

**TECHNICAL UNIVERSITY OF CRETE**  
**SCHOOL OF MINERAL RESOURCES ENGINEERING**  
MSc in Petroleum Engineering

---



MSc Thesis

Design of a continuous gas lift system to initiate production  
in a dead well

Ioannis E. Tectoros

Environmental Engineer

Scientific advisor: Dr. Vassilios Gaganis

Chania 2015



# TECHNICAL UNIVERSITY OF CRETE

## SCHOOL OF MINERAL RESOURCES ENGINEERING

### MSc in Petroleum Engineering

---

The undersigned certifies that the members of the Examination Committee have read and approve the content of the thesis, entitled “*Design of a continuous gas lift system to initiate production in a dead well*” submitted by *Ioannis Tectoros* in partial fulfilment of the requirements of the degree of Master of Science in Petroleum Engineering.

---

Prof. Nikolaos Varotsis

*(Supervisor - Member Committee)*

---

Prof. Nikolaos Kalogerakis

*(Member Committee)*

---

Prof. Nikolaos Pasadakis

*(Member Committee)*

Date \_\_\_\_\_



# Table of Contents

---

<b>List of Figures.....</b>	<b>vii</b>
<b>List of Tables .....</b>	<b>x</b>
<b>Acknowledgments .....</b>	<b>xi</b>
<b>Abstract.....</b>	<b>xiii</b>
<b>1. Introduction .....</b>	<b>1</b>
1.1 Importance of crude oil .....	1
1.2 Well deliverability and Nodal Analysis .....	1
1.3 Artificial lift .....	2
1.4 PROduction and System PERformance analysis software (PROSPER) .....	3
1.5 Thesis contents .....	3
<b>2. Well Deliverability .....</b>	<b>5</b>
2.1 Introduction.....	5
2.2 Nodal Analysis.....	5
2.3 Inflow Performance Relationship (IPR) .....	7
2.3.1 Productivity Index.....	7
2.3.2 IPR curve in undersaturated reservoirs .....	9
2.3.3 IPR in saturated reservoirs .....	10
2.3.4 Factors affecting the IPR .....	11
2.4 Vertical Lift Performance (VLP) .....	13
2.4.1 Pressure drop calculations.....	13
2.4.2 Tubing Performance Curve.....	15
2.4.3 Factors affecting the VLP curve .....	15
2.5 Multiphase Flow .....	17
2.5.1 Flow regimes.....	17
2.5.2 Superficial velocity and flow regime maps .....	18
2.5.3 Slip effect .....	20
<b>3. Artificial Lift .....</b>	<b>23</b>
3.1 Introduction.....	23
3.2 Selection of an Artificial Lift System .....	23
3.3 Types of Artificial Lift.....	24
3.3.1 Sucker Rod Pump .....	24

3.3.2	Electric Submersible Pumps (ESP).....	25
3.3.3	Hydraulic Jet Pumps .....	27
3.3.4	Progressive Cavity Pumps (PCP).....	28
3.4	Gas Lift .....	29
3.4.1	Historical Development .....	29
3.4.2	Overview of a Gas Lift System.....	30
3.4.3	Elements of Mechanical Efficiency .....	30
3.4.4	Continuous Gas Lift .....	30
3.4.4.1	Unloading process .....	31
3.4.4.2	Gas Lift Equipment .....	34
3.4.4.3	Gas Lift Valves .....	35
3.4.5	Intermittent Gas Lift .....	36
<b>4.</b>	<b>Model setup in PROSPER .....</b>	<b>37</b>
4.1	About PROSPER .....	37
4.2	Input data .....	37
4.2.1	PVT data .....	37
4.2.2	Well data .....	38
4.2.3	Reservoir data .....	38
4.2.4	Gas lift data .....	39
4.2.5	Well test data.....	39
4.3	Setting up the model in PROSPER.....	40
4.3.1	Options summary .....	41
4.3.2	PVT Data Input .....	45
4.3.3	Equipment Data Input .....	49
4.3.3.1	Deviation Survey .....	50
4.3.3.2	Surface Equipment .....	52
4.3.3.3	Downhole equipment.....	53
4.3.3.4	Geothermal gradient .....	55
4.3.3.5	Average heat capacities .....	56
4.3.4	IPR Data Input .....	57
4.3.5	Gas lift data input.....	58
4.3.6	VLP/IPR match and quality check.....	58
4.3.6.1	Well Test 1 Quality check .....	59
4.3.6.2	Well Test 2 Quality check .....	61
4.3.6.3	Correlation comparison .....	62

4.3.6.4	VLP matching .....	64
4.3.6.5	IPR/VLP matching .....	65
4.3.6.5.1	Sensitivity analysis on various water cuts .....	67
4.3.6.5.2	Sensitivity analysis on various water cuts with an ESP .....	69
4.3.6.5.3	Sensitivity analysis on various wellhead pressures .....	71
<b>5.</b>	<b>Gas lift design in PROSPER.....</b>	<b>73</b>
5.1	Input data .....	73
5.2	Design strategy.....	73
5.3	Sensitivity analysis for tubing ID selection .....	74
5.4	Methodology of valve spacing in PROSPER .....	76
5.5	Gas lift design process for $P_r = 2,850$ psi and water cut 50% (Case 1).....	78
5.5.1	Revision of Case 1 .....	86
5.6	Gas lift design process for $P_r = 3,100$ psi and water cut 40% (Case 2).....	92
5.7	Gas lift design process for $P_r = 3,400$ psi and water cut 30% (Case 3).....	97
5.7.1	Revision of Case 3 .....	100
5.8	Gas lift design process for $P_r = 3,795.2$ psi and water cut 20.3% (Case 4)..	103
5.8.1	Revision of Case 4 .....	106
<b>6.</b>	<b>Conclusions.....</b>	<b>111</b>
	<b>References.....</b>	<b>113</b>
	<b>Nomenclature .....</b>	<b>117</b>
	<b>APPENDIX A-1.....</b>	<b>119</b>
	<b>APPENDIX A-2.....</b>	<b>122</b>
	<b>APPENDIX A-3.....</b>	<b>125</b>



# List of Figures

---

<b>Figure 2.1:</b> Locations of various nodes [1] .....	6
<b>Figure 2.2:</b> Inflow and outflow curve at a specific node (Courtesy of Heriot Watt University) .....	7
<b>Figure 2.3:</b> Straight IPR (undersaturated reservoir) [2].....	10
<b>Figure 2.4:</b> Combined IPR curve for saturated and undersaturated reservoir (Courtesy of Heriot Watt University) .....	11
<b>Figure 2.5:</b> Effect of oil viscosity on the IPR: Oil a is more viscous than oil B (Courtesy of Heriot Watt University) .....	12
<b>Figure 2.6:</b> Effect of reservoir pressure to the IPR: Pressure is lowered from right to left.....	12
<b>Figure 2.7:</b> Effect of skin factor on the IPR: Skin factor is decreasing from left to the right (Courtesy of Heriot Watt University) .....	13
<b>Figure 2.8:</b> Typical tubing performance curve [6] .....	15
<b>Figure 2.9:</b> Effect of increasing tubing diameter on the VLP: Diameter is increasing from left to right (Courtesy of Herriot Watt University).....	16
<b>Figure 2.10:</b> Effect of increasing water cut on the VLP: Water is increasing from right to left (Courtesy of Herriot Watt University) .....	17
<b>Figure 2.11:</b> A generic two-phase vertical flow map [9] .....	19
<b>Figure 2.12:</b> A generic two-phase horizontal flow map [9] .....	19
<b>Figure 3.1:</b> Schematic of a sucker rod pumping system [19].....	25
<b>Figure 3.2:</b> Typical oil well with an ESP installed.....	26
<b>Figure 3.3:</b> Pump characteristic chart (Courtesy of Heriot Watt University) .....	27
<b>Figure 3.4:</b> Sketch of a hydraulic pump installation [18].....	28
<b>Figure 3.5:</b> Side pocket mandrels placed in the production tubing [24].....	31
<b>Figure 3.6:</b> Well unloading sequence [12] .....	33
<b>Figure 3.7:</b> A Side Pocket Mandrel (Courtesy of Heriot Watt University).....	34
<b>Figure 3.8:</b> Schematic view of gas lift valve in a SPM.....	35
<b>Figure 4.1:</b> Options summary in PROSPER .....	42
<b>Figure 4.2:</b> Simple schematic of temperature varying along the length of the well .....	44
<b>Figure 4.3:</b> PVT Input data section .....	46
<b>Figure 4.4:</b> PVT Match data screen.....	47
<b>Figure 4.5:</b> Correlation matching regression screen.....	49
<b>Figure 4.6:</b> Matching parameters 1 and 2 for all black oil correlations .....	49
<b>Figure 4.7:</b> Equipment data input main screen.....	50
<b>Figure 4.8:</b> Well's trajectory description .....	51
<b>Figure 4.9:</b> Profile of the well. On the x axis is the cumulative displacement while on the y axis is the measured depth.....	52
<b>Figure 4.10:</b> Surface Equipment data input screen .....	53
<b>Figure 4.11:</b> Downhole Equipment data input screen .....	54
<b>Figure 4.12:</b> Simple schematic of the downhole equipment .....	55
<b>Figure 4.13:</b> Geothermal Gradient data input screen .....	56
<b>Figure 4.14:</b> Average heat capacities data input screen .....	56

<b>Figure 4.15:</b> IPR data input main screen (1) .....	57
<b>Figure 4.16:</b> IPR data input screen (2) .....	57
<b>Figure 4.17:</b> Gas lift data input main screen .....	58
<b>Figure 4.18:</b> Match VLP/IPR section main screen .....	59
<b>Figure 4.19:</b> Estimated U-value for well test 1 .....	59
<b>Figure 4.20:</b> PvD diagram: Quality check for well test 1 .....	61
<b>Figure 4.21:</b> Estimated U value for well test 2 .....	61
<b>Figure 4.22:</b> Quality check for well test 2.....	62
<b>Figure 4.23:</b> Correlation comparison plot: All correlations plotted (Red point corresponds to the well test 1 point) .....	63
<b>Figure 4.24:</b> Matched parameters for all tubing correlations.....	65
<b>Figure 4.25:</b> Close look at the IPR/VLP curve intersection (IPR/VLP matching section).....	67
<b>Figure 4.26:</b> Revised value of the skin factor after IPR adjustment .....	67
<b>Figure 4.27:</b> Water cut cases examined .....	68
<b>Figure 4.28:</b> IPR adjustment option: Adjusted Pressure .....	68
<b>Figure 4.29:</b> ESP selection screen.....	70
<b>Figure 4.30:</b> Well head pressure cases examined .....	71
<b>Figure 5.1:</b> Sensitivity analysis: Effect of various injections depths and gas rate to the oil rate .....	75
<b>Figure 5.2:</b> Sensitivity analysis: Effect of various tubing ID to the oil rate .....	76
<b>Figure 5.3:</b> Illustration of valve spacing calculations: PvD diagram [28] .....	78
<b>Figure 5.4:</b> Gas lift design input: Main screen (Case 1) .....	80
<b>Figure 5.5:</b> Gas lift design: Calculation screen (Case 1).....	81
<b>Figure 5.6:</b> Gas lift performance curve (Case 1).....	82
<b>Figure 5.7:</b> Gas lift design: PvD plot (Case 1).....	84
<b>Figure 5.8:</b> Stability criteria (Case 1).....	86
<b>Figure 5.9:</b> Gas lift design input: Main screen (Case 1 revised).....	87
<b>Figure 5.10:</b> Gas lift design: Calculation screen (Case 1 revised) .....	88
<b>Figure 5.11:</b> Gas lift performance curve (Case 1 revised) .....	88
<b>Figure 5.12:</b> Gas lift design: PvD plot (Case 1 revised) .....	90
<b>Figure 5.13:</b> Stability criteria (Case 1 revised) .....	91
<b>Figure 5.14:</b> Pressure and liquid hold versus depth (Case 1 revised) .....	92
<b>Figure 5.15:</b> Gas lift design: Calculation screen (Case 2).....	93
<b>Figure 5.16:</b> Gas lift performance curve (Case 2).....	93
<b>Figure 5.17:</b> Gas lift design: PvD plot (Case 2) .....	95
<b>Figure 5.18:</b> Stability criteria (Case 2).....	96
<b>Figure 5.19:</b> Pressure and liquid hold versus depth (Case 2).....	97
<b>Figure 5.20:</b> Gas lift design: Calculation screen (Case 3).....	98
<b>Figure 5.21:</b> Gas lift performance curve (Case 3).....	98
<b>Figure 5.22:</b> Gas lift design: PvD plot (Case 3).....	99
<b>Figure 5.23:</b> Gas lift design (Case 3 revised).....	100
<b>Figure 5.24:</b> Gas lift design: PvD plot (Case 3 revised) .....	101
<b>Figure 5.25:</b> Stability criteria (Case 3 revised) .....	102
<b>Figure 5.26:</b> Pressure and liquid hold versus depth (Case 3 revised) .....	103
<b>Figure 5.27:</b> Gas lift design: Calculation screen (Case 4).....	104

<b>Figure 5.28:</b> Gas lift performance curve (Case 4) .....	104
<b>Figure 5.29:</b> Gas lift design: PvD plot (Case 4) .....	106
<b>Figure 5.30:</b> Gas lift design: Calculation screen (Case 4 revised) .....	107
<b>Figure 5.31:</b> Stability criteria (Case 4) .....	108
<b>Figure 5.32:</b> Pressure and liquid hold versus depth (Case 4 revised) .....	109

## List of Tables

---

<b>Table 4.1:</b> Fluid PVT properties .....	38
<b>Table 4.2:</b> Basic Reservoir characteristics .....	39
<b>Table 4.3:</b> Well test data .....	40
<b>Table 4.4:</b> Results of the sensitivity analysis for various water cuts.....	69
Table 4.5: Sensitivity analysis results on various water cuts with the introduction of an ESP.....	70
<b>Table 4.6:</b> Sensitivity analysis results on various wellhead pressures .....	71
<b>Table 5.1:</b> Valve spacing results (Case 1) .....	83
<b>Table 5.2:</b> Valve spacing results (Case 1) .....	89
<b>Table 5.3:</b> Valve spacing results (Case 2) .....	94
<b>Table 5.4:</b> Valve spacing results (Case 3) .....	99
<b>Table 5.5:</b> Valve spacing results (Case 3 revised) .....	101
<b>Table 5.6:</b> Valve spacing results (Case 4) .....	105

## **Acknowledgments**

---

First of all, I would like to thank Professor Nikolaos Varotsis for supervising my MSc Thesis. I would also like to thank Professor Nikolaos Kalogerakis for being part of my thesis committee.

I want to express my gratitude to Professor Nikolaos Pasadakis, not only for being a member of my thesis committee but also for his efforts to organize the MSc course and his willingness to help each and every one student throughout the year.

The present thesis would not have been completed without the guidance of my Scientific Advisor Dr. Vassilis Gaganis. I would like to thank him for his enthusiasm, insightful comments and his advice during the preparation of the present thesis.

After seven years in Chania, I would like to thank all the friends I've made here for the good memories and, most of all, my family for their unlimited support in every choice of my life

.



## Abstract

---

Artificial lift systems are among the most widely used production technologies in global oil and gas operations. Wells that cannot produce liquids to the surface under their own pressure require lift technologies to enable production. Some liquid wells need lift assistance from the beginning and almost all require it sooner or later. The majority of the producing wells worldwide currently use artificial lift.

One of the most popular artificial lift methods applied in the oil industry, in order to enhance oil recovery, is the gas lift method. Its main principal is the injection of gas in the well to reduce the average density of the fluids produced from the reservoir, hence the weight of the fluid column. As a result, the declined reservoir pressure is sufficient to lift the fluids up to the surface.

The present MSc thesis is based upon a fictitious onshore well named A-1, in the Alpha field. Due to the field's declined pressure (3,844 psi) and the increasing water cut (20.3%), production may cease in the upcoming months.

The main task is to design a gas lift system which will not only assist production during the current operating conditions, but also in future unfavorable situations where according to the reservoir forecasting, water cut is expected to increase up to 50% and reservoir pressure will drop down to 2,850 psi. The procedure of designing an optimized gas lift system in PROSPER is thoroughly described.

The main idea behind the design process was to recomplet the well once to ensure that the project will be economically viable and, on the other hand, maximized production was achieved during all operating conditions. Minimum oil production rate was set at 2000 bopd.

A continuous gas lift system design was carried out, based on the worst case scenario. Side pocket mandrels for the unloading process were set at certain depths, according to the calculations. Then, the rest of the cases, with lower water cut levels and higher reservoir pressure, were adapted to the initial side pocket mandrel spacing plan. Results showed that in all cases, the system was capable of delivering oil rates well over the minimum requested rate. Initial tubing diameter was also varied to ensure production optimization. The lowest oil rate achieved is 3,300 stb/day and the best rate is obtained at current operating conditions and is equal to 8,593 stb/day. Stability analysis of all designs indicated stable gas lift systems for all cases. The predicted production levels showed that the existing completion plan can serve for even worse scenarios in terms of system productivity.



# 1. Introduction

---

## 1.1 Importance of crude oil

Crude oil is the most important natural source of energy in all industrialized countries. As modern civilization and its remarkable accomplishments would not exist without oil. What makes it so important in our everyday lives is its broad variety of uses. Apart from fueling cars, airplanes etc., its components can be used to manufacture many types of chemical products such as plastics, medicine, detergents and many other things.

Even though oil is not an unlimited source of energy, the proven reserves indicate that crude oil can supply the planet's energy demands for many decades to come. According to OPEC, the total proven reserves of all oil producing countries are 1.3 trillion barrels of oil. To realize the magnitude of the above figures, it is estimated that we have already consumed about 1 trillion barrels. Global demand on energy is continuously growing and oil is produced in larger quantities than it used to some decades ago. Continuous discovery of new fields in combination with the optimization of production on the existing ones has become more essential than ever.

The concept of production optimization was not introduced from the beginning of the oil age. Ever since, the progress in technology has provided the tools to Petroleum Engineers to exploit the oilfields as efficiently as possible and maximize recovery factors.

## 1.2 Well deliverability and Nodal Analysis

Back in the late 1800s till the beginning of the 20<sup>th</sup> century, the analysis of a petroleum production system was yet unknown. When the first oil reservoirs started to suffer from severe depletion, the concept of production optimization became a necessity. Due to the uncertainty and large amount of risk behind exploration for new fields, the need to exhaust all possibilities within the existing reservoirs became urgent.

Engineers in the oil industry seek production optimization in three domains. From the reservoir engineering point of view, software specialized in reservoir simulation was developed in order to reduce the uncertainty that lies in a reservoir and predict the flow of fluids in porous media and make production forecasts. Software using the principles of material balance were also introduced to simplify calculations.

The second domain which was thoroughly studied is the fluid flow from the reservoir, through the tubing, down to the surface facilities, in other words the

ability of the well to deliver fluids to the surface. The need to reduce pressure losses in the tubulars led the engineers to confront this challenge by studying the system as a unit comprised by several interacting components. The present MSc thesis is involved in this domain and a system like the one described above will be created and studied in detail.

Lifting the fluids up to the surface is not enough. The fluids produced comprise mostly of oil, water and gas and these phases must be separated and treated accordingly. Similarly to the other domains of interest, specialized software on treatment plant design is used by all oil companies around the world.

The analysis of the well as system of components was introduced in mid 50s by Gilbert. The main objective of such analysis is to combine the characteristics of each component in order to estimate production rates and optimize the system's productivity.

Initial reservoir pressure is generally large enough to lift the reservoir fluids up to the surface. As production continues, the pressure becomes gradually lower and the liquid rates are deteriorated. For this reason, the principles of fluid flow in porous media and pipelines were thoroughly examined. As the produced fluids travel from the reservoir to the surface facilities, a significant amount of pressure is wasted due to a series of factors. The optimization of these factors, so that the lowest pressure drop possible in a well occurs, is the reason behind the development of system analysis or else Nodal Analysis. In other words, the well needs to be optimized so that the maximum possible flowrates which could be achieved by the reservoir would not be restricted due to the design of the well.

In Nodal Analysis, the whole production system is considered as a unit. Then, a certain point in the system e.g. the bottomhole or the wellhead is chosen to be analyzed. Upstream of node is called inflow and downstream of node is called outflow. Both inflow and outflow performance are combined to provide the flowing pressure at the node for a specific flow rate. Nodal Analysis is the base for the majority of calculations run in Petroleum Production Engineering. All calculations run in the present thesis use the principles of Nodal Analysis which will be discussed in detail throughout this study.

### **1.3 Artificial lift**

The reservoir pressure, after a long period of production, will drop to such levels that the observed oil rates will not be economically viable. The worst case might be encountered when the pressure is insufficient to lift the liquids up to the surface and production will eventually seize. The need to maintain production for as long as possible, led the engineers among the industry to develop methods in order to reinitiate or increase production.

The production optimization methods are called artificial lift methods and refer to the use of mechanical means (such as pumps) to assist production by reducing

pressure drop along the well, or the lightening of the hydrostatic column by injecting gas into the production tubing. The vast majority of oil wells around the world produce with some type of artificial lift.

More specifically, the second category of artificial lift mentioned above is called “gas lift” method. The decrease of the weight of the hydrostatic column in the well renders it possible to increase the flow rate above what would flow naturally with the current reservoir pressure. One of the main advantages of gas lift that makes it popular among the oil industry is its versatility under various operating conditions.

The application of Nodal Analysis in the design process of these methods is imperative in order to exploit their full capacity in production optimization. Nevertheless, economic restrictions and field experience combined should always be taken into consideration.

#### **1.4 PROduction and System PERformance analysis software (PROSPER)**

PROSPER is the industry standard single and multilateral well performance design and optimization software. It can model and optimize most types of well completions and artificial lifting methods. Sensitivity analyses for a wide range of operating conditions can be held by means of Nodal Analysis. PROSPER generates a model for each component of the producing well system separately which contributes to overall performance, and then allows to verify each model subsystem by performance matching. In this way, the program ensures that the calculation is as accurate as possible. All calculations in study regarding the generation of a well model, sensitivity analyses and design of an optimum gas lift system have been carried out by using PROSPER.

#### **1.5 Thesis contents**

The main task of this study is to design a gas lift system in an oil well when the reservoir pressure will be insufficient to support economically viable production. All topics mentioned in the previous chapter are analytically discussed in the following chapters of this study. More specifically:

- The principles of Nodal analysis and its applications on production systems are described in **Chapter 2**. A discussion on various parameters affecting the productivity of such systems and methods applied to simplify calculations are also included.
- A general discussion on the most popular artificial lift systems used in the oil industry, their component parts and how they operate is given in

**Chapter 3** followed by an analytical description of the gas lift systems, their configuration and mechanism.

- In **Chapter 4** the available data for the case under study is presented and the setting up of the model in PROSPER is thoroughly analyzed step by step. After the generation of a reliable model, calculations for the current and future operating conditions follow.
- The final design of the gas lift system for the available data, the theory behind the calculations, the strategy followed to maximize production and how PROSPER actually applies all these in practice, are discussed in **Chapter 5**.
- Finally in **Chapter 6**, an evaluation of all the results obtained by PROSPER during model set up and the effectiveness by the implementation of the gas lift design is made.

## 2. Well Deliverability

---

### 2.1 Introduction

The "deliverability" of a system refers to its capacity to deliver liquid and gas as a function of pressure. In Petroleum Engineering, the combination of well inflow and outflow performance determines the deliverability of a well. The former describes the deliverability of the reservoir and the latter counts for the resistance of flow in the production string. The main purpose of this analysis is the prediction of achievable fluid production rates from reservoirs with specified production string characteristics. The technique of this analysis is better known as "Nodal Analysis".

### 2.2 Nodal Analysis

Nodal Analysis has been applied for many years to analyze the performance of systems composed of interacting components. Electrical circuits, complex pipeline networks and centrifugal pumping systems are all analyzed using this method. Its application to well producing systems was first proposed by Gilbert in 1954 and Mach, Proano, and Brown in 1979 further developed the concept.

In Nodal Analysis, a specific point in the system is chosen (node) and the system is divided in two parts. All of the components upstream of the node comprise the inflow section and all components downstream of the node comprise the outflow section. Each component behavior in the system is directly related to flow rates and pressure drop. The flow rate through the whole system can be determined once the following requirements are satisfied:

1. Flow into the node equals flow out of the node.
2. Only one pressure can exist at a node.

The various locations of the nodes are illustrated in **Figure 2.1**:

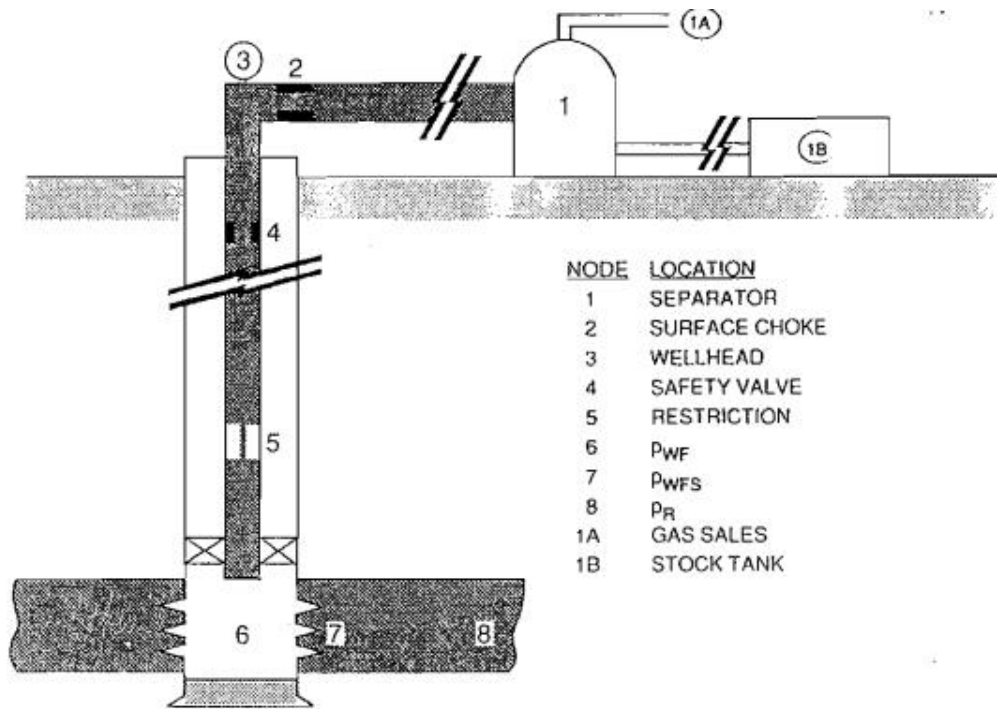


Figure 2.1: Locations of various nodes [1]

The pressures of both reservoir and separator or wellhead, are fixed. Since the node has a unique pressure, the following expressions can be used:

$$\bar{P}_r - \Delta P_{upstream} = P_{node} \quad \text{Eq. 2.1}$$

$$P_{wh} + \Delta P_{downstream} = P_{node} \quad \text{Eq. 2.2}$$

Where,  $P_r$ : the average reservoir pressure, psi

$P_{wh}$ : the pressure at the wellhead, psi

$\Delta P_{upstream}$ : the pressure loss due to upstream components, psi

$\Delta P_{downstream}$ : the pressure loss due to upstream components, psi

Note that the pressure drops both in the inflow and outflow depend on geometry, equipment etc. but most importantly on flowrate. If a sensitivity analysis on various liquid rates is made, the following diagram of node pressure versus flow rate can be derived (Fig. 2.2): The inflow and outflow curves cannot be used individually to find the flowing pressure and flow rate at the selected node. The point where these curves intersect is the operating point, i.e. the point which satisfies both constraining equations above. If these two curves do not intersect, then, no flow is established through the node, i.e. the well is dead. Generally, during a well system analysis, the solution node is set bottomhole. The purpose of this is the separation of the system into those components that comprise the

reservoir and those that comprise the well itself up to the top node. The analytical description of both inflow and outflow relationships is given in the following two sections.

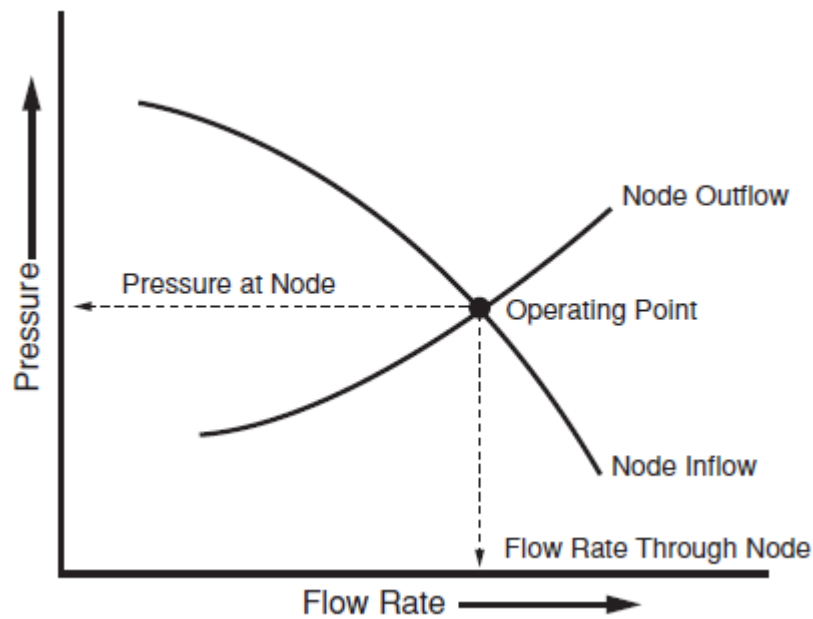


Figure 2.2: Inflow and outflow curve at a specific node (Courtesy of Heriot Watt University)

## 2.3 Inflow Performance Relationship (IPR)

### 2.3.1 Productivity Index

First of all, the ability of the reservoir to deliver fluids to the production well has to be examined. The productivity index (PI) which is denoted with the letter  $J$ , is the measure of the ability of the well to produce fluids. The productivity index is generally measured during a production test on the well. The well is shut-in until the static reservoir pressure is reached. The well is then allowed to produce at a constant flow rate of  $q$  and a stabilized bottom-hole flow pressure of  $P_{wf}$ . This type of flow theoretically represents a semisteady-state type of flow. Since a stabilized pressure at surface does not necessarily indicate a stabilized  $P_{wf}$ , the bottomhole flowing pressure should be recorded continuously from the time the well is to flow [2].

It is derived by the Darcy's equation for radial semi-steady state flow and it is the ratio of liquid flow rate to the pressure drawdown (Eq. 2.3). It can be applied only in single phase flow, hence in the case of an undersaturated reservoir.

$$J = \frac{q}{\bar{P}_r - P_{wf}} = \frac{2\pi kh}{\mu B_o} \frac{1}{\ln\left(\frac{r_e}{r_w}\right) - \frac{3}{4} + S} \quad (\text{Semisteady - state}) \quad \text{Eq. 2.3}$$

Where q: liquid rate, stb/day

J: productivity index, stb/day/psi

$\bar{P}_r$ : average reservoir pressure (static pressure), psi

$P_{wf}$ : downhole flowing pressure, psi

$r_w$ : wellbore radius, ft

$r_e$ : External drainage radius, ft

S: Skin factor, dimensionless

h: Reservoir thickness, ft

$\mu$ : viscosity, cp

$B_o$ : formation volume factor, bbl/stb

The productivity index is proved to be a very useful tool in Petroleum Engineering in order to predict future performance of wells, since, during a well's lifespan; flow regimes are approximating the pseudosteady-state ones. It should be underlined that unexpected declines in the value of J can be concrete indications for a series of well issues such as damages due to workover, completion, mechanical problems etc.

The semi-steady state inflow equation is restrictive in that it only applies for a well producing from the center of a circular shaped drainage area. When a reservoir is producing under semi-steady state conditions each well will assume its own fixed drainage boundary and the shapes of these may be far from circular. As a result, **Eq. 2.3** must be modified to comply with this lack of symmetry. To achieve that, semi-steady state inflow equation will be expressed in a generalized form by introducing the so-called Dietz shape factor denoted by  $C_A$ . Dietz shape factor exhibits various values, depending on the shape of the drainage area and the position of the well in this area. The denominator of **Eq.2.3** can be rearranged to get:

$$\begin{aligned}
\ln\left(\frac{r_e}{r_w}\right) - \frac{3}{4} + s &= \frac{1}{2} \ln\left(\frac{r_e^2}{r_w^2}\right) - \frac{3}{4} + s \\
&= \frac{1}{2} \ln\left(\frac{4\pi r_e^2}{4\pi r_w^2}\right) - \ln(e^{\frac{3}{4}}) + s \\
&= \frac{1}{2} \ln\left(\frac{4\pi r_e^2}{4\pi r_w^2}\right) - \ln(e^{\frac{3}{4}}) + s \\
&= \frac{1}{2} \ln\left(\frac{4A}{56.32r_w^2}\right) + s \\
&= \frac{1}{2} \ln\left(\frac{4A}{31.6\gamma r_w^2}\right) + s \\
&= \frac{1}{2} \ln\left(\frac{4A}{\gamma C_A r_w^2}\right) + s
\end{aligned} \tag{Eq. 2.4}$$

Where  $\gamma$  is the exponential of Euler's constant, and is equal to 1.781 (Euler's constant is 0.5772) and  $C_A$  is the Dietz shape factor. The combination of **Eq. 2.3** and **Eq. 2.4** gives the generalized inflow equation which now takes into account the geometry of the drainage area.

$$q = \frac{2\pi kh}{\mu B \left[ \frac{1}{2} \ln\left(\frac{4A}{\gamma C_A r_w^2}\right) + s \right]} \tag{Eq. 2.5}$$

### 2.3.2 IPR curve in undersaturated reservoirs

If the previous equation is rewritten, it can represent a linear relationship between the liquid flow rate and the pressure drawdown, for a single constant value of productivity index, as seen below:

$$q = J(\bar{P}_r - P_{wf}) \tag{Eq. 2.6}$$

Graphically, it is represented by a straight line with a slope equal to  $-1/J$  (**Fig. 2.3**). Note that the above methodology can only be applied to reservoirs with pressures above the bubble point pressure. When  $P_{wf}$  is equal to the average

reservoir pressure, no flow is observed due to zero pressure drawdown value. On the other hand, maximum liquid rate occurs when  $P_{wf}$  is zero and it is called absolute open flow (AOF). For saturated reservoirs, the IPR curve is no longer a straight line and will be discussed in the next paragraph.

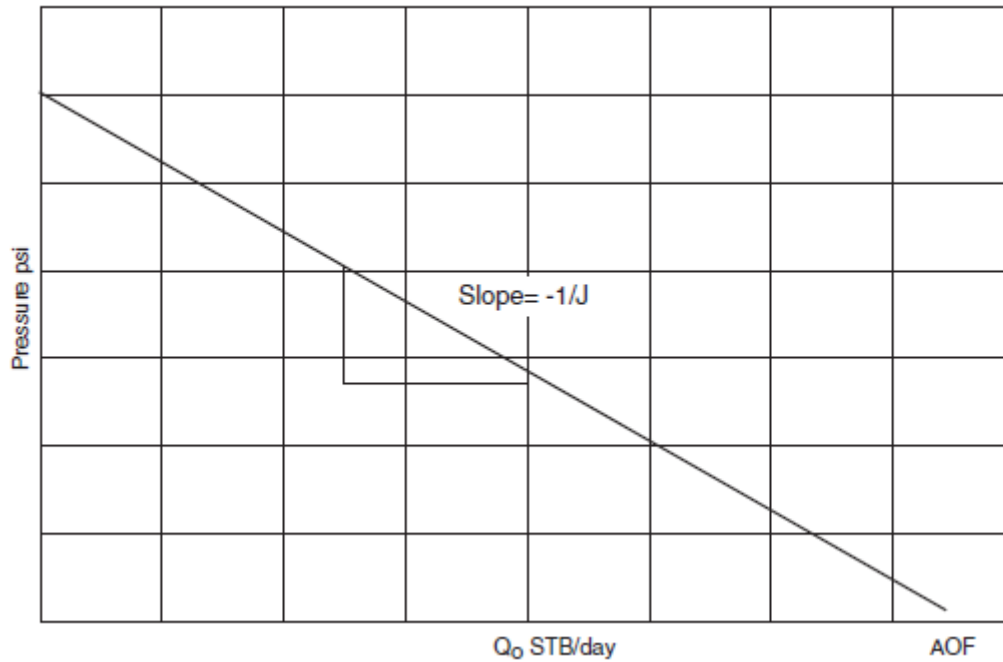


Figure 2.3: Straight IPR (undersaturated reservoir) [2]

### 2.3.3 IPR in saturated reservoirs

Evinger and Muskat [3] proposed that, for multiphase flow, a curved relationship existed between flow rate and pressure and that the straight-line is no longer applicable. Vogel [4], in 1968, proposed the following equation for predicting a well's inflow performance under a solution gas drive (two phase flow) conditions based on a large number of well performance simulations.

$$\frac{q}{q_{max}} = 1 - 0.2 \left( \frac{P_{wf}}{P_r} \right) - 0.8 \left( \frac{P_{wf}}{P_r} \right)^2 \quad \text{Eq. 2.7}$$

Where  $q_{max}$  : Absolute Open Flow (AOF), bbl/day

The combination of the straight and Vogel's curved IPR can fully describe the inflow performance at any pressure. Above  $P_b$ , the IPR is a straight line, while below  $P_b$  it is curved. In **Figure 2.4**, the area created between A and C represents the occurrence of two phase flow.

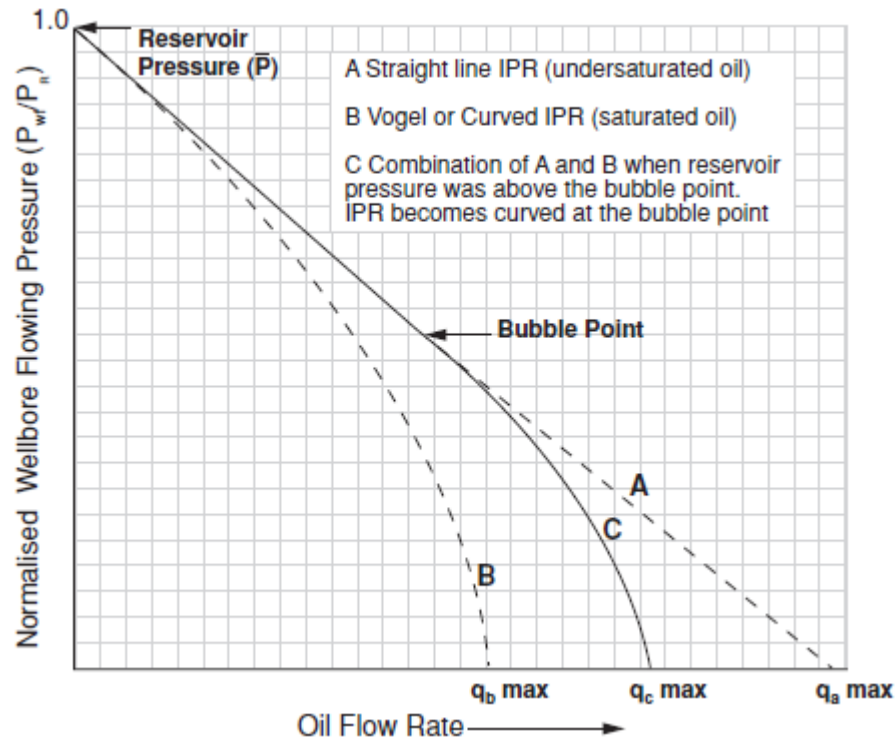


Figure 2.4: Combined IPR curve for saturated and undersaturated reservoir (Courtesy of Heriot Watt University)

### 2.3.4 Factors affecting the IPR

IPR is influenced by parameters related to the reservoir. It is already mentioned that the solution node is set bottomhole in order to separate the system in the components related to the reservoir and the components related to the flow in the tubing up the surface. The most notable components affecting an IPR curve are the following:

- Rock Properties
- Fluid Properties
- Reservoir Pressure
- Well Geometry
- Well Flowing pressure

Indicative examples can be seen in **Figures 2.5, 2.6, 2.7**. In the first image (**Fig. 2.5**), the effect of viscosity to the inflow performance of the reservoir is demonstrated. **Figure 2.6** shows the effect of reservoir depletion to the IPR. Increasing oil viscosity affects the mobility of the oil through the porous media and leads to a lower productivity index.

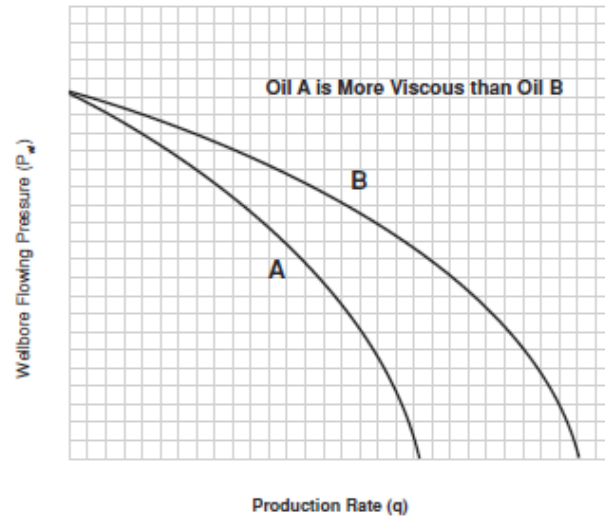


**Figure 2.5:** Effect of oil viscosity on the IPR: Oil a is more viscous than oil B (Courtesy of Heriot Watt University)

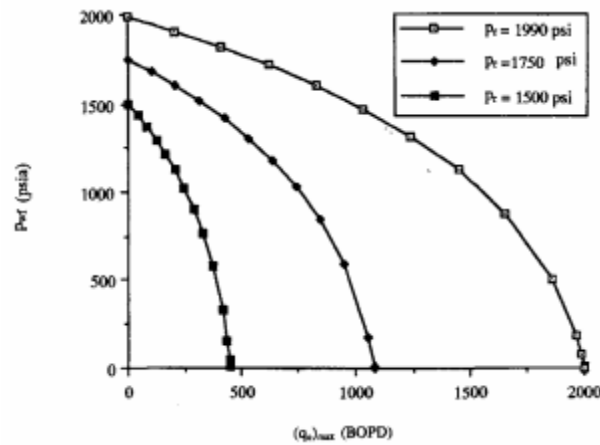


**Figure 2.6:** Effect of reservoir pressure to the IPR: Pressure is lowered from right to left

A decrease in the skin factor increases the deliverability of a system up to a point. **Figure 2.7** shows the effect of well stimulation techniques, such as fracturing or acidizing, on the inflow performance. When skin factor is further reduced, productivity of the system is unaffected.

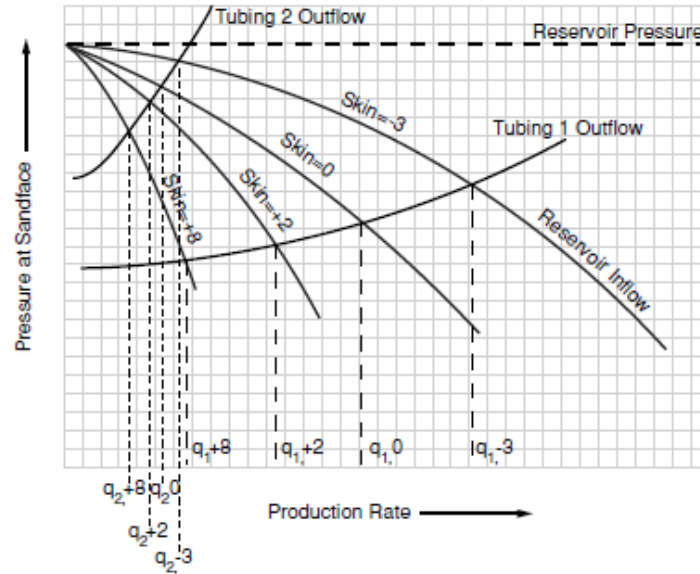


**Figure 2.7:** Effect of skin factor on the IPR: Skin factor is decreasing from left to the right (Courtesy of Heriot Watt University)

## 2.4 Vertical Lift Performance (VLP)

One of the major factors affecting the production performance of a well is the pressure loss in the tubulars. As much as 80% of the total pressure loss in a flowing well may occur in lifting the fluid to the surface, while the rest is lost in the reservoir. Vertical lift performance expresses the bottomhole flowing pressure as a function of liquid rate in the wellbore during the production of reservoir fluids [6]. According to Golan and Whitson [7], the outflow performance depends on several factors; liquid rate, fluid type (gas-liquid ratio, water cut), fluid properties and tubing size.

### 2.4.1 Pressure drop calculations

Generally, the total pressure drop in a well is the summation of the pressure drop due to frictional forces ( $\Delta P_f$ ), gravitational energy change ( $\Delta P_g$ ) and kinetic energy changes ( $\Delta P_k$ ), with the last one to be omitted as its value is usually negligible compared to the previous two sources (**Eq. 2.8**).

$$\Delta P = \Delta P_f + \Delta P_g + \Delta P_k \quad \text{Eq. 2.8}$$

**Pressure drop due to potential energy change:**

$$\Delta P_g = \rho g L \sin \theta \quad \text{Eq. 2.9}$$

where  $g$ : the acceleration due to gravity,

$\rho$ : the density of the fluid,

$L$ : the length of the pipe and

$\theta$ : the angle between horizontal and the direction of flow

**Pressure drop due to kinetic energy change:**

$$\Delta P_k = \rho(u_2^2 - u_1^2) \quad \text{Eq. 2.10}$$

**Pressure drop due to frictional forces:**

$$\Delta P_f = \frac{2f_f \rho u^2 L}{D} \quad \text{Eq. 2.11}$$

Where  $f$ : the Moody friction factor

In laminar flow it is a simple function of the Reynolds number.

$$f = \frac{64}{N_{Re}} \quad \text{Eq. 2.12}$$

$$N_{RE} = \frac{\rho u D}{\mu} \quad \text{Eq. 2.13}$$

The Reynolds number determines the type of flow which is distinguished by certain boundaries between flow regimes.

$N_{Re} \leq 2000$ : Laminar flow

$2000 < N_{Re} \leq 4000$ : Transition between laminar and turbulent flow

$4000 < N_{Re}$ : Turbulent flow

Estimation of the friction factor during turbulent flow is more complicated and other methods are used for its calculation. The most common is the use of the Moody chart which requires the knowledge of the roughness ( $\epsilon$ ) of the examined pipe.

Specialized software can perform all these complex calculations of pressure drop in pipelines. To do so, the pipelines are split in a set of many small segments and pressure drop calculations are held for each segment individually. The splitting is done adaptively so that are exhibiting big contribution to the total pressure loss are simulated with small segments, while in others of minor interest the software uses larger segments.

### 2.4.2 Tubing Performance Curve

In **Section 2.2** it is discussed that the solution node, in a system analysis of a well, lies bottomhole. The generation method of the inflow performance curve is already analyzed. The outflow performance is also necessary to estimate the bottomhole flowing pressure  $P_{wf}$  which is one of the most important tasks in Petroleum Production Engineering. This can be easily done, by using the following method. For various flowrates and for a fixed wellhead pressure, the total pressure loss can be calculated using the Equation 2.8 for the whole length of the production tubing. The outcome of this approach is the Tubing Performance curve (or else known as VLP curve) and its importance lies on the fact that it captures the required flowing bottomhole pressure needed for various liquid rates. The VLP depends on many factors including PVT properties, well depth, tubing size, surface pressure, water cut and GOR. A schematic example of a VLP curve is shown below (**Fig. 2.8**):

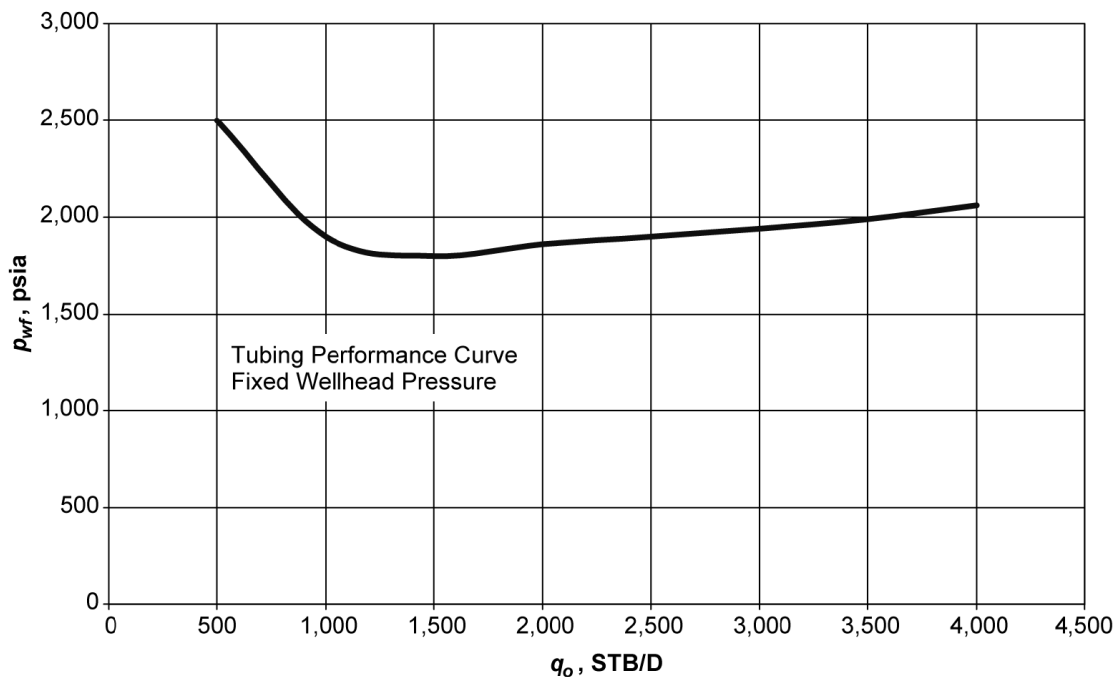


Figure 2.8: Typical tubing performance curve [6]

### 2.4.3 Factors affecting the VLP curve

Some of the factors affecting the vertical lift performance of the well are:

- Production Rate
- Well Depth
- GOR/GLR
- Tubing Diameter
- Water cut
- Restrictions (Scale, waxes, SSSV etc)

In general, an increase of the tubing diameter proves to be beneficial to the productivity of a system (**Fig. 2.9**). There is a point, though, where very large tubing size results in the large decrease of the upward gas flow velocity that it is no longer sufficient to efficiently lift the liquid to the surface (see **Section 2.5**).

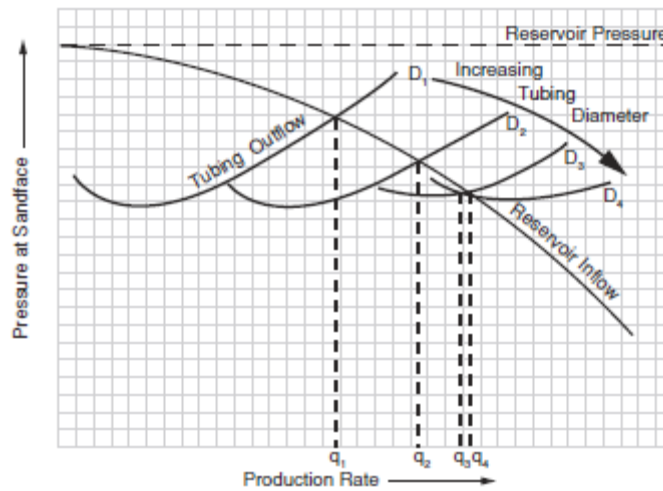


**Figure 2.9:** Effect of increasing tubing diameter on the VLP: Diameter is increasing from left to right  
(Courtesy of Herriot Watt University)

Water cut is also an important parameter that must be taken into consideration. An increasing water cut reduces the gas-liquid ratio. Less oil means that less gas will be evolved from it, and in combination with the greater density of the water in respect to that of the oil, the average density of the fluid will be greater than initially was. This eventually leads to an increase of the hydrostatic head between the reservoir and the surface (**Fig. 2.10**). Heavier flowing fluid requires more pressure from the reservoir to be lifted up to the surface.

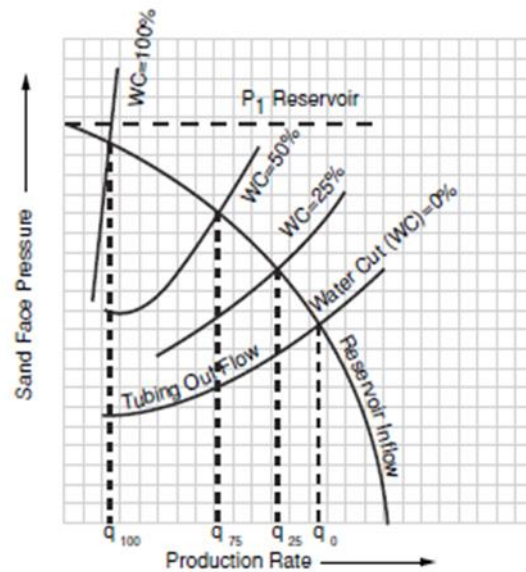


**Figure 2.10:** Effect of increasing water cut on the VLP: Water is increasing from right to left (Courtesy of Herriot Watt University)

## 2.5 Multiphase Flow

### 2.5.1 Flow regimes

In oil and gas production, multiphase flow often occurs in wells and pipelines because the wells produce gas and oil simultaneously. This is called two-phase flow. In addition to gas and oil, water is also often produced at the same time. This is called three-phase flow. The calculations of pressure drop along the production tubing become more complex than the ones described in **paragraph 2.4.1**. Common single-phase characteristics such as velocity profile, turbulence and boundary layer, are thus inappropriate for describing the nature of such flows. The flow structures are classified in flow regimes, whose characteristics depend on a number of parameters such as operating conditions, fluid properties, flow rates and the orientation and geometry of the pipe through which the fluids flow. The distribution of the fluid phases in space and time differs for the various flow regimes, and is usually not under the control of the designer or operator [9].

All flow regimes however, can be grouped into dispersed flow, separated flow, intermittent flow or a combination of these:

- Dispersed flow: Bubble and mist flow are characteristic examples of this category. The main characteristic of this type of flow is the uniform distribution of phases in both radial and axial directions.

- Separated flow is characterized by a non-continuous phase distribution in the radial direction and a continuous phase distribution in the axial direction. Examples of such flows are stratified and annular.
- The intermittent flow regime is characterized by discontinuity in liquid and vapor flow. In this flow regime, vapor slugs or plugs are formed, surrounded by a thin liquid coating on the periphery and blocked by a liquid slug between successive vapor bubbles [10].

### 2.5.2 Superficial velocity and flow regime maps

The term superficial velocity is often used on the axes of flow regime maps. Flow regime maps are a qualitative tool used to define the type of flow, when superficial velocities are known. The velocity of a single phase vapor or a liquid (through vessels, pipes, etc.) is equal to the volumetric flow rate divided by the cross-sectional flow area of the pipe. For the superficial liquid velocity, in multiphase flow, the same can be derived and the simple expressions are given in **Equations 2.14** and **2.15**.

$$V_{s,gas} = \frac{q_{gas}}{A} \quad \text{Eq. 2.14}$$

$$V_{s,liquid} = \frac{q_{liquid}}{A} \quad \text{Eq. 2.15}$$

In vertical flows, as the superficial gas velocity increases, multiphase flow will pass through all flow regimes (bubble - slug - churn and annular) as seen on **Figure 2.11**.

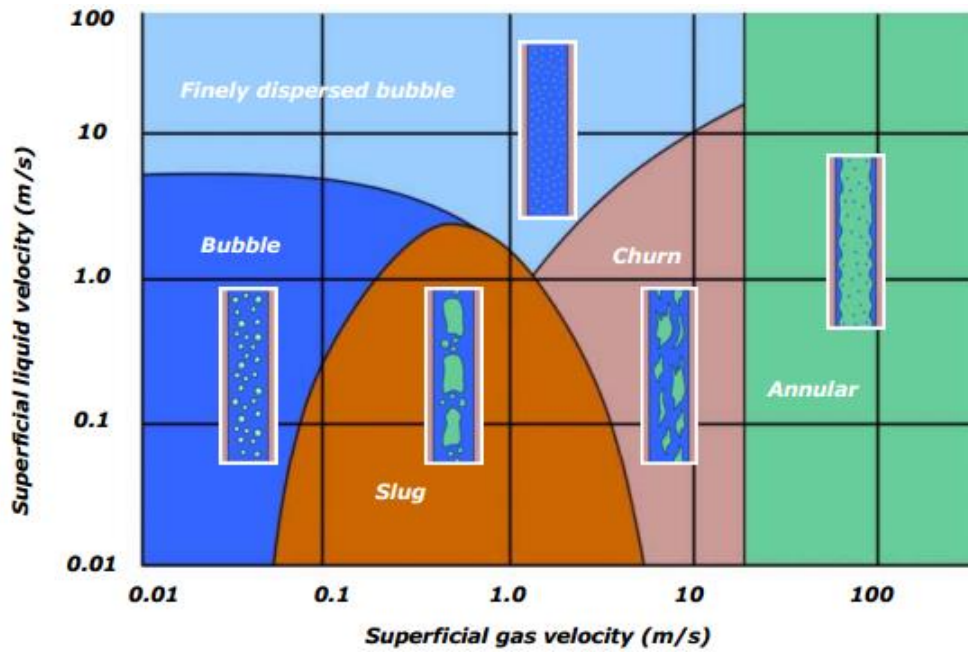


Figure 2.11: A generic two-phase vertical flow map [9]

In horizontal flows as well, the flow regime transitions depends upon many factors such as gas-liquid velocities, fluid properties, orientation of conduit, tube diameter ( $D$ ) and operating conditions [11]. The following map (Fig. 2.12) shows qualitatively, how flow regime transitions are dependent on superficial gas and liquid velocities in horizontal multiphase flow. A map like this will only be valid for a specific pipe, pressure and a specific multiphase fluid.

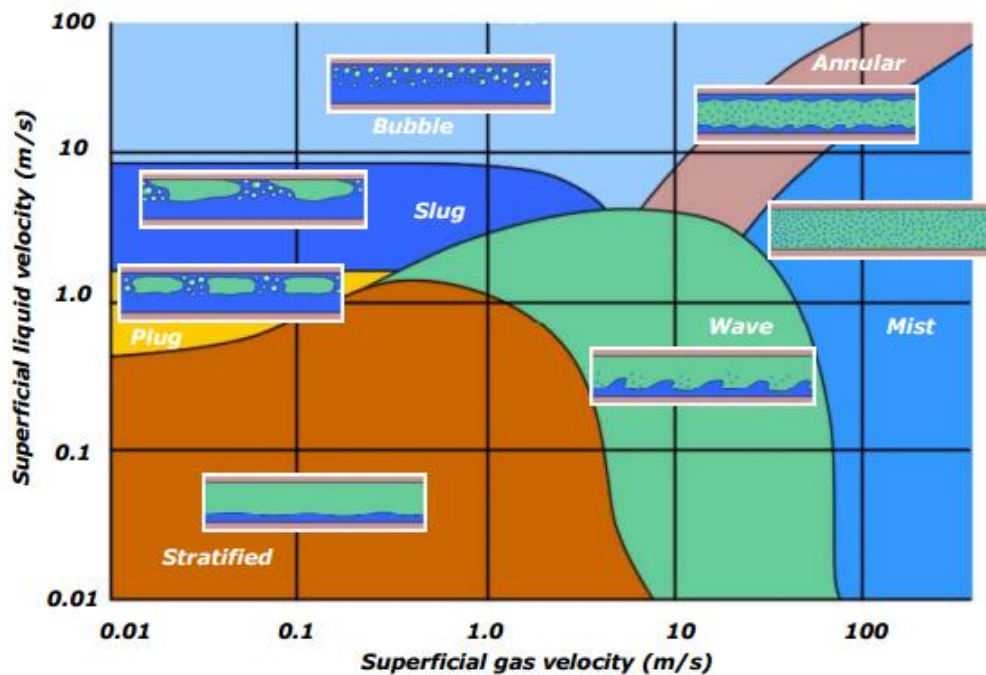


Figure 2.12: A generic two-phase horizontal flow map [9]

### 2.5.3 Slip effect

Multiphase flow would be greatly simplified if the two phases behaved as a homogeneous mixture whose properties were an appropriately averaged value of the individual phase properties. However, experiments have shown that this is not the case and that one fundamental phenomenon occurring in inclined multiphase flow (oil-gas, water-oil, etc.) is the concept of slip and hold-up. These phenomena are most important for the gas/liquid case since the density differences are greatest: Slip refers to the ability of the less dense (“lighter”) phase to flow at a greater velocity than the denser (“heavier”) phase. Hold-up is a consequence of slip - the volume fraction of the pipe occupied by the denser phase is greater than would be expected from the (relative) in – and outflow of the two phases - since its flow velocity is slower than that for the light phase [5]. This is something which severely affects calculations of pressure drop in a pipe. When more gas is present in a pipe segment, friction is the main factor of pressure loss due to its increased actual velocity. On the other hand, pipe segments almost full of liquid, exhibit pressure losses due to the increased gravity term.

Unlike the superficial velocities discussed previously, which represent velocities of each phase as if the pipe was occupied by only this phase, the phase velocities are the real velocities of the flowing phases. They may represent velocities in a local scale in the pipe cross section or a velocity of a cross sectional average of the pipe. They are defined by:

$$V_{gas} = \frac{q_{gas}}{A_{gas}} \quad \text{Eq. 2.16}$$

$$V_{liquid} = \frac{q_{liquid}}{A_{liquid}} \quad \text{Eq. 2.17}$$

where  $A_{liquid}$  and  $A_{gas}$  are the pipe areas occupied by the liquid and gas respectively. Gas and liquid will flow at different phase velocities within the pipe. The relative phase velocity or slip velocity is defined by:

$$V_s = |V_{gas} - V_{liquid}| \quad \text{Eq. 2.18}$$

Liquid hold – up and gas void fraction are defined as the ratio of the area occupied by each phase (liquid or gas) to the total cross sectional area of the pipe.

$$\lambda_{liquid} = \frac{A_{liquid}}{A_{pipe}} \quad \text{Liquid Hold - up} \quad \text{Eq. 2.19}$$

$$\lambda_{gas} = \frac{A_{gas}}{A_{pipe}} \quad \text{Gas void fraction} \quad \text{Eq. 2.10}$$

$$\lambda_{liquid} + \lambda_{gas} = 1 \quad \text{Eq. 2.21}$$

Only under no-slip conditions is the gas void fraction equal to the gas volume fraction, and the Liquid Hold-up is equal to the Liquid Volume Fraction. The flow in this case is homogeneous and the two phases travel at equal velocities. In reality, however, the Liquid Hold-up will be larger than the Liquid Volume Fraction and, consequently, the gas void fraction will be smaller than the gas volume fraction.

Multiphase flow correlations are used to predict the liquid holdup and frictional pressure gradient. Depending on the particular correlation, flow regimes are identified and specialized holdup and friction gradient calculations are applied for each flow regime. The density difference between gas and either water and oil is far greater than the density difference between oil and water. The multiphase flow correlations lump oil and water together as liquid and calculations are based on liquid/gas interactions. Such flow correlations are more accurately described as two-phase methods. The calculation errors resulting from lumping the water and oil together have been found to be insignificant for the majority of oil well pressure calculations. The primary purpose of a flow correlation is to estimate the liquid holdup (and hence the flowing mixture density) and the frictional pressure gradient.

Some of the correlations most widely accepted for oil wells are:

- Duns and Ros
- Hagedorn and Brown
- Orkiszewski
- Beggs and Brill



## 3. Artificial Lift

---

### 3.1 Introduction

In Petroleum Engineering, artificial lift refers to the use of artificial means to increase the flow of liquids or reinitiate the flow from wells whose production has been seized. Mechanical means can be used to assist production such as pumps, or methods that change some physical properties of the produced reservoir fluid in the tubing (i.e. injection of gas at certain depth to decrease the weight of the hydrostatic column) and render possible the optimized production at the same reservoir pressure.

Oil reservoirs will eventually not be able to produce fluids at economical rates unless natural driving mechanisms (e.g., aquifer and/or gas cap) or pressure maintenance mechanisms (e.g., water flooding or gas injection) are present to maintain reservoir energy. Higher production rates can be obtained by lowering the bottomhole flowing pressure and increasing the pressure drawdown by means of artificial lift. Most oil wells require artificial lift at some point in the life of the field, and many gas wells benefit from artificial lift to take liquids off the formation so that gas can flow at a higher rate. Approximately 50% of the wells worldwide need artificial lift systems [12].

In this chapter, a brief discussion of the various types of artificial lift is made. An analytic description of continuous gas lift systems, the basic principles and a description of its main component is also given in **Section 3.4**.

### 3.2 Selection of an Artificial Lift System

To realize the maximum potential from developing any oil or gas field, the most economical artificial lift method must be selected. The methods historically used to select the lift method for a particular field vary broadly across the industry. The methods include [13].

- Operator experience
- What methods are available for installations in certain areas of the world
- What is working in adjoining or similar fields
- Determining what methods will lift at the desired rates and from the required depths
- Evaluating lists of advantages and disadvantages
- “Expert” systems to both eliminate and select systems
- Evaluation of initial costs, operating costs, production capabilities, etc. with the use of economics as a tool of selection, usually on a present-value basis

Each method has applications for which it is the optimum installation. Proper selection of an artificial lift method for a given production system (reservoir and fluid properties, wellbore configuration, and surface facility restraints) requires a thorough understanding of the system [12]. Artificial lift methods should be designed before completion in order to minimize additional costs due to future workovers and recompletions but this is often not the case.

### 3.3 Types of Artificial Lift

The major forms of artificial lift are sucker rod (beam) pumping, electrical submersible pumps (ESP), gas lift and jet hydraulic pumping systems. Also, plunger lift and progressive cavity pumps (PCP) are becoming more common. There are other methods, which are mentioned as appropriate, such as the electrical submersible progressive cavity pump (ESPCP) for pumping solids and viscous oils, in deviated wells. This system has a PCP with the motor and some other components similar to an ESP. Other methods include modifications of beam pump systems, various intermittent gas-lift methods, and various combination systems [14]. The most widely artificial lift methods are described in the next paragraphs.

#### 3.3.1 Sucker Rod Pump

The history of artificial lifting of oil wells began shortly after the birth of petroleum industry. At those times, cable tools were used to drill the wells, and this technology relied on a wooden walking beam which lifted and dropped the drilling bit hung on a cable. When the well ceased to flow, it was quite simple to use this walking beam to operate a bottomhole plunger pump. It became common practice to leave the cable-tool drilling rig on the well so that it could later be used for pumping. The sucker-rod pumping system was born, and its operational principles have not changed since today [15].

A sucker-rod pumping system consists of various components, the ones that operate at the surface and the ones that operate underground. Linked rods attached to an underground pump are connected to the surface unit. The linked rods are normally called sucker rods and are usually long steel rods, from 5/8 to more than 1 or 1 1/4 in. in diameter. The steel rods are normally screwed together in 25 or 30-ft lengths; however, rods could be welded into one piece that would become a continuous length from the surface to the downhole pump. The steel sucker rods typically fit inside the tubing and are stroked up and down by the surface-pumping unit. This activates the downhole, positive-displacement pump at the bottom of the well. Each time the rods and pumps are stroked, a volume of produced fluid is lifted through the sucker-rod tubing annulus and discharged at the surface [16].

When this type of system is used, it is usually called a beam-pump installation. The more-generic name of sucker-rod lift, or sucker-rod pumping, should be used to refer to all types of reciprocating rod-lift methods. A schematic description of the various components of a sucker rod pumping system is shown at the figure below (**Fig. 3.1**)

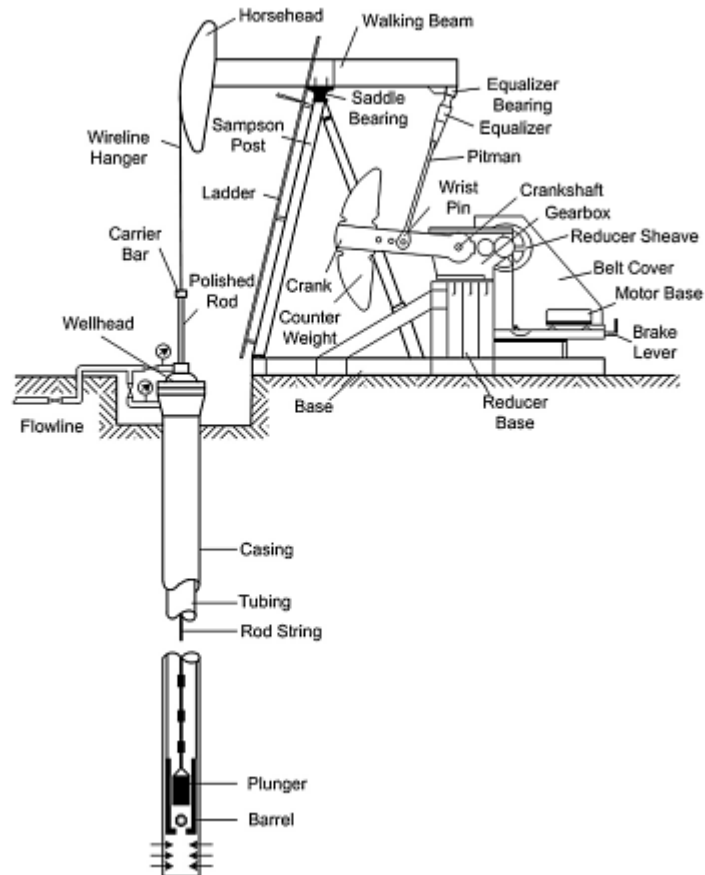


**Figure 3.1:** Schematic of a sucker rod pumping system [19]

### 3.3.2 Electric Submersible Pumps (ESP)

An electrical submersible pump (ESP) is a multistage centrifugal pump that offers a great deal of flexibility. ESP's are capable of producing very high volumes of fluid, unlike sucker rod pumps they can be used efficiently in deeper wells and are able to handle some free gas in the pumped fluid. The pump is driven by an electric motor connected by cables to a three-phase power source at the surface. The motor is situated so that the produced fluids flow around the motor, providing cooling, either by setting the pump above the producing interval, or by equipping the pump with a shroud that directs the fluids past the motor before entering the pump intake. Should the gas fractions be higher than

20% to 40%, a rotary gas separator may be included as part of the pump intake. In **Figure 3.2** a typical ESP installation is demonstrated.

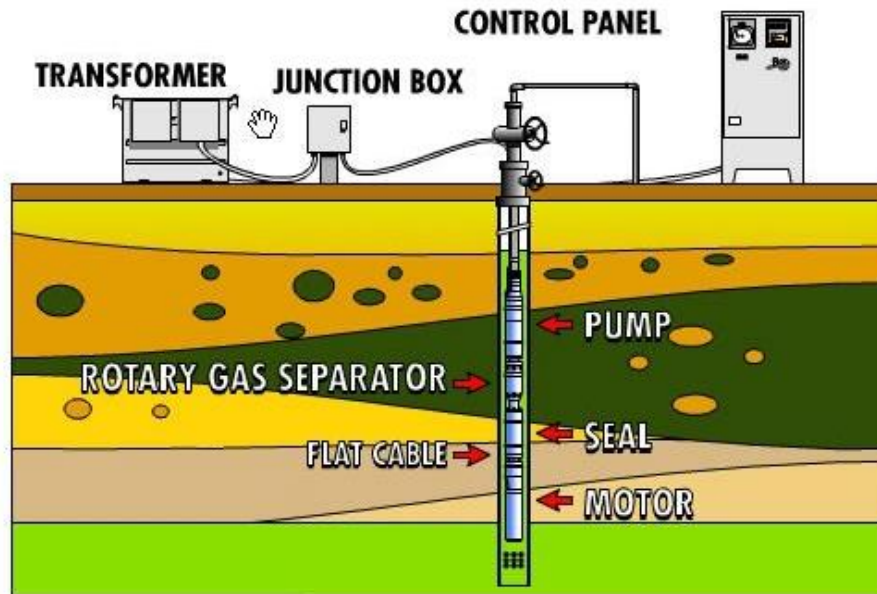


**Figure 3.2:** Typical oil well with an ESP installed

Centrifugal pumps do not displace a fixed amount of fluid, as do sucker-rod pumps, but rather create a relatively constant amount of pressure increase to the flow stream. The flow rate through the pump will thus vary, depending on the back pressure held on the system. The pressure increase provided by a centrifugal pump is usually expressed as pumping head, the height of the produced fluid that the  $\Delta p$  created by the pump can support [18].

$$h = \frac{\Delta P_{pump}}{0.433 \cdot \gamma_l} \quad \text{Eq. 2.1}$$

As mentioned above, the centrifugal pump unit employed in ESP's is a dynamic-displacement pump in which the pump rate depends on the pressure head generated; the pump rate is low when the pressure head is high and vice versa. This is different from the positive displacement pumps discussed earlier in which the pump rate and discharge pressure are independent to each other. The relationship between pump rate and pressure generated for dynamic displacement pumps is called the pump characteristic (**Fig. 3.3**). It is measured by the pump manufacturer in laboratory tests using a standard fluid (water) [5].

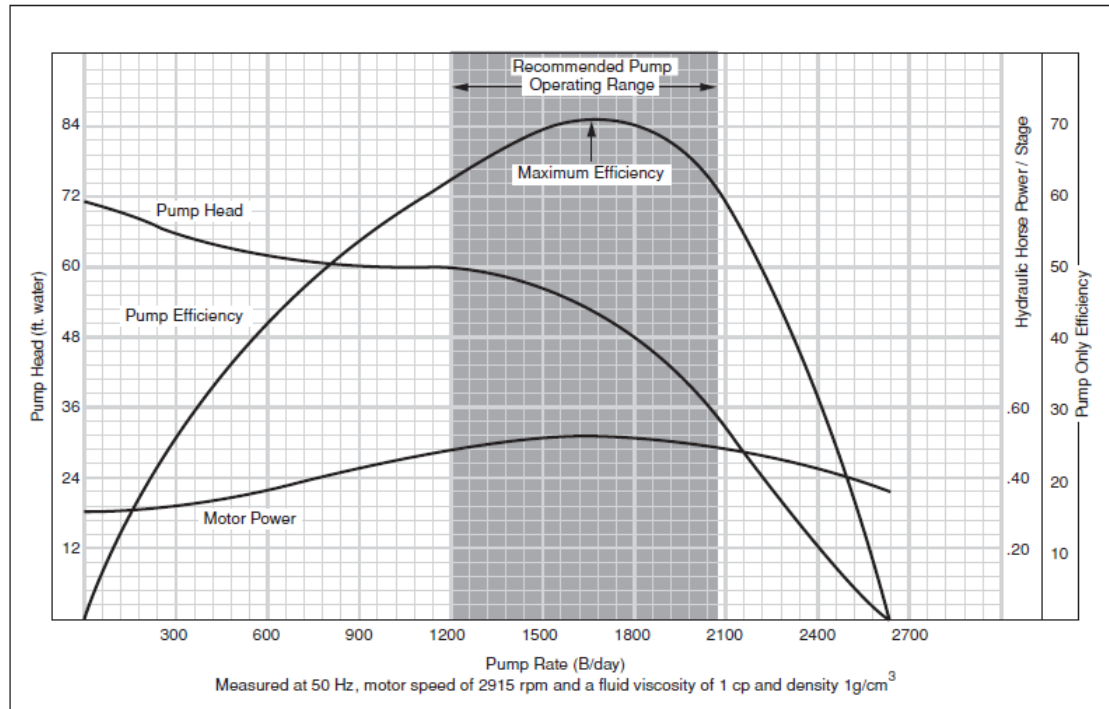


Figure 3.3: Pump characteristic chart (Courtesy of Heriot Watt University)

The pump characteristics given by the manufacturers must be corrected if the fluid being pumped has a higher viscosity. High fluid viscosity decreases the efficiency of a centrifugal pump and can affect the head developed.

### 3.3.3 Hydraulic Jet Pumps

The hydraulic jet pumps convert the energy from the injected power fluid (water or oil) to pressure that lifts production fluids. Because there are no moving parts involved, dirty and gassy fluids present no problem to the pump. The jet pumps can be set at any depth as long as the suction pressure is sufficient to prevent pump cavitation. The disadvantage of hydraulic jet pumps is their low efficiency (20–30%).

The working principle of a hydraulic jet pump can be seen in **Figure 3.4**. It is a dynamic-displacement pump which increases the pressure of the pumped fluid with a jet nozzle. The power fluid enters the top of the pump from an injection tubing. It is then accelerated through the nozzle and mixed with the produced fluid in the throat of the pump. As the fluids mix, the momentum of the power fluid is partially transferred to the produced fluid and increases its kinetic energy (velocity head) [18]. The power fluid consists of oil or production water (the large oil inventory in the surface power fluid system makes oil accounting difficult once high water cuts are being produced). The power fluid is supplied to the downhole equipment via a separate injection tubing.

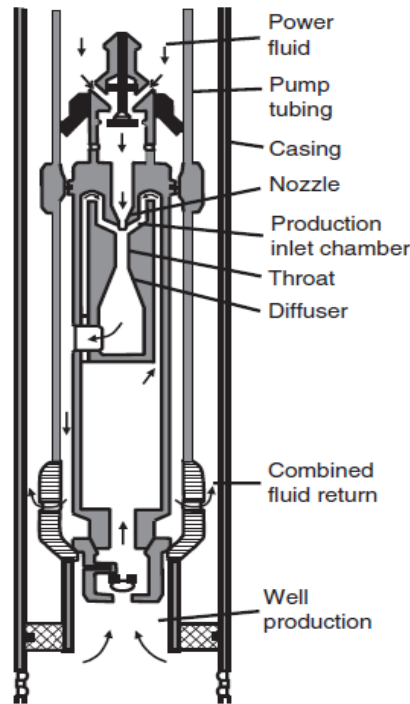


Figure 3.4: Sketch of a hydraulic pump installation [18]

Some of the kinetic energy of the mixed stream is converted to static pressure head in a carefully shaped diffuser section of expanding area. If the static pressure head is greater than the static column head in the annulus, the fluid mixture in the annulus is lifted to the surface [12].

### 3.3.4 Progressive Cavity Pumps (PCP)

The PCPs have been the most widely used pumping systems, since these pumps have demonstrated higher mechanical efficiency than rotodynamic pumping systems (ESP's) together with lower initial investment and energy consumption. Besides, the PCP can handle sand and greater quantities of gas than the Sucker-Rod pumping system [19].

The two key features that differentiate PCP systems from other forms of artificial lift are the downhole PC pumps and the associated surface drive systems. Although other major components, such as the production tubing and sucker rod strings, are found in other lift systems, the design and operational requirements typically differ for PCP applications. Also, many additional equipment components may be used in conjunction with PCP systems to contend with specific application conditions [20].

PCP is a screw pump with a single, helical rotor [21]. The downhole PC pump is a positive displacement pump that consists of two parts:

- Helical steel “rotor”
- “Stator” comprised of a steel tubular housing with a bonded elastomeric sleeve formed with a multiple internal helix matched suitably to the rotor configuration

The stator is typically run into the well on the bottom of the production tubing, while the rotor is connected to the bottom of the sucker rod string. Rotation of the rod string by means of a surface drive system causes the rotor to spin within the fixed stator, creating the pumping action necessary to produce fluids to surface [22]. Its low (300 to 600 rev/min) operating speed enables the pump to maintain long periods of downhole operation if not subjected to chemical attack or excessive wear or it is not installed at depths greater than approximately 4,000 to 6,000 ft. The pump has only one moving part downhole with no valves to stick, clog, or wear out. The pump will not gas lock, can easily handle sandy and abrasive formation fluids, and is not normally plugged by paraffin, gypsum, or scale [14]. PCP’s are highly energy efficient (55% to 75%), can easily handle sand production high amounts of free gas. They do not require costly maintenance and are relatively simple in installing and operating. On the other hand, limited production rates or limited lift capability along with their incompatibility when horizontal or deviated wells are present, dictates the need for more appropriate alternatives. Generally, if configured and operated properly in appropriate applications, PCP systems currently provide a highly efficient and economical means of artificial lift.

## **3.4 Gas Lift**

### **3.4.1 Historical Development**

The actual removal of liquids by means of gas lift goes back to the 18<sup>th</sup> century. The lifting medium then was air and the application was to remove water from flooded mine shafts. The technique was first applied to the lifting of oil in Pennsylvania oil fields around 1865. The 'law-lift' reached the Texas-Louisiana Gulf Coast oil fields about 1900, where it began to receive intensive application. California began to utilize the method about 10 years later and gas rather than air as the lifting medium made its appearance shortly thereafter [23]. Natural gas proved more satisfactory than air because it was safer, it did not have the corrosive effects of air, and it was often available in quantity and under pressure.

### 3.4.2 Overview of a Gas Lift System

Gas lift technology increases oil production rate by injection of compressed gas in to the lower section of the tubing through the casing- tubing annulus. Upon entering the tubing, the compressed gas improves liquid flow in two ways: **(a)** the energy of expansion pushes the oil to the surface and **(b)** the gas aerates the oil so that the effective density of the fluid is less, while the bottomhole pressure is reduced which leads to a greater pressure differential within the reservoir to attain a desired flow rate. Well depth is not a limitation. It is also applicable to offshore operations. Lifting costs for a large number of wells are generally very low. Gas-lift is used only in wells that produce economically with relative high bottomhole pressures, typically high productivity reservoirs. It is also preferable when the well has a multi-inclination trajectory, in which installation and operation of bottomhole pump are mechanically difficult. There are two types of gas lift: Intermittent gas lift and continuous gas lift. In the present Master's Thesis, the use of the term "Gas Lift" suggests continuous gas lift systems.

### 3.4.3 Elements of Mechanical Efficiency

The three main elements consuming energy during the flow of a fluid are:

- the weight of oil and the distance lifted,
- the weight of the gas itself and distance lifted,
- the frictional resistance of the upward moving column of oil and gas, and
- the slippage (see **paragraph 2.5.3**) of the oil in the upward flowing gas.

The first represents the useful work to be done, and, of course, is irreducible; therefore efforts to increase mechanical efficiency must primarily be directed to decreasing friction and slippage.

Friction increases with velocity according to well-known laws, but in the gas lift it is difficult to determine a friction constant for a well, and as there is an acceleration of velocity from the bottom to the top of the tubing, the computation of the total friction is a complex problem.

### 3.4.4 Continuous Gas Lift

A continuous gas lift operation can be considered as a steady-state flow of the aerated fluid from the near bottom of the well to the surface. It is usually applied on wells with high productivity indices (PI) (see **paragraph 2.3.1**). Because of the abundance of gas and low operating cost, the gas-lift is one of the major artificial lift systems used extensively around the world. The principle underlying the continuous flow gas lift method is that energy resulting from expansion of

gas from a high pressure to a lower pressure as well as the reduction of fluid column gravity is utilized in promoting the flow of well fluids which otherwise would not have been able to be produced in efficient rates.

It is generally intended that, during continuous flow gas lift, only one valve (usually an orifice) will be delivering gas to the production tubing and that valve will be as deep as the available gas pressure will permit. A typical configuration of a continuous gas lift system is illustrated in **Fig. 3.5**.

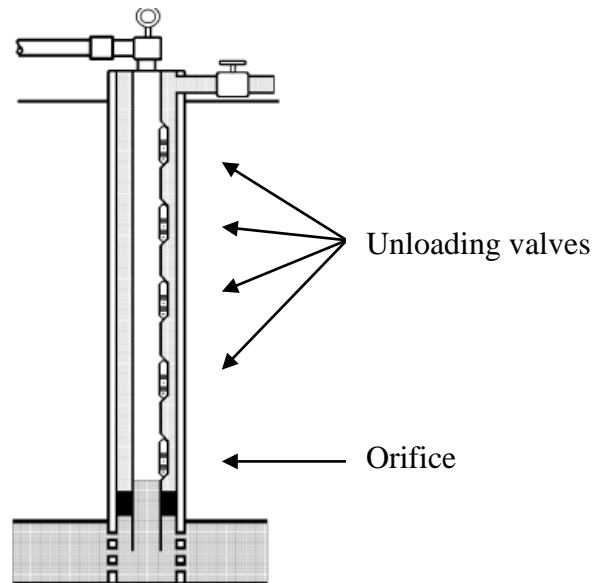


**Figure 3.5:** Side pocket mandrels placed in the production tubing [24]

It should be pointed out that, apart from the operating valve, additional valves are set along the tubing in predefined positions, according to the completion design. At these positions Side Pocket Mandrels (SPM), which will be examined in the next chapter, are installed.

#### 3.4.4.1 Unloading process

As stated previously, more than one valves lie in the production tubing. The purpose of their use is crucial when gas lifted production is to be initiated. Generally, the gas compressor cannot provide the desired pressure with the available gas down to the designed depth of gas injection because the static pressure of the fluid in that depth is greater than the pressure of the injected gas, hence a sequence of unloading valves should be placed. The positioning of the gas lift valves and their number is a matter of wellbore hydraulics optimization [18]. In most cases, the operating valve is not the deepest one, as more valves can be placed and used in latter stages of the reservoir's life when low pressures and high water cut levels may be encountered.

The static and flowing pressure conditions during the unloading process are described analytically below.

Initially, all valves are open and the pressure gradient in the tubing is that of the static fluid column ( $G_s$ ) (**Fig. 3.6**). By the time the injected gas reaches the top valve, gas is entering into the tubing and bubble flow is observed. Fluids above the valve flow to the wellhead as production is assisted by the expansion of gas while it travels upwards. This partial evacuation reduces the fluid density in the tubing above the top gas lift valve and ensures further casing fluid to be unloaded through the rest of the valves. A flow of liquids may occur bottomhole back to the reservoir if no check valve is installed. Meanwhile, a pressure drawdown is being generated at the reservoir level and the flow of formation fluid from the reservoir into the wellbore is induced i.e. the well is starting to produce. As the gas continues to occupy more space in the annulus, it reaches the second valve. The pressure gradient in the tubing is further decreased and increased liquid rate is observed at the surface. When casing pressure operated valves are used, a slight reduction in the casing pressure causes the top valve to close. On the other hand with, with fluid operated and proportional response valves, a reduction in the tubing pressure at valve depth causes the top valve to close. The pressure drawdown becomes continuously higher. Finally, the injected gas reaches the operating valve (orifice type valve) at the deepest point which remains always open, establishing a steady state flow.

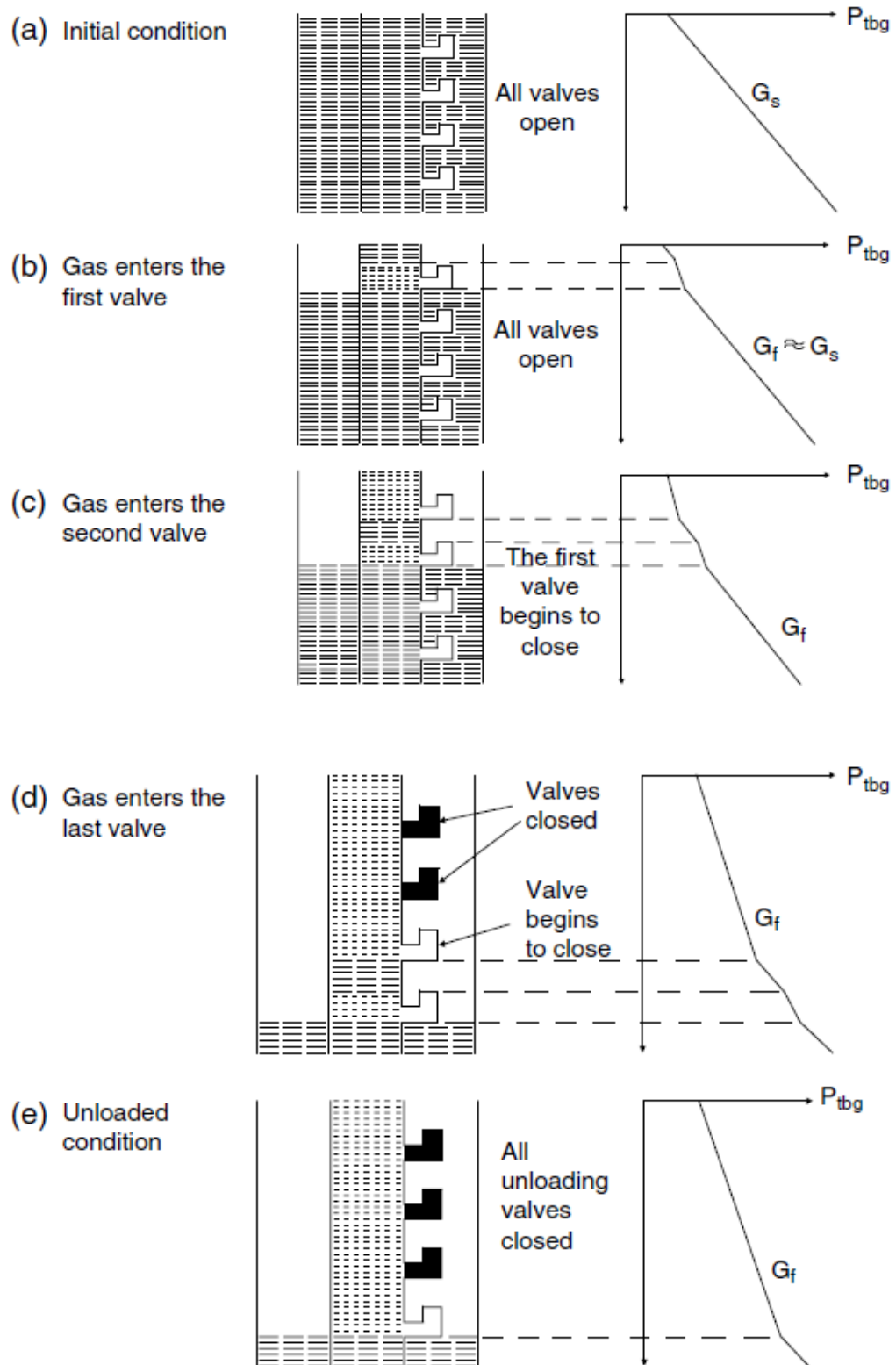


Figure 3.6: Well unloading sequence [12]

### 3.4.4.2 Gas Lift Equipment

The gas lift equipment can be divided into two categories: surface and downhole equipment. As far as the surface equipment is concerned, a gas compressor is indispensable in order to minimize space requirements and provide the desired injection pressure. A distribution manifold is also required. It consists of a control valve, gas meter, and distribution line to each well. Downhole gas lift equipment consists mainly of the gas lift valves and the mandrels in which the valves are placed.

#### Side Pocket Mandrels

The side pocket mandrels allow gas lift valves to be installed (and recovered) in a live well using wireline techniques. Side pocket mandrels are oval shaped accessories with an outside diameter slightly greater than that of the tubing (**Fig. 3.7**). This shape allows the gas lift valve to be installed in the pocket placed to one side of the tubing conduit while maintaining fullbore access throughout the complete tubing length [5]. They lie at predefined positions according the well design and can be reconfigured only after workovers. Most side pocket-type mandrels have a full-bore inside diameter (ID) equal to the tubing ID.

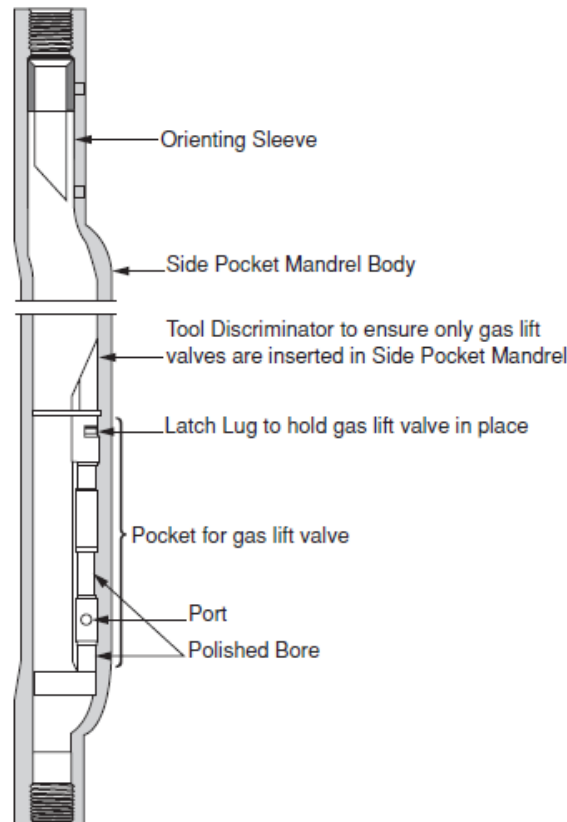


**Figure 3.7:** A Side Pocket Mandrel (Courtesy of Heriot Watt University)

### 3.4.4.3 Gas Lift Valves

The design of a valve spacing program for a continuous-flow gas in a well requires the calculation of several pressures (see **Section 5.4**). After their calculation and prior to installation, gas lift valve operating characteristics must be adjusted to support the unloading process. The main components of a gas lift valve (GLV) are indicated in **Figure 3.8**. GLV contain a dome which is charged with a high pressurized gas, usually nitrogen. The pressure of the gas forces the bellows to keep the valve closed. At the initiation of the unloading process, the injected gas reaches the unloading valve at a specific pressure. Since the pressure is known according to the design, the pressure of the dome is less than the casing pressure. In this case, the valve's stem tip lifts off the valve seat and the valve opens. The valve will close when gas is injected with a lower pressure and the gas gradient plus the injection pressure no longer overcomes the dome pressure. Since this pressure interval is crucial, the dome pressure must be adjusted accurately for the downhole operating conditions. The amount of uncertainty though, makes it imperative to apply a safety factor in the spacing of the valves.

There are two types of gas lift valves:

- Injection pressure or casing pressure operated valves and,
- Production pressure or fluid operated valves.

In this study, only the first category is considered.

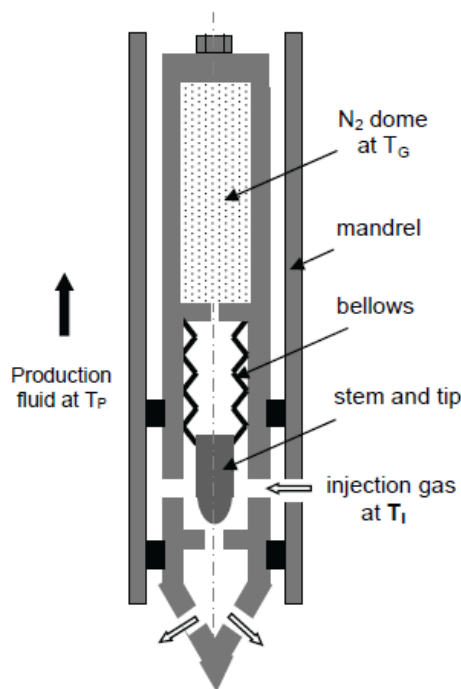


**Figure 3.8:** Schematic view of gas lift valve in a SPM

### 3.4.5 Intermittent Gas Lift

If a well has a low reservoir pressure or a very low producing rate, it can be produced by a special form of gas lift called intermittent flow. As its name implies, this system produces intermittently or irregularly and is designed to produce at the rate at which fluid enters the wellbore from the formation. In the intermittent flow system, fluid is allowed to accumulate and build up in the tubing at the bottom of the well. High pressure gas is injected into the liquid column on a cyclic or intermittent basis generating a gas bubble which expands pushing the liquid above it to the surface in a slug. The frequency of gas injection in intermittent lift is determined by the amount of time required for a liquid slug to enter the tubing. The length of gas injection period will depend upon the time required to push one slug of liquid to the surface. While it is normally associated with low volume producers, intermittent lift has successfully lifted wells at rates in excess of 500 barrels of liquid per day, although such a rate could probably have been lifted more efficiently with continuous flow. Wells with high productivity indices (PI) and low bottom hole pressure or wells with low PI's requiring low flowing bottomhole pressures are most suited to this type of lift [25].

#### **Plunger lift**

A type of intermittent gas lift is the plunger assisted lift. Plunger lift utilizes a free piston (plunger) cycling up and down inside the tubing (or casing) of a well. Generally, no packer is set in the well or an existing packer is breached to allow gas storage space in the casing-tubing annulus. When the gas pressure in this annulus space is sufficient, the flowline at the surface is opened and the plunger with its liquid slug load begins traveling up the tubing. As the plunger arrives at the surface, the liquid slug is produced into the flowline, the flowline is closed, and the plunger falls to the bottom of the well. While the well is shut in, and the plunger is falling, the pressure in the well is building up in order to re-cycle the plunger [26].

## 4. Model setup in PROSPER

---

### 4.1 About PROSPER

PROSPER is the industry standard single well performance design and optimization software. It can model most types of well completions and artificial lifting methods. Sensitivity analyses for a wide range of operating conditions can be held with the use of Nodal Analysis. PROSPER makes a model for each component of the producing well system separately which contributes to overall performance, and then allows to verify each model subsystem by performance matching. In this way, the program ensures that the calculation is as accurate as possible. All calculations in this MSc thesis have been done using PROSPER.

The process of setting up a reliable model with the available PVT, well and reservoir data is described in the chapter. PROSPER is used throughout this MSc thesis for all calculations regarding setting up of a reliable model and building on it a highly productive continuous gas lift system (see **Chapter 5**).

### 4.2 Input data

The developed model in this MSc thesis is based upon a fictitious onshore well named A-1, in the Alpha field. Due to the long life of the reservoir, its pressure has dropped to a very low level and as a result, production may cease in the upcoming months. Thus, it is necessary to install an artificial lift system in order to optimize production and prolong the well's lifespan. The available data is separated into various categories and will be presented in this chapter. Each data category will be modeled separately and subsequently all of them will be joint in a unified model. When this model is tuned to real field data, PROSPER can confidently predict the well's performance under various scenarios. In this MSc thesis, several scenarios based on various operating conditions will be carried out and a continuous gas lift system (see **Chapter 5**) will be designed. A detailed explanation of the role of each data category will be analyzed in **Section 4.3** along with the way it is introduced to the software.

#### 4.2.1 PVT data

The available PVT data is related to a direct flash (single stage separation) of the reservoir fluid from reservoir conditions down to standard conditions (**Table 4.1**). According to its API gravity, the oil can be categorized as volatile and relatively easy to flow in a pipeline. At the current reservoir conditions, it is monophasic, as the reservoir pressure is above bubble point.

**Table 4.1:** Fluid PVT properties

Property	Value	Units
$P_b@T_{res}$	2,241	psig
$R_g@P_b$	493	scf/stb
API gravity	38.7	API
$\gamma_g$	0.798	
$\rho@P_b$	694.45	kg/m <sup>3</sup>
$\mu@P_b$	0.41	cp
Water salinity	80,000	ppm

#### 4.2.2 Well data

The well path is a typical “build and hold” deviated one. The kick off point (KOP) is set at 1,000’ and the build angle rate is 3 degrees per 100’. The target inclination angle is 45 degrees and the target TVD is 11,500 ft. The well is a 2D one, i.e. no azimuth angle change is present. The wellbore diameter at the payzone depth is 8.5”.

The production casing diameter is 7” OD with a thickness of 0.3”. The tubing ID diameter is 4.052”. As no measurements of the pipelines roughness are available, the regular value of 0.0006” will be used. A subsurface safety valve (SSSV) with an internal diameter of 3.72” has been set at 800’. The production packers have been set at 11,000 TVD. The overall heat transfer coefficient is estimated at 8.2 BTU/hr/ft<sup>2</sup>/F.

#### 4.2.3 Reservoir data

A general description of the reservoir data is given in **Table 4.2**. The Dietz shape factor is calculated at 30.9, a value that corresponds to the shape of the drainage area which is approximately square and the well is placed in the center. The role of Dietz shape factor was discussed in detail in **Section 2.3**. The skin factor, from well tests conducted, is estimated to be 0.5.

**Table 4.2:** Basic Reservoir characteristics

Property	Value	Units
$P_r$	3,844	psig
k	100	mD
A (drainage area)	100	acres
h (thickness)	100	ft
S	0.5	Dimensionless
Dietz shape factor	30.9	Dimensionless

The reported temperature gradient is 1.6522 °F/100ft. Therefore, the reservoir temperature can be calculated by multiplying the temperature gradient multiplied by the true vertical depth (TVD) and adding the ambient temperature:

$$T_r = 60 \text{ } ^\circ F + 11500 \text{ ft} * 1.6522 \frac{^\circ F}{100 \text{ ft}} = 250 \text{ } ^\circ F \quad \text{Eq. 4.1}$$

#### 4.2.4 Gas lift data

A gas lift system has been installed in the well and the available gas lift gas gravity is 0.7 with negligible impurity levels. The gas is injected at a casing pressure of 1,900 psig. The pressure loss across the orifice is assumed to be equal to 100 psi. This data does not infer to the finally designed continuous gas lift system. The calculations and the final configuration of the designed gas lift system can be found in **Chapter 5**.

#### 4.2.5 Well test data

Two well tests have been carried out at the same operating conditions (same reservoir and wellhead pressure and same water cut level). The gauge pressure measurements have been taken at different depths for each case. The first test is conducted without any form of artificial lift, while the second test is carried out with a continuous gas lift system under operation. The gas lift system injects 1 MMscf/day of gas at 8,000'. The well test data is analytically described in **Table 4.3**.

Table 4.3: Well test data

Name	Tubing Head Pressure	Tubing Head Temperature	Liquid Rate	Gauge Depth (MD)	Gauge Pressure	Water Cut	Injection Depth (MD)	Gas Injection Rate
	(psig)	(°F)	(stb/day)	(ft)	(psig)	(%)	(ft)	(MMscf/day)
Test Point 1	264	124.8	5,045	14,800	3,382	20.3	-	-
Test Point 2	264	124.8	1,100	1,500	500	20.3	8,000	1

It is obvious that one of the two tests cannot be taken into account due to erroneous output data. Indeed, although both well tests have been held at the same reservoir conditions, the flow rates differ significantly. The flow rate from Test 1 was found to be 5,045 stb/day, while that from Test 2 is 1,100 stb/day, despite the presence of a gas lift system which has been installed to increase oil production. A quality check on the well test data needs to be done in order to decide which set of data needs to be discarded (See VLP/IPR matching section in this chapter).

### 4.3 Setting up the model in PROSPER

As mentioned at the beginning of **Chapter 4**, the main objective is to generate a mathematical model, tuned against real field data that can describe as accurately as possible the well's behavior under various future production scenarios. Each category of data will be modeled separately and the developed sub-models will be joined to develop a complete model capable of predicting both the inflow and outflow performance of the well.

The general workflow starts with the introduction of the basic information about the examined well in the summary section. After that, PVT data is entered and the appropriate fluid PVT property correlations are selected. The system is described in terms of downhole and surface equipment and trajectory of the well. As the temperature plays an important role to pressure drop calculations, the geothermal gradient (i.e. rate of increasing temperature of the surrounding formation with respect to increasing depth) and average heat capacities (ratio of the amount of heat energy transferred to oil, water or gas over the resulting increase in their temperature) are also take into consideration. The way they are involved in temperature and pressure calculations is discussed in **paragraph 4.3.1**. In the IPR section, the available data on reservoir properties is used to generate the IPR curve for the current reservoir pressure. Then, a quality control of the well test data is run in the VLP section to discard unrealistic

measurements. Subsequently, the correlation that best describes the multiphase flow in the tubing is matched against the measured data. After completing all the above tasks, nodal analysis (see **Section 2.2**) and investigation of future production scenarios is possible.

### 4.3.1 Options summary

In this section, the main characteristics of the well are entered (**Fig. 4.1**). Recall that it is a single branch producing well, with a cased hole, no sand control, while production fluids travel through the production tubing. As a continuous gas lift system is about to be designed, the appropriate selection at the artificial lift option is made as seen below. The options selected are the following:

- Fluid: Oil and Water
- Method: Black Oil
- Separator: Single-Stage Separator
- Emulsions: No
- PVT Warnings: Disable Warning
- Water Viscosity: Use default correlation
- Viscosity Model: Newtonian Fluid
- Flow Type: Tubing Flow
- Well Type: Producer
- Artificial Lift Method: Gas Lift (Continuous)
- Type: Friction Loss in Annulus
- Predict: Pressure and Temperature (on land)
- Temperature Model: Rough Approximation
- Range: Full System
- Well Completion: Cased hole
- Sand Control: None
- Inflow Type: Single Branch
- Gas Coning: No

Done	Cancel	Report	Export	Help	Datestamp
Fluid Description			Calculation Type		
Fluid	Oil and Water		Predict	Pressure and Temperature (on land)	
Method	Black Oil		Model	Rough Approximation	
Separator	Single-Stage Separator		Range	Full System	
Emulsions	No				
PVT Warnings	Disable Warning				
Water Viscosity	Use Default Correlation				
Viscosity Model	Newtonian Fluid				
Well			Well Completion		
Flow Type	Tubing Flow		Type	Cased Hole	
Well Type	Producer		Sand Control	None	
Artificial Lift			Reservoir		
Method	Gas Lift (Continuous)		Inflow Type	Single Branch	
Type	Friction Loss In Annulus		Gas Coning	No	
User information			Comments (Cntl-Enter for new line)		
Company	TUC				
Field	Alpha				
Location	Greece				
Well	A-1				
Platform					
Analyst	Tetoros Ioannis				
Date	Τετάρτη , 2 Σεπτεμβρίου 2015				

Figure 4.1: Options summary in PROSPER

### Comments on selected options

The options are set so that **emulsions** (droplets of one liquid in another immiscible liquid) and **hydrates** (ice-like solids that form when free water and natural gas combine at high pressure and low temperature) are not taken into consideration. The reason is that they are mainly a matter of concern in surface facilities (pipelines, manifolds, separators etc.) not the wellbore. Gas hydrates cause major and potentially hazardous flow assurance problems in offshore operations. Transfer lines from the wellhead to the production platform where low seabed temperatures and high operation pressures increase the risk of blockage due to gas hydrate formation. As far as the emulsions are concerned, they lead to operational problems at the separating stage of oil and water and can severely affect pumps. Since this is not the case under study, as the design of a continuous gas lift system is about to take place, calculations based on emulsions and hydrates will be omitted.

As far as the **rheology** of the fluids travelling through the wellbore is concerned, all phases are treated as Newtonian ones as it is usually the case when modelling fluid flow in pipelines. It should be noted that the rheological behavior of the fluids is related to the prevailing pressure loss along the tubing.

To predict **water viscosity**, the default correlation implemented in PROSPER is used. All water viscosity models available in PROSPER are based on the original work of [27]. Note that water viscosity at reservoir conditions is low almost always less than 1 cp. Although a pressure corrected correlation is also available in Prosper, it is not worth utilizing as water viscosity does not greatly vary with pressure. This is due to the small amount of gas dissolved in the water and its minor effect on viscosity.

For the **temperature calculations**, the Rough Approximation model is selected. It calculates the heat loss from the well to the surrounding formation with the use of a heat transfer coefficient, the temperature difference between the fluids and the formation and the average heat capacities. Note that the heat transfer coefficient is related to the easiness of heat transfer flowing from the hot flowing fluids to the surroundings whereas the heat capacity of the three phases determines the temperature reduction of the fluids due to the heat dissipation. The geothermal gradient entry screen is used to input formation temperatures at measured depth points. The formation temperature profile is then derived by interpolation between the input values. The importance of a temperature modeling of the wells lies on the fact that temperature changes affect pressure drop calculations. Generally, the (hot) reservoir fluids travel through the tubing towards the (cool) surface. Inevitably, a heat loss will occur along the way from the liquid to the formation. In general, the higher the production rate, the hotter the fluid will be at any given depth (since the increase in the (rate of) supply of energy (heat) is to the production increase while the heat losses from the wellbore by thermal conductivity are a only function of the temperature difference between the well and the surroundings i.e. independent of the production rate. This temperature change will affect the average fluid properties, which in turn will alter the pressure drop calculation (and hence the temperature change) [4]. The temperature model of “Rough Approximation” uses the following methodology [28].

**Figure 4.2** depicts the geothermal gradients  $G_1$  and  $G_2$  of a specific formation. Ambient temperature at any point can be easily calculated since the geothermal gradient is known:

$$T(x) = T_{a1} - G_2(x - L_1)\cos\theta$$

Where  $T(x)$ : ambient temperature at a segment depth  $x$ , °F

$T_{a1}$ : ambient temperature at  $L_1$ , °F

$G_2$ : Geothermal gradient, °F/ft

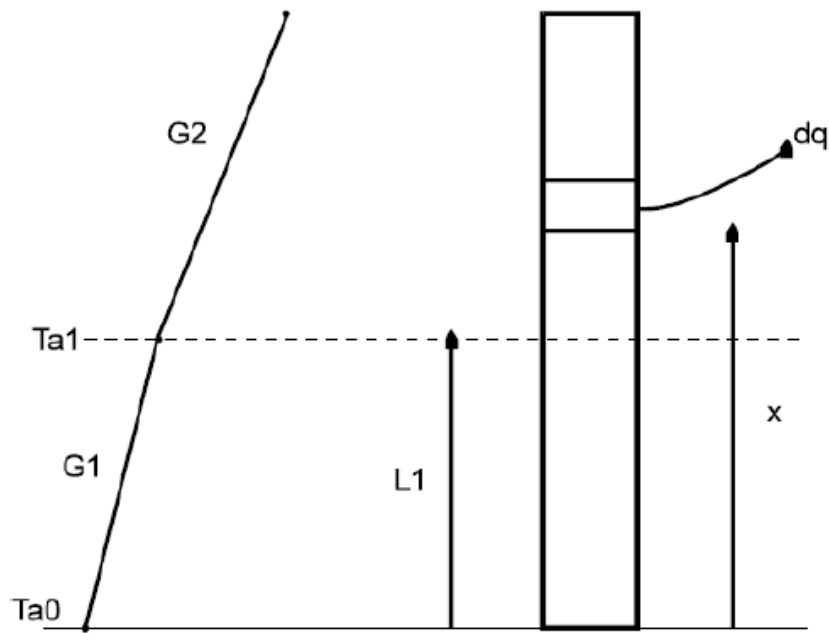


Figure 4.2: Simple schematic of temperature varying along the length of the well

As mentioned previously, the simplified description of all heat transfer mechanisms is captured by the overall heat transfer coefficient  $U$ . The heat transferred from the hot produced fluid to the surroundings instantly for a small segment of the pipe  $\Delta x$  is equal to:

$$Q_{transf} = UA(T(x) - T_{fluid,ave}) = U\pi D\Delta x(T_{sur} - T_{fluid,ave}) \quad \text{Eq.4.2}$$

where  $U$ : the heat transfer coefficient, BTU/h/ft<sup>2</sup>/°F

$T(x)$ : ambient temperature at a segment depth  $x$ , °F

$T_{fluid,ave}$ : The average temperature of the fluid in a segment depth  $x$ , °F

$D$ : the diameter of the pipe containing the fluid, ft

Once the heat transferred to the surroundings is known, it is assumed that the energy transferred is obtained from the heat generated when the fluid drops in temperature. This can be calculated by multiplying the average heat capacity of each phase by the mass flow rate of the phase and then by the temperature drop in the fluid.

$$Q_{obt} = (m_{oil}C_{p,oil} + m_{gas}C_{p,gas} + m_{water}C_{p,water})(T_{in} - T_{out}) = \dot{m}\bar{C}_p\Delta T \quad \text{Eq. 4.3}$$

Where  $C_{p,oil}$ : average heat capacity of oil, BTU/lb/°F

$C_{p,water}$ : average heat capacity of water, BTU/lb/°F

$C_{p,gas}$ : average heat capacity of gas, BTU/lb/°F

$T_{in}$  Temperature of the fluid before entering segment x, °F

$T_{out}$  : Temperature of the fluid after exiting segment x, °F

$\bar{C}_p$ =Weighted average specific heat capacity for all the phases, BTU/lb/°F

If **Eq. 3.1** and **Eq. 3.2** are equated, the heat transferred with the heat obtained from the drop in temperature a single equation is derived, which implies that the rate of change of temperature with depth is:

$$\frac{dT}{dx} = -\frac{U\pi D}{\dot{m}\bar{C}_p} [T_{fluid,ave} - T_{a1} + G_2(x - L_1)\cos\theta] \quad \text{Eq. 4.4}$$

For a complete temperature profile, PROSPER divides the well in numerous segments (i.e slices) and proceeds with the above mentioned calculations one segment after another from the reservoir up to the wellhead.

An enthalpy balance model to predict the temperature of the fluid as it travels up the well is also available in PROSPER. This is a very detailed model which takes into account the different heat transfer mechanisms which are present within the well; however, it requires a large amount of input data and also the time taken to complete calculations is increased. It should be used only when precision in the temperature prediction is required i.e. flow assurance calculations (hydrate formation in subsea wells).

### 4.3.2 PVT Data Input

The surface PVT data given, such as Solution GOR (equal to  $R_s$  in this case because reservoir pressure is above  $P_b$ ), API gravity, gas gravity and water salinity are used as input as seen in **Figure 4.3**. This data provides a rough description of the thermodynamic behavior of the reservoir fluid. In fact, it is treated as a mixture of two component fluids, STO and STG while GOR denotes the contribution of each component to the reservoir fluid. This is why it is only a

rough description compared to a fully compositional model. No gas impurities were reported.

Figure 4.3: PVT Input data section

The next step is to match the available laboratory PVT measured data with the black oil correlations. A unique matching point is available (at  $P_b$ ). The properties at this point (GOR, oil viscosity) are also used as input. As density is not commonly used as a tuning point as opposed to the  $B_o$ , the  $B_o$  value at  $P_b$  will be computed as shown below:

$$\begin{aligned}
 FVF &= \frac{V_o^{RC}}{V_o^{SC}} = \frac{m^{RC}}{\rho_o^{RC}} = \frac{m_o^{SC} + m_g^{SC}}{\rho_o^{SC} \cdot V_o^{SC}} = \frac{\rho_o^{SC} V_o^{SC} + \rho_g^{SC} V_g^{SC}}{\rho_o^{RC} V_o^{SC}} = \frac{\rho_o^{SC} V_o^{SC} + \rho_g^{SC} GOR \cdot V_o^{SC}}{\rho_o^{RC} V_o^{SC}} \\
 &\Leftrightarrow \\
 &\Leftrightarrow B_o = \frac{\rho_o^{SC} + \rho_g^{SC} \cdot GOR}{\rho_o^{RC}} \quad \text{Eq. 4.5}
 \end{aligned}$$

The densities of gas and oil at standard conditions required at Eq. 4.5 are calculated from the following expressions.

$$\begin{aligned}
 API &= \frac{141.5}{SG_o} - 131.5 \Leftrightarrow SG_o = \frac{141.5}{API - 131.5} = 0.83 \\
 \rho_o^{SC} &= SG_o \cdot \rho_w^{SC} = 0.83 \cdot 999 \frac{kg}{m^3} = 829.17 \frac{kg}{m^3}
 \end{aligned}$$

$$\rho_g^{SC} = SG_g \cdot \rho_{air}^{SC} = 0.798 \cdot 1.2922 \frac{kg}{m^3} = 1.03 \frac{kg}{m^3}$$

$$GOR = 493 \frac{scf}{stb} = 87.81 \frac{m^3}{m^3}$$

The  $B_o$  at bubble point can now be derived from **Equation 4.5** since all parameters are known:

$$B_o = \frac{829.17 + 1.032 \cdot 87.81}{694.45} = 1.32 \text{ bbl/stb}$$

The reservoir temperature is already calculated previously (**paragraph 4.2.3**) and it is equal to 250 °F. All the above data are introduced in the PVT match data screen (**Fig. 4.4**)

Point	Pressure (psig)	Gas Oil Ratio (scf/STB)	Oil FVF (RB/STB)	Oil Viscosity (centipoise)
1	2241	493	1.32	0.41
2				
3				
4				
5				
6				
7				

**Figure 4.4:** PVT Match data screen

Many authors have developed black oil correlations to predict the  $P_b$ ,  $B_o$ , GOR,  $\mu_{oil}$  based on experimental data of various crude oil/natural gas mixtures. The input variables for these correlations can be surface data,  $P_b$  and  $T_{res}$ . PROSPER supports several built-in correlations for the calculations of the aforementioned properties. More specifically, for the calculation of  $P_b$ ,  $B_o$ , GOR the following correlations are implemented:

- Glaso's correlations
- Standing's correlations
- Lasater's correlations
- Vasquez and Beggs' correlations
- Petrosky et al correlations
- Al-Marhoun's correlations

For the calculation of  $\mu_{oil}$  the built-in correlations are the ones developed by:

- Beal et al
- Beggs et al
- Petrosky et al
- Egbogah et al
- Bergman and Sutton

After entering the full set of available data, the software calculates the PVT properties mentioned above and compares them to the experimental values which have been introduced in order for the software to proceed to the matching process. PROSPER performs a nonlinear regression which adjusts the correlations to best-fit the laboratory measured PVT data (Test point). The nonlinear regression technique applies a multiplier (Parameter 1) and a shift (Parameter 2) to the correlations. The standard deviation is also displayed, which represents the overall closeness of fit. The lower the standard deviation, the better the fit. The best overall model is the one that has Parameter 1 closest to unity and Parameter 2 close to 0.

The reported values of the following PVT properties are used as match variables (**Fig. 4.5**):

**P<sub>b</sub>**: Bubble point pressure.

**GOR**: Gas oil ratio versus pressure.

**Oil FVF**: Oil formation volume factor versus pressure.

**Oil viscosity**: Oil viscosity versus pressure.

As explained in **Chapter 2**, the main cause of pressure drop in the tubulars is the gravity and the corresponding hydrostatic term. The density of gas and liquid phase at various pressures and temperatures, as well as the knowledge of the proportion of the pipe occupied by liquid (holdup) (see **paragraph 2.5.3**) are closely related with the PVT data. Thus, a consistent PVT model is essential. Glaso's correlation for P<sub>b</sub>, oil FVF and solution GOR is selected while Beggs' correlation is selected to model the oil viscosity as the values of Parameters 1 and 2 lie closer to 1 and 0 respectively compared to any other correlation. PVT data at every any pressure and temperature can now be predicted with the adjusted black oil correlations.

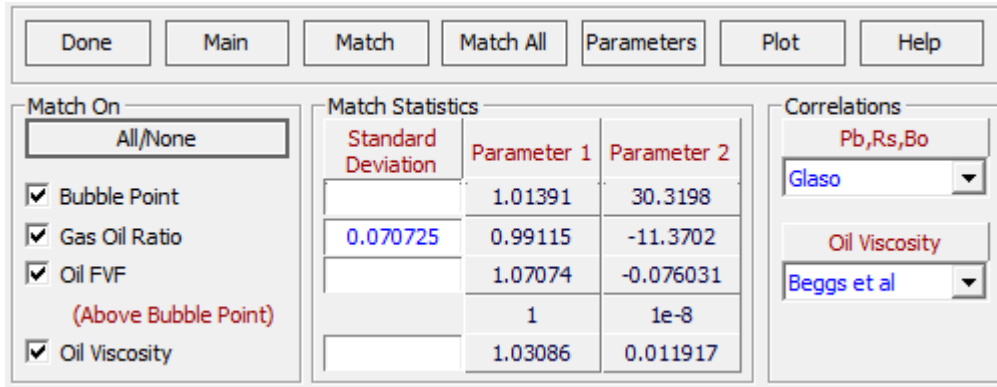


Figure 4.5: Correlation matching regression screen

An overview of the matching parameters for all black oil correlations is given in Figure 4.6.

	Done	Cancel	Main	Export	Report	Reset All	Help	Pb, Rs, Bo	Uo
								Glaso	Beggs et al
<b>Bubble Point</b>									
	Glaso	Standing	Lasater	Vazquez-Beggs	Petrosky et al	Al-Marhoun			
Parameter 1	1.01391	1.04638	1.16985	0.95336	0.99061	0.98053			
Parameter 2	30.3198	95.0523	283.523	-115.332	-21.4443	-45.4022			
Std Deviation									
	Reset	Reset	Reset	Reset	Reset	Reset			
<b>Solution GOR</b>									
	Glaso	Standing	Lasater	Vazquez-Beggs	Petrosky et al	Al-Marhoun			
Parameter 1	0.99115	0.91161	0.76333	1.12748	1.3987	1.05894			
Parameter 2	-11.3702	-6.24889	-0.15231	-2.02712	-182.715	-0.94316			
Std Deviation	0.070725				0.70725	0.070799			
	Reset	Reset	Reset	Reset	Reset	Reset			
<b>Oil FVF</b>									
	Glaso	Standing	Lasater	Vazquez-Beggs	Petrosky et al	Al-Marhoun			
Parameter 1	1.07074	0.9229	0.92296	0.9111	0.94192	0.89837			
Parameter 2	-0.076031	0.075615	0.07554	0.087593	0.043969	0.094896			
Parameter 3	1	1	1	1	1	1			
Parameter 4	1e-8	1e-8	1e-8	1e-8	1e-8	1e-8			
Std Deviation									
	Reset	Reset	Reset	Reset	Reset	Reset			
<b>Oil Viscosity</b>									
	Beal et al	Beggs et al	Petrosky et al	Egbogah et al	Bergman-Sutton				
Parameter 1	1.13339	1.03086	0.96039	0.63209	1.35946				
Parameter 2	0.043177	0.011917	-0.017637	-0.56802	0.085757				
Std Deviation				0.000789					
	Reset	Reset	Reset	Reset	Reset				

Figure 4.6: Matching parameters 1 and 2 for all black oil correlations

### 4.3.3 Equipment Data Input

In this section of PROSPER, a detailed description of the well's trajectory, surface and downhole equipment, geothermal gradient and average heat capacities is given (Fig. 4.7)

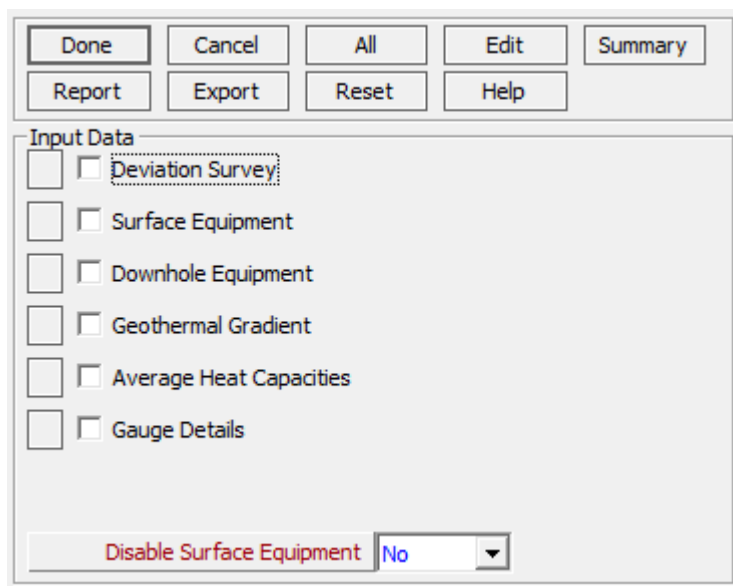


Figure 4.7: Equipment data input main screen

### 4.3.3.1 Deviation Survey

As stated in the introduction of the available data in **paragraph 4.2.2**, the well is a typical “build and hold” one. That means that, it is vertical down to a certain point. Below this point, an inclination angle is built with a constant angle step. Once the required maximum inclination angle is reached, the well reaches the target depth by keeping this angle constant. In order for the software to recreate the deviation survey it requires pairs of measured depth Measured Depth (MD) and True Vertical Depth (TVD). MD is the total length of the well (from the point of interest up to first point of the well at the surface) while TVD is the vertical distance of the point of interest up to the surface. PROSPER uses a linear interpolation scheme between two consecutive MD points in order to draw the trajectory of the well. For each straight line section of the well, two data points are sufficient. In the present case, for the part of the well where the inclination angle is being built, as many data points as possible were introduced, to capture the curvature of the well as accurately as possible. In the final segment of the well, since a straight line is implemented, again very few pairs of depths were given. Given this data, the software calculates the inclination angle at each depth and the cumulative horizontal displacement. The analytical method of calculating the pairs of depths to describe the well path is given in **APPENDIX A-1**. In **Figures 4.8** and **4.9** the description of the well and the profile of the well are illustrated respectively:

A consistent deviation survey is necessary to obtain accurate calculations in the VLP section. The concept of pressure losses along the production pipeline was discussed in **Chapter 2**. TVD of the well is essential for the calculation of the pressure drop due to gravity (or vertical elevation) since it only depends on the change in elevation and the density of the fluid. On the other hand, the very

sensitive issue of pressure loss due to friction and the generation of the corresponding temperature profile are intimately related to accurate values of MD. All equipment placed in the production tubing is always described in terms of MD.

Point	Measured Depth (feet)	True Vertical Depth (feet)	Cumulative Displacement (feet)	Angle (degrees)
1	0	0	0	0
2	1000	1000	0	0
3	1100	1099.9	4.47102	2.56256
4	1300	1298	31.9736	7.90394
5	1500	1494	71.7731	11.4783
6	1800	1776.5	172.737	19.6666
7	2000	1954.5	263.929	27.1267
8	2200	2122.2	372.91	33.0179
9	2400	2277	499.547	39.2855
10	2500	2348	569.967	44.7651
11	2715	2500	722.023	45.0105
12	4836	4000	2221.57	44.9913
13	6250	5000	3221.27	44.9913
14	9079	7000	5222.08	45.0116
15	11907	9000	7221.47	44.9913
16	15443	11500	9722.13	45.0075
17				

**Figure 4.8:** Well's trajectory description

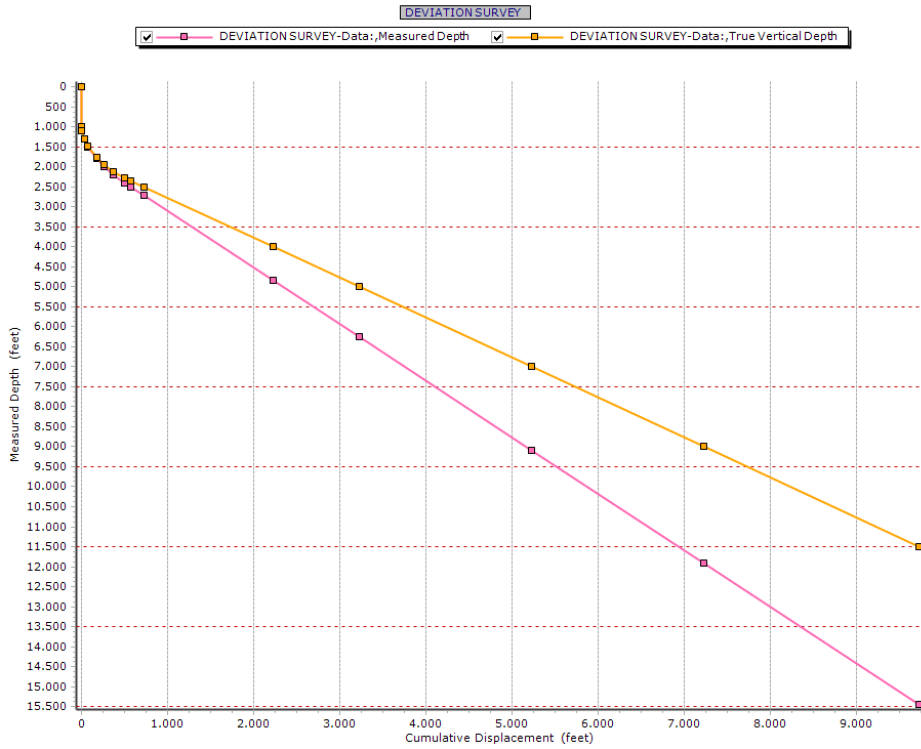


Figure 4.9: Profile of the well. On the x axis is the cumulative displacement while on the y axis is the measured depth

### 4.3.3.2 Surface Equipment

As the wellhead pressure was provided in the well tests, it was decided, for the Nodal analysis calculations, the set top node at the wellhead. For this reason, the manifold TVD was set at 0' TVD. The only values set in this form are the ambient temperature at 60 °F and the overall heat transfer coefficient at 8.2 BTU/h/ft<sup>2</sup>/°F (Fig. 4.10).

Point	Label	Type	Pipe Length (feet)	True Vertical Depth (feet)	Pipe Inside Diameter (inches)	Pipe Inside Roughness (inches)	Rate Multiplier
1		Manifold		0			
2							
3							
4							
5							
6							
7							
8							
9							
10							

Figure 4.10: Surface Equipment data input screen

#### 4.3.3.3 Downhole equipment

Similarly to the deviation survey, the description of the well's equipment is necessary to calculate the VLP of the well and the pressure and temperature gradients. As already discussed, the calculations performed by the "Rough Approximation" model depends on the tubing ID. Tubing's ID and inside roughness are also used to estimate frictional pressure losses during production. Introduction of casing data is also of great importance, mainly in the gas lift design section which will be discussed in **Chapter 5**.

The Downhole Equipment screen (**Fig. 4.11**) enables the downhole completion data to be entered. The production packers are set at 11,000' TVD. The MD at this point is 14,734'. The production tubing ends a few feet deeper at 14,900'. The production casing runs from the surface and reaches bottomhole at 15,443' MD.

Input Data										
Point	Label	Type	Measured Depth (feet)	Tubing Inside Diameter (inches)	Tubing Inside Roughness (inches)	Tubing Outside Diameter (inches)	Tubing Outside Roughness (inches)	Casing Inside Diameter (inches)	Casing Inside Roughness (inches)	Rate Multiplier
1		Xmas Tree	0							
2		Tubing	800	4.052	0.0006	4.5	0.0006	6.4	0.0006	1
3		SSSV		3.72						1
4		Tubing	14900	4.052	0.0006	4.5	0.0006	6.4	0.0006	1
5		Casing	15443					6.4	0.0006	1
6										
7										
8										
9										
10										
11										
12										
13										
14										
15										
16										
17										

Figure 4.11: Downhole Equipment data input screen

A schematic representation of the downhole equipment, as obtained by PROSPER, is presented below (Fig. 4.12):

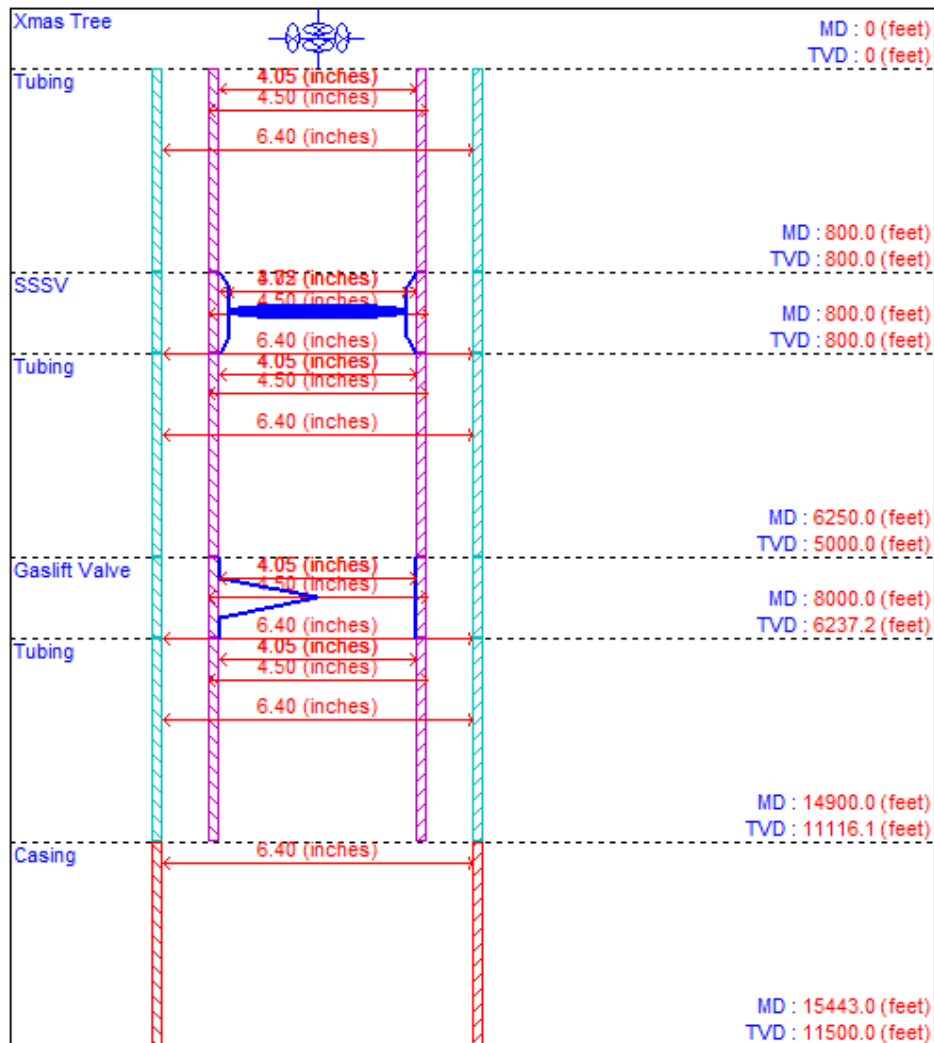


Figure 4.12: Simple schematic of the downhole equipment

### Comments on the selected options

The rate multiplier at the right hand side of the screen in **Figure 4.11** is related to the calculation of pressure losses due to friction in dual completion wells. Due to the fact that the well is a single branch one, the value of this variable was set to its default value of 1.

#### 4.3.3.4 Geothermal gradient

The formation temperature at any depth can be computed by PROSPER by the means of the geothermal gradient. A rough approximation of the temperature profile can be achieved by introducing the known values of temperature at the surface and at the reservoir. The depth where each temperature is measured can be introduced as a measured depth or a true vertical one. PROSPER then interpolates linearly all points given by the user and models the temperature distribution of the formation in the various depths. Because of the linear

interpolation, at least two data points must be introduced. The geothermal gradient and overall heat transfer coefficient are also introduced in this section and take part in the produced fluids' temperature prediction calculations, as explained in the former paragraphs of this chapter.

Point	Formation TVD (feet)	Formation Measured Depth (feet)	Formation Temperature (deg F)
1	0	0	60
2	11500	15443	250
3			
4			

Figure 4.13: Geothermal Gradient data input screen

#### 4.3.3.5 Average heat capacities

The average heat capacities of water, oil and gas are used in the “Rough Approximation” temperature model to calculate the dissipated heat when the fluid changes temperature. A good approximation can be given by using the default values of  $C_p$  of oil, water and gas (For more information, see **Section 4.3**). However, it should be noted that,  $C_p$  for oil and gas is not a constant value since their composition changes and thus their properties change along depth (**Fig. 4.14**).

Parameter	Value	Units
Cp Oil	0.53	BTU/lb/F
Cp Gas	0.51	BTU/lb/F
Cp Water	1	BTU/lb/F

Figure 4.14: Average heat capacities data input screen

### 4.3.4 IPR Data Input

This section defines the Reservoir Inflow Performance curve. Calculating an IPR curve results in a relationship between the bottomhole pressure and the flow rate passing in the well. In this case the “Darcy” model is used. The software uses the Darcy’s equation above the bubble point and the Vogel’s model below the bubble point. The Vogel’s model applies by the time when the flowing pressure at the bottom node ( $P_{wf}$ ) becomes equal to the bubble point and hydrocarbon two phase flow takes place. The IPR curve derivation and its role on Nodal analysis were well-discussed in **Chapter 2**. The main screen of the IPR section is given in **Figures 4.15** and **4.16**.

The screenshot shows the IPR data input main screen (1). It is divided into two main sections: Reservoir Data and Model Data.

**Reservoir Data:**

Reservoir Pressure	3844
Reservoir Temperature	250
Water Cut	20.3
Total GOR	493
Compaction Permeability Model	No
Relative Permeability	No

**Model Data:**

Reservoir Model: Mech-Geom Skin | Dev-PP Skin | Sand Control | Rel Perms | Viscosity | Compaction

Darcy Reservoir Model

Reservoir Permeability	100	md
Reservoir Thickness	100	feet
Drainage Area	100	acres
Dietz Shape Factor	30.9972	
Wellbore Radius	2.9	feet

Buttons: Calculate Dietz

Figure 4.15: IPR data input main screen (1)

The screenshot shows the IPR data input screen (2). It is divided into two main sections: Reservoir Data and Model Data.

**Reservoir Data:**

Reservoir Pressure	3844
Reservoir Temperature	250
Water Cut	20.3
Total GOR	493
Compaction Permeability Model	No
Relative Permeability	No

**Model Data:**

Reservoir Model: Mech-Geom Skin | Dev-PP Skin | Sand Control | Rel Perms | Viscosity | Compaction

Enter Skin By Hand Mechanical Skin Model

Mechanical Skin	0.5
Enable Wong Clifford Model	No

Figure 4.16: IPR data input screen (2)

### 4.3.5 Gas lift data input

One of the well tests was carried out in the presence of a gas lift system. It was reported that the injection point was at 8,000'. It is a fixed point of injection. Gas lift gas gravity and impurity levels are also used as input (**Fig. 4.17**). More information on Gas lift systems can be found in **Section 3.4**. Note that, all these information is necessary for the VLP matching process, as the multiphase flow correlations should be adapted to the presence of a gas lift system (see next paragraph). However, this section should not be confused with the final gas lift design as it shall be used only for the VLP matching section.

Input Data			Gaslift Details		
GasLift Gas Gravity	0.7	sp. gravity	Gaslift Valve Depth (Measured)	8000	feet
Mole Percent H2S	0	percent	Orifice Diameter	32	64ths inch
Mole Percent CO2	0	percent	Thornhill-Craver DeRating Value	100	percent
Mole Percent N2	0	percent			
GLR Injected	0	scf/STB			
Injected Gas Rate	1	MMscf/day			
GLR/ Rate ?	<input type="checkbox"/> Use GLR Injected <input checked="" type="checkbox"/> Use Injected Gas Rate				
Gas Lift Method	<input checked="" type="checkbox"/> Fixed Depth of Injection <input type="checkbox"/> Optimum Depth of Injection <input type="checkbox"/> Valve Depths Specified				

**Figure 4.17:** Gas lift data input main screen

### 4.3.6 VLP/IPR match and quality check

Once the IPR and the gas lift data were given to the model, the essential quality check of the well test data could be carried out. The general procedure in this section implies, first of all, the introduction of the well test data to the main screen. Afterwards, the procedure of processing the data is done by following 4 steps in sequence. These steps are highlighted in red colour in **Figure 4.18**.

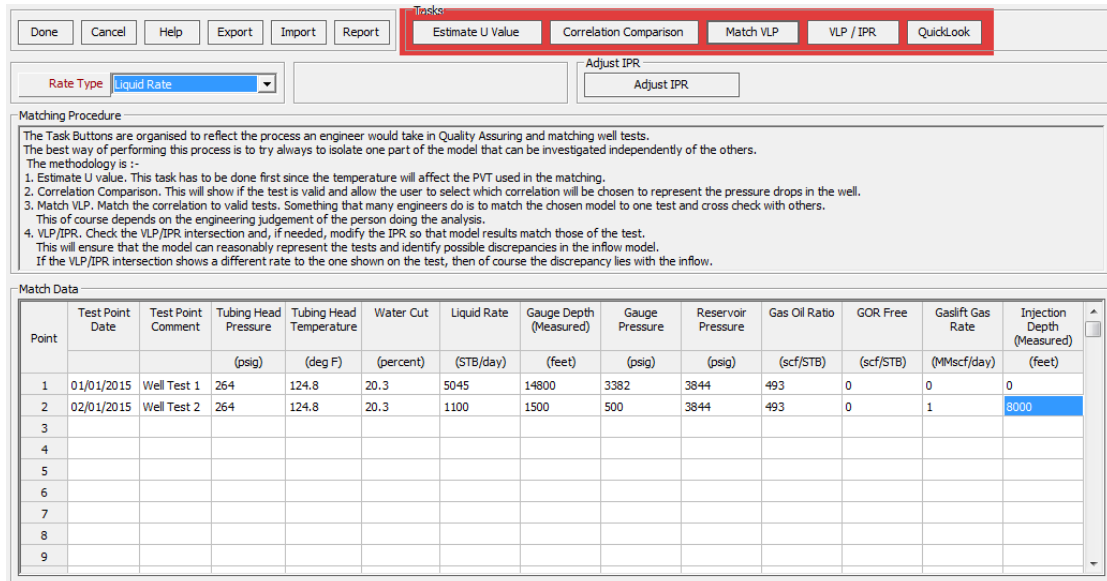


Figure 4.18: Match VLP/IPR section main screen

### 4.3.6.1 Well Test 1 Quality check

#### Estimate U-value

PROSPER estimates the overall heat transfer coefficient that matches the wellhead temperature of the well test. The calculations for temperature prediction along the wellbore can be more accurate with the revised U-value. The following screen appears (Fig. 4.19):

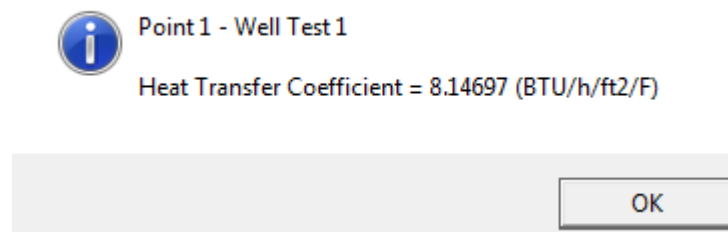


Figure 4.19: Estimated U-value for well test 1

The value is very close to the initial 8.2 BTU/h/ft<sup>2</sup>/F. value which was an initial estimation. The optimized value will replace the initial one in all successive calculations.

#### Correlation comparison

Prior to the selection of the most appropriate correlation to describe pressure drop in the tubing, a quality check of the well test data shall be made. According to PROSPER 9 manual [28], the quality check for a well test can be done in the

tubing correlation comparison section by plotting in a pressure versus depth diagram, the specific point which represents the well test and two pressure gradient curves based on correlations that present extreme cases of pressure drop. These two correlations create an envelope. The existence of the plotted well test point in this envelope indicates data consistency, while, on the other hand, revision of the provided data is essential, if it lies outside the envelope. The latter means that the measured data have no physical meaning since the correlations are modified to represent the worst and the best cases once the pressure losses in the system are considered. Like the PVT matching section, a valid test point is of great importance once the matching process takes place. If correlations are about to be matched with erroneous data, they can result to erroneous output in turn. The extreme correlations are **Duns and Ross modified** and **Fancher and Brown** which are described below. Related information on pressure drop calculations, slip effect and multiphase flow in pipelines have been thoroughly discussed in **Chapter 2**.

- **Fancher and Brown:** This is a no-slip correlation which means that the gas and liquid are assumed to be travelling at the same velocity. The no-slip conditions will predict the lowest possible hold-up and this will have the impact of calculating the lowest pressure drop which is physically possible.
- **Duns and Ross modified:** This correlation is modified by Petroleum Experts to over predict the pressure drop when the well is producing in the slug-flow regime.

**Figure 4.20** shows that well test 1 is clearly in the limits created by the two pressure gradient curves. Consequently, it is considered as consistent with the model data and can be used in the matching process

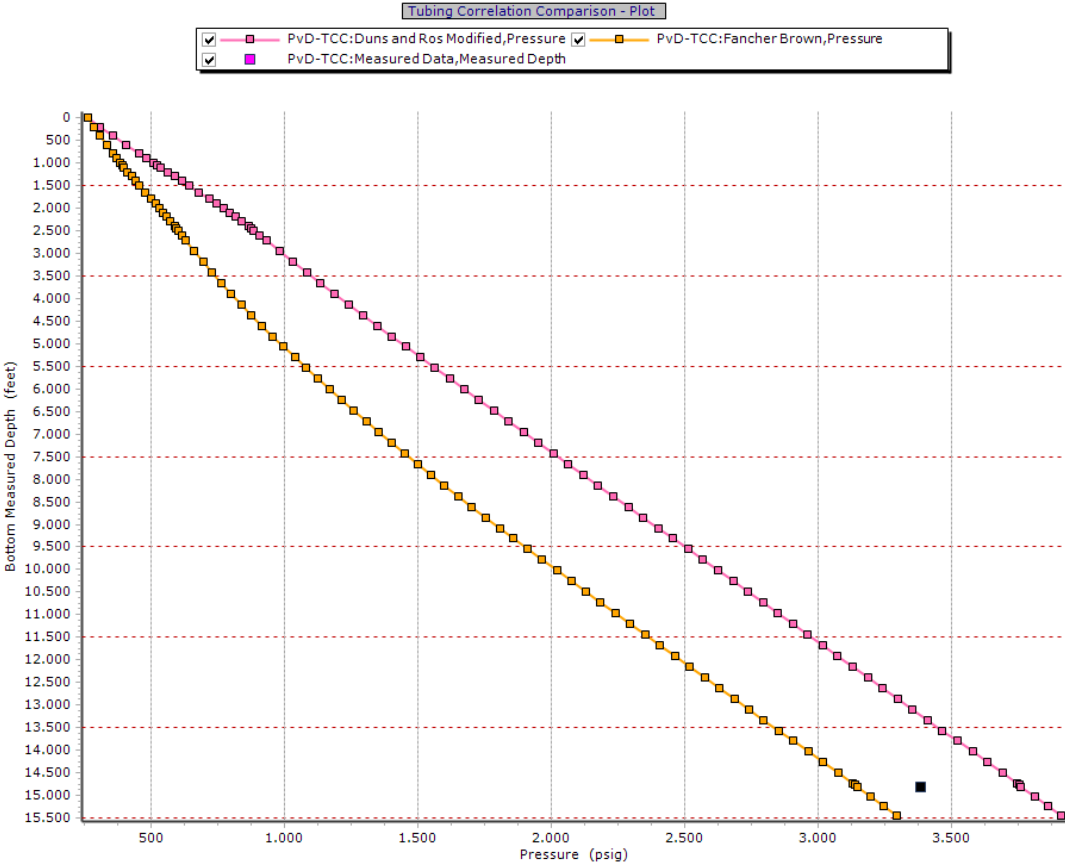


Figure 4.20: PvD diagram: Quality check for well test 1

### 4.3.6.2 Well Test 2 Quality check

#### Estimate U-value

The U-value provided by PROSPER is equal to 1.99 BTU/h/ft<sup>2</sup>/F (Fig. 4.21). According to PROSPER manual [28], it should be used as a rule of thumb that oil have U values ranging from 5 to 8. The calculated value is far away from the initial estimate. It can be commented that the system is behaving like an insulated one which, in practice, is not the case.

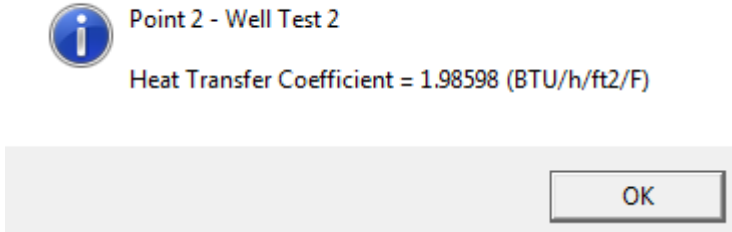


Figure 4.21: Estimated U value for well test 2

### Correlation comparison

The second test is plotted along with the pressure gradients derived by the two correlations, as previously (Fig. 4.22). The results show that test point 2 lies outside the envelope and on the right hand side of the pressure gradient calculated by Duns n Ross correlation. Recall that Duns n Ross correlation does not consider hold-up phenomena, and represents an unrealistic situation with the least pressure drop possible along the tubing. Well test 2, with the presence of a gas lift system and, hence, the larger possibility of pressure losses due to friction as a result of large quantities of gases (gas lift gas and gas previously dissolved in oil) travelling through the tubulars, appears to be somewhat unaffected by that fact. Given the previous results, VLP matching cannot be performed with the use of well test 2.

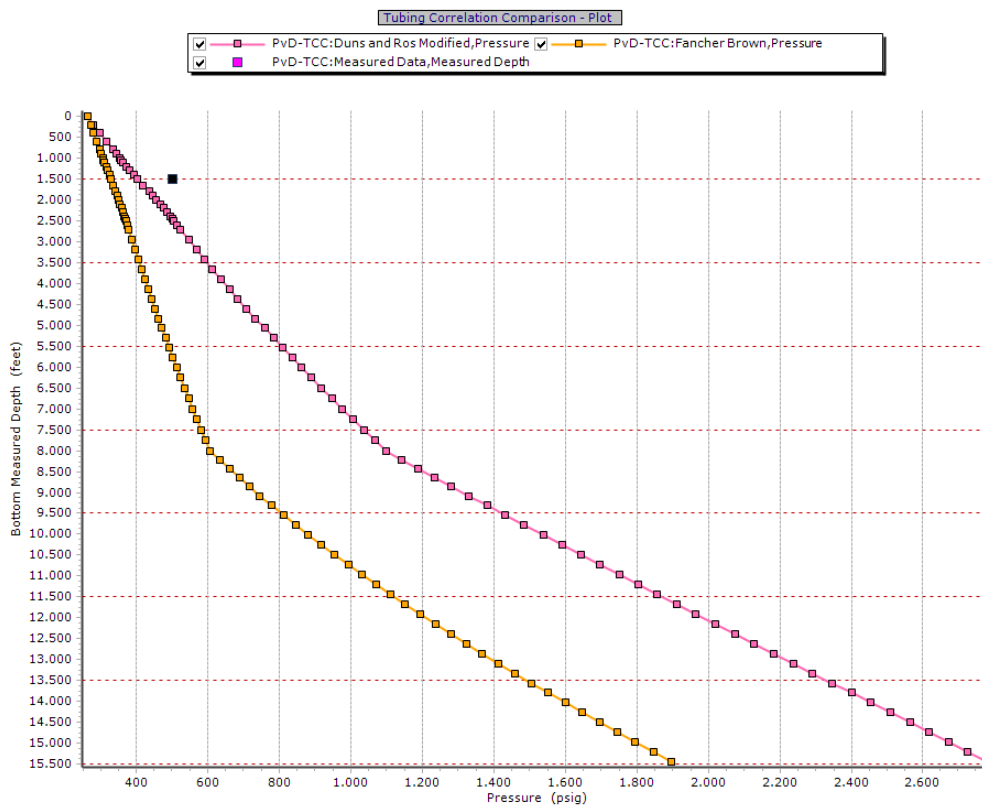
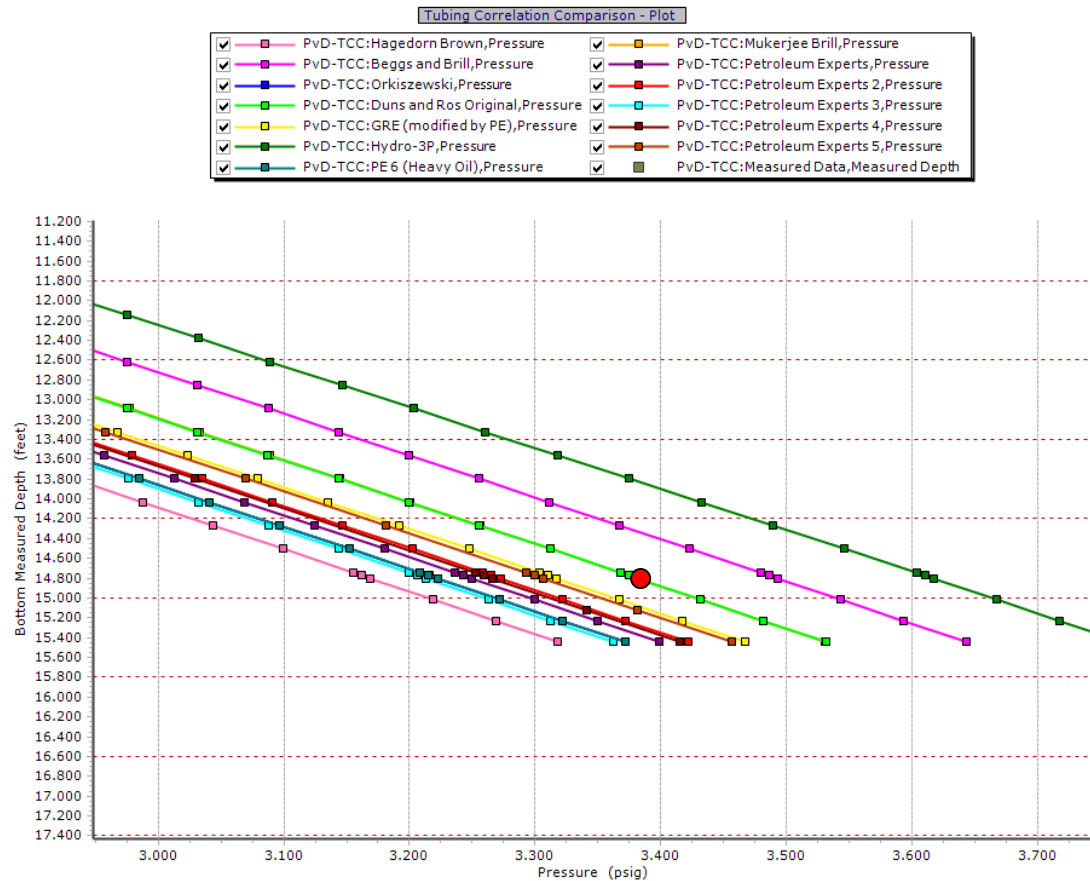


Figure 4.22: Quality check for well test 2

#### 4.3.6.3 Correlation comparison

The VLP/IPR matching process will be held by using only the first well test data point. PROSPER provides many built-in multiphase flow correlations. A brief discussion on the role of these correlations is given in paragraph 2.5.3. The concept of this section is to find which correlations exhibit the closest match to the test point before the actual matching regression is carried out. Those correlations are expected to require least tuning to match perfectly the well test

data. Multiphase flow correlations take into account many parameters in order to produce the pressure gradient curve of the well and model flow regimes at each depth along the well. In this case, they are plotted for a certain top node pressure and flow rate, those of the well test. The correlation to which the plotted measurement of pressure is closer to the gradient curves can be confidently chosen to be tuned (**Fig. 4.23**). It is clear that the correlations that match best with the test point are the “Duns and Ross Original” and “Mukherjee and Brill”.



**Figure 4.23:** Correlation comparison plot: All correlations plotted (Red point corresponds to the well test 1 point)

An important observation is that since no significant deviation is visible between the rest of the correlations and the test point, as pressure deviate is less than 100 psi (**Fig. 4.23**), the Petroleum Experts 2 correlation is selected as a more reliable one compared to those of Mukherjee and Brill or Duns n Ross Original. Duns n Ross Original correlation behaves best in gas condensate production [29], while Mukherjee and Brill correlation even though it adapts to the various inclinations and flow regimes, it fails to predict the flow regime in some cases [30]. Petroleum Experts 2 correlation includes the older Petroleum Experts 1 correlation and combines the best features of existing correlations plus original work on predicting low-rate VLPs and well stability. PE2 has also been externally tested as the most reliable well flow correlation irrespective of fluid type, flow regime or pipe specification [28].

#### 4.3.6.4 VLP matching

The qualitative work done in the previous chapter now becomes more quantitative. The matching of the correlations with the reported field data is done in this section. The method of VLP matching proposed by PETEX is the following: Since pressure losses in the tubing are caused mainly due to gravitational forces and friction, Prosper introduces 2 parameters (similar to the ones in the PVT data matching process). Parameter 1 is the multiplier for the gravity term in the correlation, while parameter 2 is the multiplier for the friction term. Then, it performs a nonlinear regression to adjust these two parameter in order to achieve the best fit. The more these two multipliers deviate from unity, the least reliable is the selected correlation. The closeness of the fit is also expressed by the standard deviation. A standard deviation value close to 0 indicates a good matching process. The solution of the regression process using the Petroleum Experts 2 correlation led to a **Parameter 1 value equal to 1.03** while the **Parameter 2 value remained unchanged and equal to the unity. Standard deviation is 0**. Along with the Petroleum Experts 2 correlation, all other correlations were indicatively adjusted and the summary of their multipliers is given in **Figure 4.24**. Even though in most cases, parameters 1 and 2 vary no more than 10% from the default value of 1, they cannot be used, as they are specialized for certain types of liquids or specific inclination i.e some correlations give good results in vertical wells only.

Point		Correlation	Parameter 1	Parameter 2	Standard Deviation
1	Reset	Duns and Ros Modified	0.89842	1	0.00048828
2	Reset	Hagedorn Brown	1.05712	1	0.00073242
3	Reset	Fancher Brown	1.06379	1	0.0012207
4	Reset	Mukerjee Brill	0.997	1	0.00073242
5	Reset	Beggs and Brill	0.97043	0.98644	0
6	Reset	Petroleum Experts	1.03589	1	0.00048828
7	Reset	Orkiszewski	1.04431	1	0.00024414
8	Reset	Petroleum Experts 2	1.02997	1	0
9	Reset	Duns and Ros Original	1.00324	1	0.00048828
10	Reset	Petroleum Experts 3	1.02312	1.4327	0.00097656
11	Reset	GRE (modified by PE)	1.00903	1.14576	0.00024414
12	Reset	Petroleum Experts 4	1.01635	1.26355	0.00048828
13	Reset	Hydro-3P	0.96717	0.69817	0
14	Reset	Petroleum Experts 5	1.01049	1.15914	0.00048828
15	Reset	PE 6 (Heavy Oil)	1.02201	1.39229	0.00024414
16	Reset	OLGAS 2P	1	1	
17	Reset	OLGAS 3P	1	1	
18	Reset	OLGAS3P EXT	1	1	
19	Reset	LedaFlow 2P	1	1	

Figure 4.24: Matched parameters for all tubing correlations

#### 4.3.6.5 IPR/VLP matching

The final step of the well set up is the IPR/VLP matching section. Since the VLP is now matched and trusted, it must be examined whether the reported liquid rate at the surface from well test 1 i.e. the intersection between the IPR and the VLP curve is close to the operating point (more information on Nodal Analysis can be found in chapter 1). The calculations indicate a liquid rate of 5,512 stb/day, that is significantly greater than the one reported by the well test (5,045 stb/day). Their difference is 13.25 % indicating that the IPR model is not representative of the actual flowing conditions. To correct this large difference in liquid rate, PROSPER gives the opportunity for the adjustment of the IPR either in terms of the **reservoir pressure** or of the **skin factor** due to the fact that these terms are considered to be the most questionable in the configuration of the IPR curve. Recall that the skin factor is a measure of the deviation of the reality from the mathematical model which has been set up to predict the flow from the reservoir. As far as the reservoir pressure is concerned, during well testing, the measurement of the average reservoir pressure is achieved by closing the choke on the surface and stopping production for a period of time. This may take a few hours. Actual reservoir pressure, though, may take several days to balance. As a

result, field engineers use extrapolation methods to predict the static pressure, which may contain a certain amount of error.

**Figure 4.25** is a close view of the sensitive area where the IPR and VLP intersection occurs. Due to the very “flat” shape of the curves, the linear interpolation method implemented between two consecutive IPR points to generate the IPR curve is inaccurate and may lead to a production difference of hundreds of barrels. This is the reason why, these operating conditions cannot be used to extract safe conclusions about which parameter is more appropriate to be altered. The investigation must be done using operating conditions where the two curves are rather complementary, i.e. exhibit inverse slope. This inverse slope is obtained only by generating a VLP curve at more favorable operating conditions. This could correspond to lower a water cut level or when the production is assisted by some type of artificial lift. For this reason sensitivity analysis for both cases was decided to be applied. Three different cases were considered: For each adjusted parameter, **(a)** liquid rates for various water cut levels, **(b)** liquid rates for various water cut levels during the application of an electric submersible pump and **(c)** liquid rates for various top node pressures were compared. In other words, an attempt was made to capture the difference in the IPR curve for certain operating conditions, and in the meantime, the same VLP would intersect these IPR curves. For a fixed top node pressure or water cut, the VLP curve is not affected. An indicative example of the attempted process is the following: For a WC level of 16%, top node pressure of 264 psi and GOR of 493 scf/stb, two different IPR curves can be generated, one for the adjusted skin factor and one for the adjusted reservoir pressure. Meanwhile, as stated previously, the VLP curves for both situations will remain practically the same because changes occur only in the reservoir, so only the IPR curves will be affected. If any significant difference in the liquid rate is reported, two different production scenarios must be considered, as this would indicate that the inflow performance is affected in a different manner by either of the two adjusted parameters. The results of the above mentioned process are given in detail in the next paragraphs.

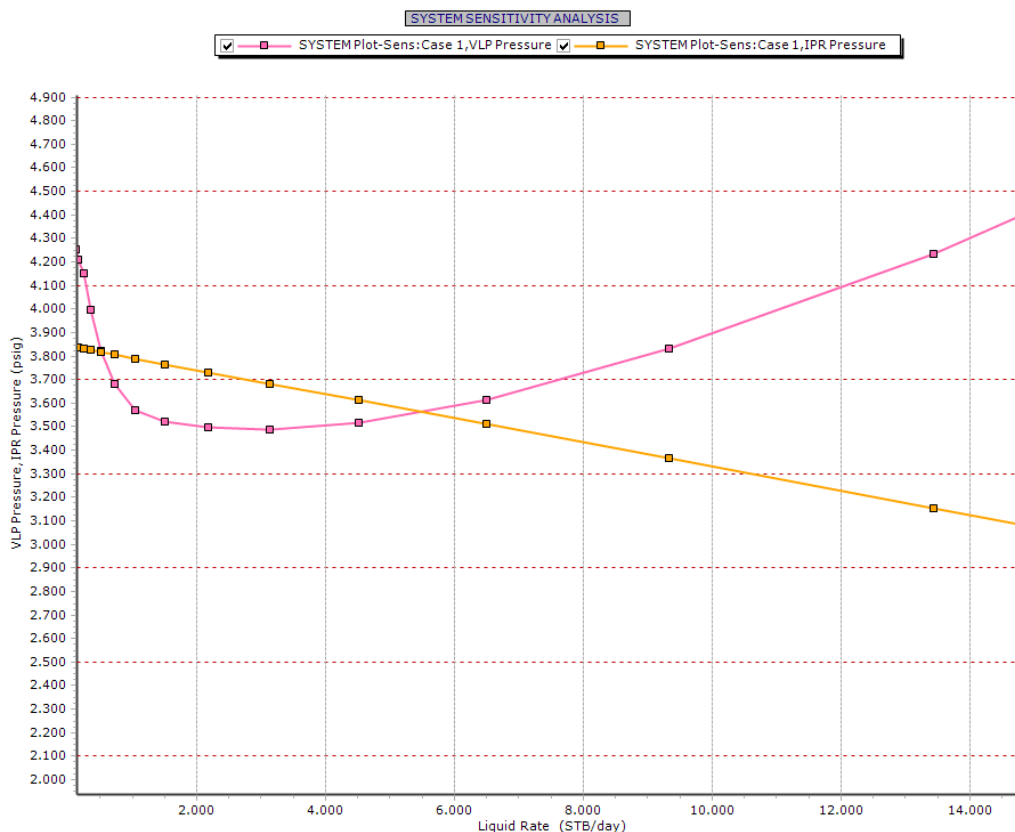


Figure 4.25: Close look at the IPR/VLP curve intersection (IPR/VLP matching section)

#### 4.3.6.5.1 Sensitivity analysis on various water cuts

##### Skin factor adjustment

In the “Adjust IPR” option of PROSPER, the IPR is adjusted in terms of skin factor to obtain a calculated liquid rate equal to the measured one. Meanwhile, the Reservoir Pressure remained the same as initially set (3,844 psi). The new skin factor value was calculated at 1.69 as depicted on **Figure 4.26**. A sensitivity analysis on various water cut cases is then held out (**Fig. 4.27**).

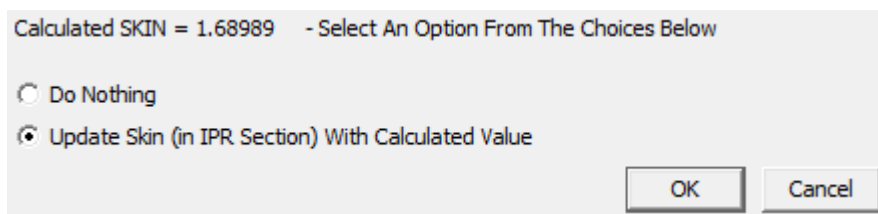


Figure 4.26: Revised value of the skin factor after IPR adjustment

	percent	Water Cut
1	10	
2	12	
3	14	
4	16	
5	18	
6	20	
7	22	
8	24	
9	26	
10		

Figure 4.27: Water cut cases examined

### Pressure adjustment

The same procedure was repeated, this time the skin factor was left unchanged in its initial value equal to 0.5, while the IPR was adjusted in terms of reservoir pressure. **Figure 4.28** shows the revised value of the the reservoir pressure (**3,795.2 psi**). Again, the same cases of water cut levels are investigated.

Calculated Reservoir Pressure = 3795.2 (psig) - Select An Option From The Choices Below

Do Nothing  
 Update Reservoir Pressure (in IPR Section)  
 Update Reservoir Pressure (in VLP/IPR Match Record(s))  
 Update Reservoir Pressure (in Both Sections)

OK Cancel

Figure 4.28: IPR adjustment option: Adjusted Pressure

### Results

**Table 4.4** shows the results of the liquid rates for each category and each case. No significant differences are observed between the two categories (skin factor and  $P_r$ ). As the IPR and the VLP curves barely intersect at water cut levels of 24 and 26% due to the unfavorable conditions in the well, a slight change in the IPR may cause a large difference in the liquid rate or even seize production. This critical area is not trustworthy and any result calculated may not lead to correct

conclusions. The 9.15 % difference in the 24% water cut case is not taken into account due to the aforementioned reason.

**Table 4.4:** Results of the sensitivity analysis for various water cuts

<b>WC</b>	<b>Liquid rate (S)</b>	<b>Liquid rate (Pr)</b>	<b>diff</b>
(%)	stb/day	stb/day	(%)
10	6758,5	6936	2,63
12	6499,5	6652,2	2,35
14	6152,1	6314	2,63
16	5791,2	5903,9	1,95
18	5421,9	5483,5	1,14
20	5041,8	5050	0,16
22	4652,1	4604,8	-1,02
24	3968,1	3605,1	-9,15
26	2801,1		

#### 4.3.6.5.2 Sensitivity analysis on various water cuts with an ESP

The next scenario is the implementation of an ESP at a fixed depth for both cases. The ESP selected and its characteristics are seen on **Figure 4.29**. More details on the ESP calculations are given in **APPENDIX A-2**. A brief discussion of an ESP configuration and mechanism is briefly described in **paragraph 3.3.2**.

Done	Cancel	Main	Help	Plot
------	--------	------	------	------

Input Data					
Head Required	1292.37	feet	Pump Intake Pressure	2017.07	psig
Average Downhole Rate	12617.7	RB/day	Pump Intake Rate	12879.3	RB/day
Total Fluid Gravity	0.74876	sp. gravity	Pump Discharge Pressure	2436.16	psig
Free GOR Below Pump	48.6193	scf/STB	Pump Discharge Rate	12511.1	RB/day
Total GOR Above Pump	493	scf/STB	Pump Mass Flow Rate	3311843	lbm/day
Pump Inlet Temperature	229.31	deg F	Average Cable Temperature	194.165	deg F

Select Pump	ESP TE11000XHT_COMP 5.38 inches (8000-14000 RB/day)
Select Motor	ODI 70KM300-E 126HP 1545.83V 56A
Select Cable	#1 Aluminium 0.33 (Volts/1000ft) 95 (amps) max

Results					
Number Of Stages	25		Motor Efficiency	90.2706	percent
Power Required	127.885	hp	Power Generated	127.885	hp
Pump Efficiency	72.0278	percent	Motor Speed	4104.01	rpm
Pump Outlet Temperature	230.67	deg F	Voltage Drop Along Cable	205.019	Volts
Current Used	50.1442	amps	Voltage Required At Surface	1750.85	Volts
Surface KVA	152.066		Torque On Shaft	163.66	lb.ft

Figure 4.29: ESP selection screen

## Results

The results for the liquid rates for adjusted  $P_r$  or  $S$  are given in **Table 4.5**. It is underlined that the deviations are very similar, always close to 3.5%. This sensitivity analysis leads to a conclusion that no significant differences can be noted for this scenario.

Table 4.5: Sensitivity analysis results on various water cuts with the introduction of an ESP

WC (%)	Liquid rate (S) (stb/day)	Liquid rate ( $P_r$ ) (stb/day)	diff (%)
10	10637,6	11020,7	3,60
12	10508,7	10882,8	3,56
14	10376,5	10741,4	3,52
16	10240,8	10596,2	3,47
18	10101,3	10446,9	3,42
20	9957,9	10293,4	3,37
22	9810,5	10135,6	3,31
24	9659	9973,2	3,25
26	9502	9805,9	3,20
28	9342,4	9633,9	3,12

### 4.3.6.5.3 Sensitivity analysis on various wellhead pressures

The final scenario is the comparison of liquid rates for various wellhead pressures (Fig. 4.30).

Figure 4.30: Well head pressure cases examined

### Results

Once again, deviations are negligible and rates are close to each other as shown in Table 4.6.

Table 4.6: Sensitivity analysis results on various wellhead pressures

Top node pressure	Liquid rate (S)	Liquid rate (P <sub>r</sub> )	diff
<i>psig</i>	stb/day	stb/day	(%)
200	6660,1	6823,2	2,45
210	6447,1	6603	2,42
220	6177,7	6339,9	2,63
230	5907,9	6034,9	2,15
240	5636,2	5726,8	1,61
250	5365,1	5418,5	1,00
260	5092,6	5108,1	0,30

To sum up, the adjustment of the IPR curve in terms of P<sub>r</sub> or S gave quite similar liquid rates for the various cases. Both adjustments are judged as reliable and

future calculations should correspond to the reality if either variable is to be adjusted. **In this study, all calculations will be done by trusting the provided skin factor (0.5) while the reservoir pressure is adjusted to 3,795 psi (from 3,844 psi).** Reservoir pressures in the well test data and the IPR section are now updated for the rest of the calculations that will take place in the continuous gas lift design in **Chapter 5**.

## 5. Gas lift design in PROSPER

---

In this chapter, the design procedure of a continuous gas lift system for various reservoir pressures and water cut levels is discussed in detail. At the beginning of this chapter, a study on various tubing sizes is held, in order to take full advantage of the well's production capacity (More information about tubing size effect can be found on **Chapter 2**). An increase of the production tubing ID leads to an optimized VLP curve and consequently to an increase in production. The pressure drop in the tubing decreases so that a greater pressure drawdown is created for the same reservoir and separator pressure. However, if the tubing size becomes too large, liquid hold up becomes a major problem and production gradually decreases. Once the optimum tubing size is determined, design of the gas lift system for the various future operating conditions, when the reservoir is being depleted, is undertaken. The gas lift system principles are introduced in **Chapter 3**. In this chapter, a detailed description on how a gas lift system is configured (valve spacing) is also provided. More information about the design parameters are given in the next paragraph.

### 5.1 Input data

For gas lift system to be designed, the maximum available injection gas is 8 MMscf/day whereas the casing has been designed to withstand injection pressures up to 2,000 psi. The gas lift system is to be designed to improve the flowing conditions which are encountered at the same time the well test data was collected.

Moreover, the designed gas lift system need to take into account the prediction of future performance of the well when the operating conditions, according to the existing reservoir simulation scenario, are expected to deteriorate to 30% WLR and  $P_r=3,400$  psi, 40% WLR and  $P_r=3,100$  psi and 50% WLR and  $P_r=2,850$  psi. According to the operating company, the minimum production rate required to sustain an economically vital well is 2,000 stb/day.

### 5.2 Design strategy

It was decided that, the gas lift system and the positions of the side pocket mandrels in the production tubing where gas lift valves are to be placed for the unloading process (see **paragraph 3.4.4**), must be done based on the worst situation in terms of well productivity. This situation corresponds to the case where the reservoir pressure will drop to 2,850 psi and the water cut will be as high as 50%. Recall that, in these conditions, water to liquid ratio is greater than the initial one and pressure losses due to gravity are much larger due to the

presence of a larger fraction of water in the tubing, which is known to have a greater density than oil. Eventually, the pressure provided by the reservoir will not be sufficient to lift the liquids up to the surface. In **Chapter 4**, during the analysis of the initial conditions, it was discussed that the well was about to seize flowing in a much larger  $P_r$  and less water cut. As a result, the future conditions will all result to a “dead well”.

Due to economic limitations, the well will be recompleted only once to ensure that the project will be economically viable. The new gas lift must thus be designed for a particular scenario of reservoir pressure and water cut and the rest of the operating conditions will be designed to fit the existing positions of the side pocket mandrels placed according to the initial scenario. According to the previous argument, the design that best fits the worst case ( $P_r=2,850$ , 50% wc), should serve all other cases, as conditions are more favorable. Generally, the deeper the gas injection point is, the larger is the column to be lightened, the less are the pressure losses due to the gravity term and hence the better are the production rates that can be achieved. For this reason, the maximum injection depth will be placed at a point very close to the production packers. Prior to the gas lift design, it was investigated whether a new tubing with a greater ID would serve the optimization purpose. Sensitivity analysis is conducted on the worst case, in terms of injection rate at various injection depths and then, the optimum combination of these two variables is examined on various tubing diameters. The optimum tubing ID derived will be used in the gas lift design process. As far as the gas lift system for the rest of the operating conditions is concerned, only well workovers are necessary to replace the unloading valves with dummy valves or orifices, depending on the needs of the unloading process. More information on gas lift principles and parts that compose the system can be seen in **Section 3.4**.

### 5.3 Sensitivity analysis for tubing ID selection

As already mentioned in the paragraphs above, before the design process, it is decided to run a set of sensitivity analyses so to figure out whether the increase in the production tubing's ID plays a beneficial role on liquid production. The only case examined in this section is the worst case of  $P_r = 2,850$  psi and 50% WC. Generally, when the tubing ID increases, the VLP curve intersects the IPR one at higher production rates up to a point. At this point, the upward gas flow velocity has decreased so much (due to the tubing diameter increase) that it is no longer sufficient to efficiently lift the liquid to the surface i.e. slip phenomena commence and liquid holdup increases. This leads to a decline of the production rate. In this paragraph, it is examined whether slip phenomenon occurs for this specific case. If liquid hold up is of minor importance and production is unaffected, the tubing ID can be safely increased and used for all cases. It should be reminded that, the other cases correspond to situations with lighter hydrostatic columns due to lower water cut and higher  $P_r$  is exhibited.

The first step is, essentially, an indirect gas lift design. The optimum combination of gas lift injection rate and gas injection depth is questioned in the sensitivity analysis. Cases vary for injection rates from 1 to 8 MMscf/day and depths from 3,000 to 12,000 ft. Note that, similarly to the very large tubing ID mentioned above, large quantities of gas present in the tubing can severely deteriorate liquid production because of the friction dominant over the gravity term. In other words, the benefits in pressure from a lighter column are counterbalanced by increased friction.

The results are plotted in **Figure 5.1**. It is clear that, above 6 MMscf/day friction becomes the dominant factor of pressure loss in the tubing. The optimum depth in terms of maximum oil rate lies at 12,000' for all test rates. Injecting more than 6 MMscf/day deeper than 12,000' does not substantially increase production, therefore, this rate is selected as the optimum one. The combination of these optimized variables is now tested for various tubing ID.

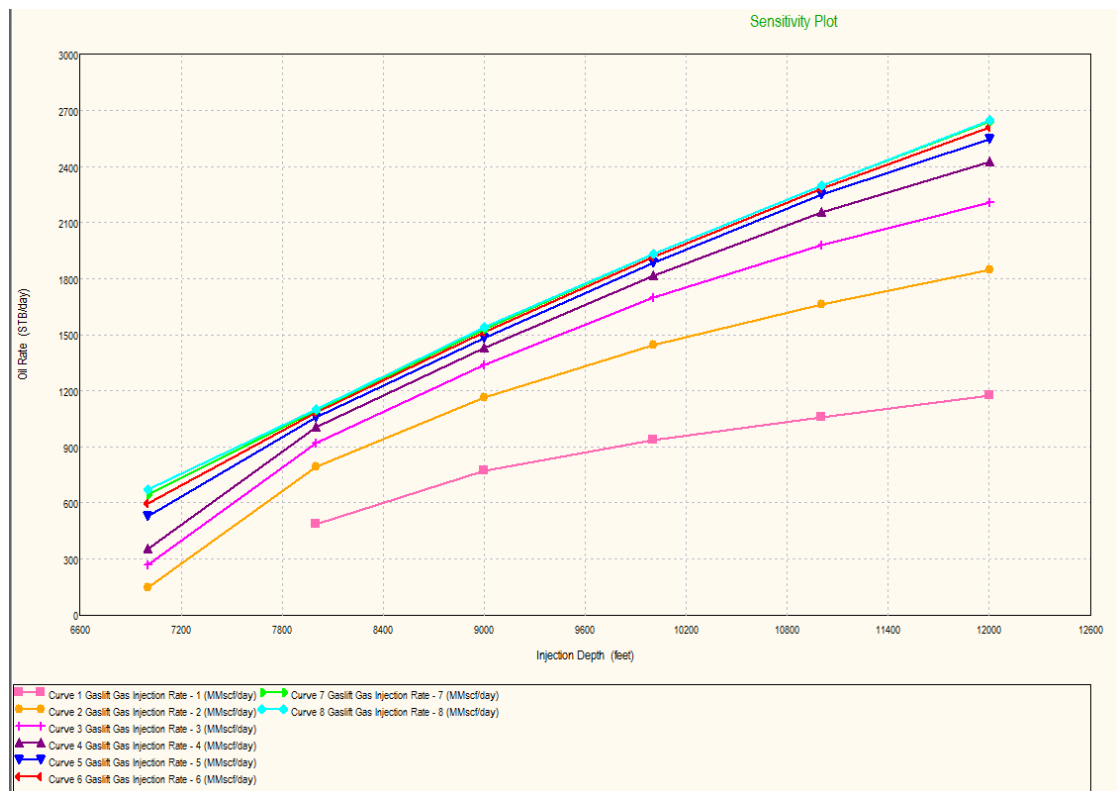


**Figure 5.1:** Sensitivity analysis: Effect of various injections depths and gas rate to the oil rate

Existing casing has an ID of 6.4" (see Downhole Equipment in **Chapter 3**), so it is necessary to choose a tubing whose size leaves enough annular space for future well workovers. Due to the size of the production tubing, the various tubing ID that could be tested, range from 4" to 4.5". Oil rate seems to be increasing linearly by larger tubing ID, according to **Figure 5.2**. For this purpose, a tubing string with 4.5" ID and wall thickness of 0.3" (5.1" OD) is set in the

recompletion process. The “Downhole Equipment” section is newly updated with the new characteristics of the production tubing.

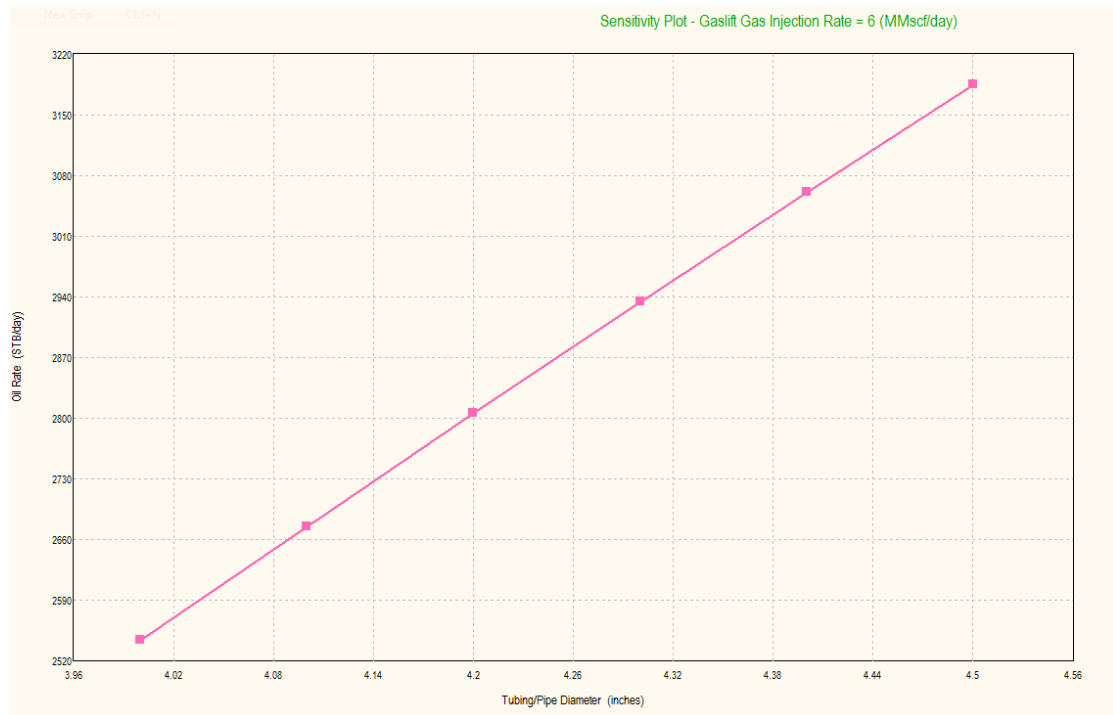


**Figure 5.2:** Sensitivity analysis: Effect of various tubing ID to the oil rate

## 5.4 Methodology of valve spacing in PROSPER

The unloading process is already analyzed in **Section 3.4**. In this section, the valve spacing calculations that will eventually serve the purpose of the unloading process, is explained. Prosper implements these procedures in the “Casing Sensitive” calculations (see **Section 5.5**).

First of all, the primary task is to perform a sensitivity analysis by assuming that all available gas is injected at various injection points. By means of Nodal Analysis, where the injection point is the node, the pressure and the flow rate at the node are calculated along with the required injection pressure at the casing head. By repeating the above procedure, the injection point that yields maximum production with the available gas injected is selected to be the objective depth during the unloading process. The equilibrium inflow/outflow curve in a pressure versus depth diagram for this specific node is then derived.

In **Figure 5.3**, the valve spacing process is illustrated in a pressure versus depth diagram. On the top right corner of the diagram, the red lines correspond to various gas injection pressures at the casing head. Green lines represent the static pressure gradient of the casing fluid, while the blue curve is the equilibrium inflow/outflow curve. The design procedure is as follows:

1. Gas injection is initiated from the casing head with a predefined pressure, always respecting the restrictions of the maximum pressure the casing at the surface can withstand. The initial injection pressure is the kick off pressure (KOP) and in **Figure 5.3**, it is the rightmost straight red line starting from top. The depth, at which the first unloading valve will be placed, is the depth where the pressure line of the gas intersects with the static pressure gradient of the casing fluid.
2. Once the position of the first unloading valve is found, gas injection pressure from the casing head is reduced by small amount of pressure, for example 50 psi. Then, a new gas pressure gradient starting from a lower pressure at the surface is created.
3. The second valve is placed when the static pressure gradient of the casing fluid (which starts from the depth where the first valve is placed, since the space above the valve is occupied by gas) intersects the new gas pressure line which is created as explained in step 3.
4. The procedure goes on in a similar way until either the maximum depth of injection is reached (at the node), or the gas will not be able to displace the casing fluid due to insufficient injection pressure at the casing head and the orifice is placed in a shallower depth.

Note that, the reduction of injection pressure is strictly related to the closing of the valves. Valves are adjusted to open when the casing pressure reaches the pressure calculated, when the intersection of the two pressure lines mentioned previously occurs. The pressure of the charged dome in the valve will have a pressure slightly less than the casing pressure but the pressure difference cannot be more than the injection pressure reduction interval. This methodology ensures that, when deeper valves are functioning, all the above ones remain closed.

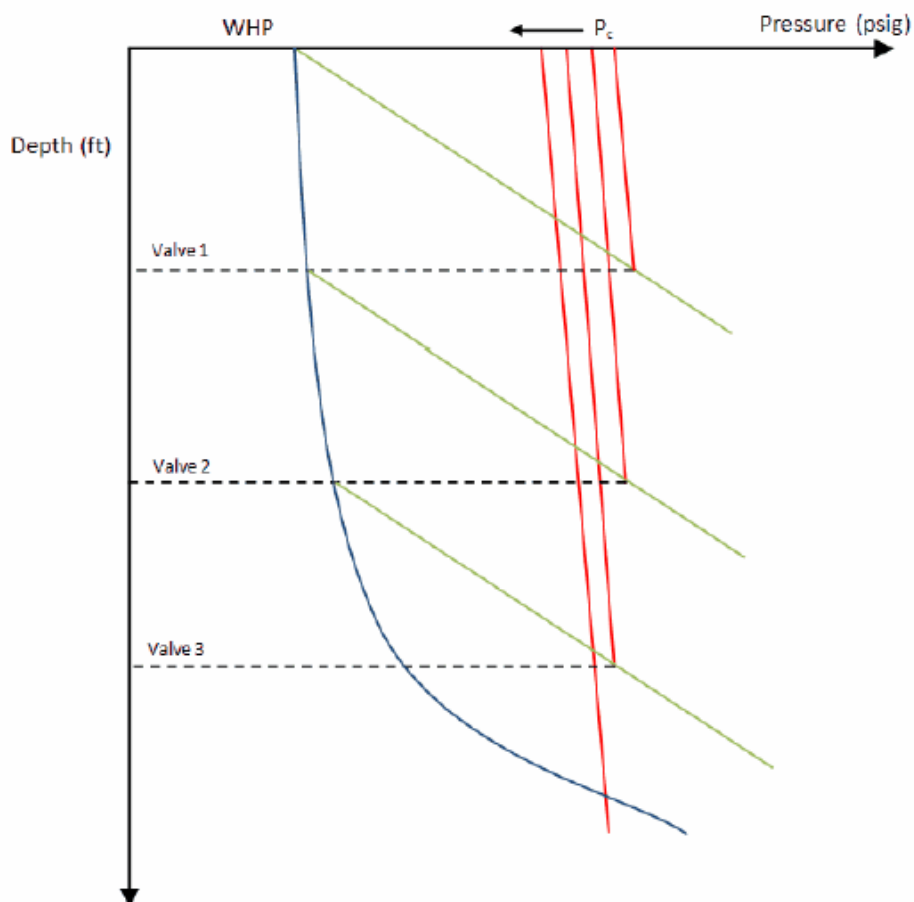


Figure 5.3: Illustration of valve spacing calculations: PvD diagram [28]

### 5.5 Gas lift design process for $\bar{P}_r = 2,850$ psi and water cut 50% (Case 1)

This case will be the groundwork for the recompletion design of the well according to the design strategy (see **Section 5.2**). All input data edited in this section will serve the purpose of the new valve spacing design, as discussed in **Section 5.4**.

The first step is to generate the IPR curve for the new reservoir conditions. New  $P_r$  and water cut level are used as input in the IPR section of PROSPER. The next step now is the design of a new continuous gas lift system. In the main gas lift design screen the following input data are inserted (**Fig. 5.4**).

The flowing and the unloading top node pressures are 264 psi as restrictions of the surface facilities still occur (see data input section in **Chapter 3**). The injection and the kick off injection pressure i.e. the initial injection pressure during the unloading process, are selected to be equal to 1,800 psi so as to respect the casing pressure restriction set initially. Note that even though the maximum casing pressure allowed at the surface is 2,000 psi, a more conservative approach is decided to be applied. The dP across valves is set to 100

psi. This means that the pressure in the annulus should be at least equal to the tubing pressure plus 100 psi that are consumed in the valve. In practice, this is a safety measurement to ensure that gas will flow through the valve. Its effect on the calculations is that during the design process, valves are placed a few feet shallower than they were intended to. Maximum depth of gas injection is set at 14,000 ft MD very close to the production packers (14,740'). Minimum spacing of the unloading valves is left to its default value (250'). If during calculations the next valve is calculated to be at a depth less than 250', calculations will stop. The completion fluid is a brine, slightly heavier than pure water and has a static pressure gradient equal to 0.45 psi/ft.

The Thornhill-Craver equation is used to capture the valve's response from subcritical to critical flow. It is found that this model overpredicts the flow through the gas lift valves. The Thornhill-Craver derating percentage of valves and orifices is the amount of reduction in the expected gas passage by when calculating the required port size using the Thornhill-Craver methodology. It can result to a larger port size or orifice size calculated. The default value (100%) is used. More information on the Thornhill-Craver methodology can be found in PROSPER manual [28].

The valve type is set to "Casing sensitive". The operating principle of the "Casing sensitive" valves as explained in the previous section. The decrease in the casing head injection pressure is set to 50 psi for all valves.

Valve settings are set to "All valves PVo = Gas Pressure". PROSPER designs using the maximum of either the dP to close valves or the calculated closing pressure drop. This method is more conservative and will ensure that valves do not close before they are intended to. However, it reduces the available injection pressure and will result in lower production rates. According to PROSPER manual [28], even though that lead to a conservative scenario, it is recommended in the design of a new GL system.

Conformance with the IPR is enabled to ensure that the calculated liquid rates can be delivered by the reservoir. This the reason why a very large amount of desired production rate is entered at the beginning, so to ensure the calculation of the highest liquid rate possible. The use of the IPR curve in the unloading process is also used. In this case, during sensitivity analysis based on various gas injection rates, the minimum gas injection rate that initiates well flow is determined. This injection rate is used to size the valve.

Finally, normal R-20 valves manufactured by Camco are selected with port sizes varying from 8 to 32 64<sup>th</sup> inch.

Port Size	R Value
8	0.017
12	0.038
16	0.066
20	0.103
24	0.147
28	0.2
32	0.26

Figure 5.4: Gas lift design input: Main screen (Case 1)

After the introduction of the basic input data, the design process follows. At the top of **Figure 5.5**, the optimum injection rate calculated by PROSPER is visible. The gas lift performance curve is plotted in **Figure 5.6**. The optimum gas injection rate according to the calculations is 8 MMscf/day, the maximum gas injection rate available. Optimum gas rate refers to the rate which yields maximum oil production. However, it is not the final gas injection rate, as the unloading process is not yet taken into consideration.

The calculation background the derivation of the gas lift performance curve is the sensitivity analysis of various injection rates at various injection depths for each rate. The depths and the injection rates are randomly spaced by PROSPER. It is important to note that, they are not plotted for a fixed maximum depth of injection and this should not be confused. In **Figure 5.6**, the red points correspond to the randomly chosen gas rates and the blue line is the fitted performance curve. The curve provides the optimum injection rate that constitutes a design parameter for the valve spacing process. After 10 MMscf/day of gas injected, the curve is declining due to the fact that, when large quantities of gas are present in the tubing friction forces prevail in the system (friction is dominant over gravity term reduction) and pressure drop in the tubing becomes larger, which eventually reduces the production rate. The gas lift performance curve is used to derive to the equilibrium curve, as mentioned in **Section 5.4**.

Calculated Rate							
GLR Injected	Liquid Rate	Oil Rate	VLP Pressure	IPR Pressure	Standard Deviation	Design Rate	Oil Production
scf/STB	STB/day	STB/day	psig	psig		MMscf/day	STB/day
1522.3	9337.0	4668.5	3164.3	2417.8	211.566	7.998	3720.8
Get Rate			Plot				

Objective Gradient				
Measured Depth	True Vertical Depth	Pressure	Temperature	Gas Injection Pressure
feet	feet	psig	deg F	psig
12562.1	9463.2	1765.0	244.9	1865.0

Valve Number 3 @ 10660.4 (md) 8118.35 (tvd) (feet)  
 Valve Number 4 @ 12154 (md) 9174.65 (tvd) (feet)  
 Operating Valve Number 5 @ 12588.9 (md) 9482.1 (tvd) (feet)  
 Valve Number 1 @ 4394.78 (md) 3687.96 (tvd) (feet)  
 Valve Number 2 @ 8166.65 (md) 6354.99 (tvd) (feet)  
 Valve Number 3 @ 10661.2 (md) 8118.96 (tvd) (feet)  
 Valve Number 4 @ 12159.6 (md) 9178.61 (tvd) (feet)  
 Operating Valve Number 5 @ 12562.1 (md) 9463.2 (tvd) (feet)

Design	Plot	Results	Main	Done	Help
--------	------	---------	------	------	------

Results			
Liquid Rate	Oil Rate	Injected Gas Rate	Injection Pressure
STB/day	STB/day	MMscf/day	psig
6928.18	3464.09	7.1194	1600

Valve Details			
Valve Type	Manufacturer	Type	Specification
Casing Sensitive	Camco	R-20	Normal

Figure 5.5: Gas lift design: Calculation screen (Case 1)

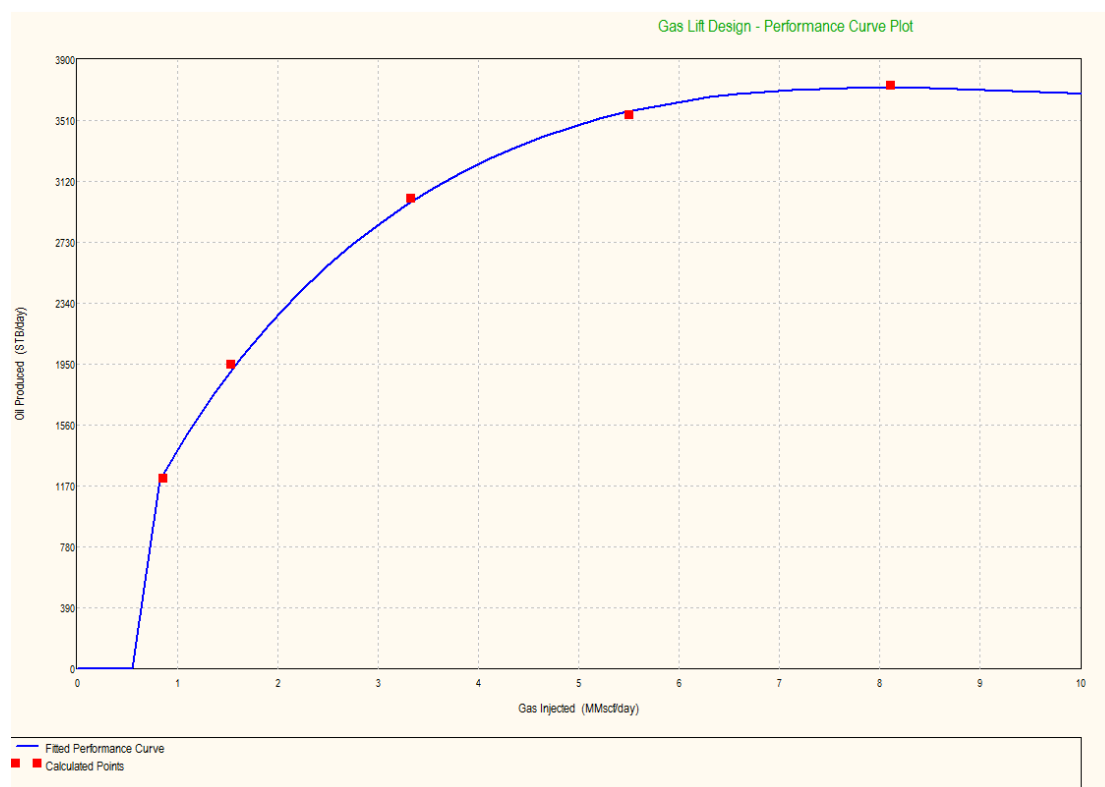


Figure 5.6: Gas lift performance curve (Case 1)

If **Figure 5.5** is recurred, at the bottom of the design screen and after the valve spacing process, the final operating conditions are visible. **A constant gas injection rate (GIR) of 7.12 MMscf/day with an injection pressure of 1,600 psi, can deliver 3,464 bbl/day of oil.**

The basic information of the valves spacing are presented in **Table 5.1**. More information on the calculated results can be found on **APPENDIX A-3**. The maximum depth of injection at 14,000' MD has not been reached and gas is injected at 12,562'. The port size of the orifice is 31 64<sup>ths</sup> inch.

It is asked to model a situation where the desired injection point lies at a very large depth. Having in mind the valve spacing method described in **Section 5.4**, the main reason of gas injection at a lower depth than the desired one is that gas injection pressure plus the gas gradient are not sufficient to displace the fluid in the annulus. In other words, the gas pressure and the annular liquid static pressure are equal well above 14,000'. Recall that, the depth at which the two above mentioned pressure lines are intersected in a pressure versus depth diagram is the depth that a valve or an orifice is placed. Due to the casing pressure restrictions, a compromise is made. Even though, the injection depth lies at a shallower depth than the desired one, oil rate obtained exceeds by far the minimum rate restriction (2,000 stb/day).

Note that, the gas injection rate is not the optimum one, as this was initially calculated at 8 MMscf/day. The new calculated gas injection rate is the optimum rate at the specific depth where the orifice is set. The main reason behind the

decrease of the gas injection rate is that gas already evolved from oil at this depth and a gas rate of 8 MMscf/day would seriously increase pressure losses due to high gas velocities in the tubing.

**Table 5.1:** Valve spacing results (Case 1)

Valve	Valve type	MD (ft)	TVD (ft)	Tubing pressure (psig)	Casing pressure (psig)	Opening CHP (psig)	Gas lift gas rate (MMscf/day)	Port size (64 <sup>ths</sup> inch)
1	Valve	4394.8	3688	790	1973.7	1800	0.712	12
2	Valve	8166.7	6355	1215.3	2040.1	1750	0.712	12
3	Valve	1066.2	8119	1516	2059.1	1700	0.712	12
4	Valve	12159.6	9178.6	1711.1	2042.8	1650	2.09	20
5	Orifice	12562.1	9463.2	1765	1865		7.12	43

The Pressure vs Depth plot illustrating the valve spacing design is given in the following figure (**Fig. 5.7**). Positioning of the valves, valves' opening and closing pressures and mainly the flowing pressure gradient in the tubing are visible. The effect of gas lift is seen at the below and above the injection point. Below this depth, the flowing pressure gradient of the produced fluid has a steeper slope, which means that the fluid column in the tubing below the orifice is heavier and the pressure gradient is larger. Above the injection point, and as a result of the large quantities of gas being injected in the production tubing combined with the free gas previously dissolved in oil, the fluid column is lighter which is depicted by the milder slope.

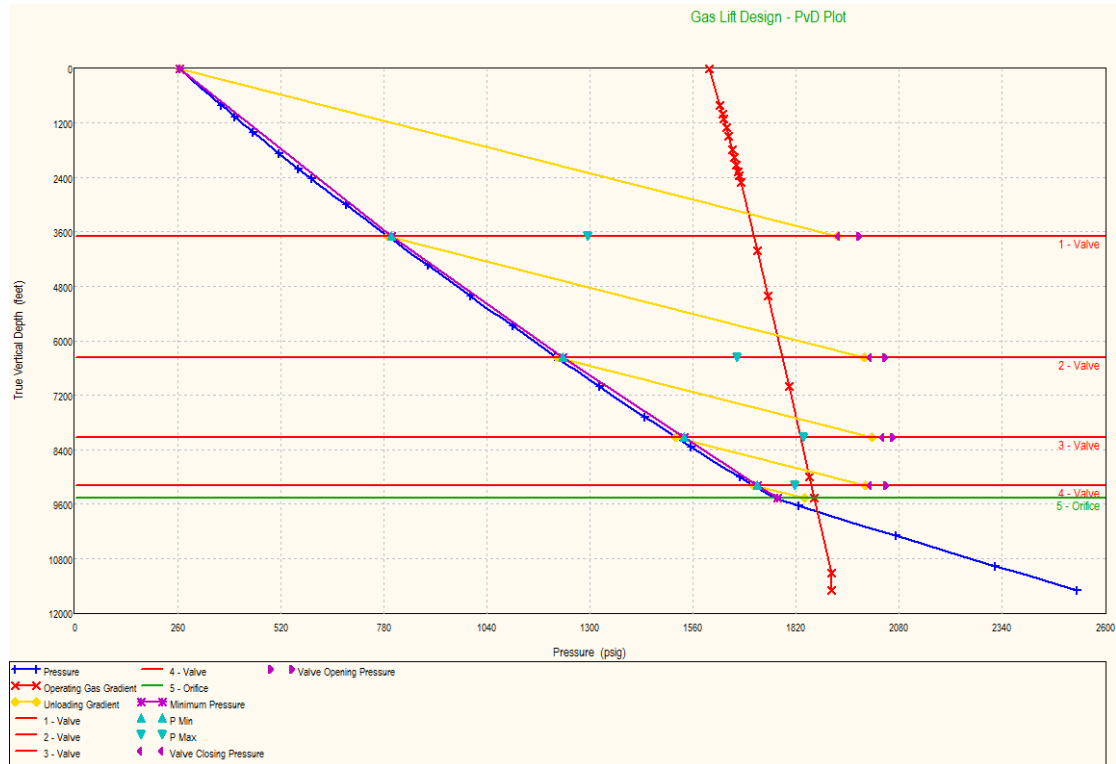


Figure 5.7: Gas lift design: PvD plot (Case 1)

The final step of the gas lift design is to check whether the system is stable or not. Harald Asheim [31] proposed the use of 2 criteria in order to evaluate a gas lift system’s stability. The first criterion (F1) is the inflow response of the well. If the reservoir fluid rate is more sensitive to pressure than the lift-gas rate, then the average density of the mixture will increase in response to a decrease in tubing pressure. This causes the tubing pressure to increase, which stabilizes the flow. This criterion is calculated as:

$$F_1 = \frac{\rho_{gsc} B_g q_{gsc}^2}{q_{Lsc}} \frac{J}{(EA_i)^2}$$

$\rho_{gsc}$  = Lift-gas density at SC

$B_g$  = FVF of gas injection point

$q_{gsc}$  = Lift-gas flow rate at standard conditions

$q_{Lsc}$  = Liquid flow rate at standard conditions

$J$  = Productivity index

$E$  = orifice efficiency factor

$A$  = Injection port area

If the first criterion is not fulfilled, tubing pressure decrease will cause the injected gas flow rate to increase more than the liquid flow rate. This will cause the tubing pressure to decrease as well as the casing pressure. If the casing pressure decreases faster than the tubing pressure, then the pressure difference between the casing and the tubing will decrease and so will the injected gas rate. This stabilizes the flow. This Criterion (F2) namely pressure-depletion response is calculated:

$$F_2 = \frac{V_t}{V_c} \cdot \frac{1}{gD} \cdot \frac{P_t}{(\rho_{fi} - \rho_{gi})} \cdot \frac{q_{fi} + q_{gi}}{q_{fi}(1 - F_1)}$$

Where:

$V_t$  = Tubing volume downstream of injection point

$V_c$  = Casing volume

$g$  = Acceleration due to gravity

$D$  = Vertical depth to injection point

$P_t$  = Tubing Pressure

$\rho_{fi}$  = Reservoir fluid density at the injection point

$\rho_{gi}$  = Lift gas density at injection point

One of the two criteria must exhibit a value greater than unity. Should both values are less than one, the system is considered unstable and the design must be reviewed. In this case, **Criteria F1 and F2 are equal to 0.52 and 0.18 respectively (Fig 5.8), indicating an unstable gas lift system.** It is stressed out that modifications on the design parameters should be made to ensure stability. Among all parameters, the maximum injection depth is the most appropriate variable to change,

Done      Main      Export      Help		
<b>Inflow Response Criterion</b>		
Lift Gas Density @ Standard Conditions	0.053662	lb/ft3
FVF of Gas @ Injection Point	0.0095486	ft3/scf
Lift Gas Flow Rate @ Standard Conditions	7.1194	MMscf/day
Liquid Flow Rate @ Standard Conditions	6928.18	STB/day
Productivity Index Of Well	23.6553	STB/day/psi
Orifice Efficiency Factor	0.9	fraction
Injection Port Size	0.35454	in2
<b>F1</b>	<b>0.51781</b>	
<b>Pressure-Depletion Response Criterion</b>		
Tubing Volume Downstream Of Injection Point	1387.44	scf
Gas Conduit Volume	1024.31	scf
Acceleration Due To Gravity	32.174	ft/sec/sec
Vertical Depth To Injection Point	9463.2	feet
Tubing Pressure @ Injection Point	1764.97	psig
Reservoir Fluid Density @ Injection Point	52.8996	lb/ft3
Lift Gas Density @ Injection Point	5.60095	lb/ft3
Liquid Flow Rate @ Injection Point	7980.2	STB/day
Lift Gas Flow Rate @ Injection Point	0.06798	MMscf/day
<b>F2</b>	<b>0.18427</b>	
F1 or F2 should be greater than 1 for Stable Flow.		
Ref. "Criteria for Gas-Lift Stability" - Harald Asheim - JPT November 1988		

Figure 5.8: Stability criteria (Case 1)

### 5.5.1 Revision of Case 1

As observed in **Section 5.5**, the basic scenario lacks stability, as described by stability criteria F1 and F2 based on Asheim's original work [31]. The only difference between Case 1 in **Section 5.5** and its revised version described in this section is the change of the maximum injection depth. This will provide new results for valve spacing, injection depth and injection rate and most importantly the oil rate obtained.

Reservoir pressure and water cut level remain the same, as this is a revised design of Case 1, hence the modeling of the IPR remains unchanged as described in **Section 5.5**

The only variation from Case 1 is the maximum injection depth set at 12,000' MD instead of 14,000' MD set previously, as seen in **Figure 5.9**. Information on the other parameters' values and their contribution to the final result can be seen in **Sections 5.4** and **5.5**.

Design Rate Method: Calculated From Max Production

Maximum Liquid Rate: 20000 STB/day

Input Parameters		
Maximum Gas Available	8	MMscf/day
Maximum Gas During Unloading	8	MMscf/day
Flowing Top Node Pressure	264	psig
Unloading Top Node Pressure	264	psig
Operating Injection Pressure	1800	psig
Kick Off Injection Pressure	1800	psig
Desired dP Across Valve	100	psi
Maximum Depth Of Injection	12000	feet
Water Cut	50	percent
Minimum Spacing	250	feet
Static Gradient Of Load Fluid	0.45	psi/ft
Minimum Transfer dP	25	percent
Maximum Port Size	32	64ths inch
Safety For Closure Of Last Unloading	0	psi
Total GOR	493	scf/STB

Valve Type: Casing Sensitive  
Min CHP Decrease Per Valve: 50 psi

Valve Settings: All Valves PVo = Gas Pressure

Injection Point: Injection Point is ORIFICE

Dome Pressure Correction Above 1200psig: Yes

Valve Spacing Method: Normal

Check Rate Conformance With IPR: Yes

Vertical Lift Correlation: Petroleum Experts 2 1.03 1.00

Surface Pipe Correlation: Beggs and Brill

Use IPR For Unloading: Yes

Orifice Sizing On: Calculated dP @ Orifice

Thornhill-Craver DeRating: DeRating Percentage For Valves: 100 percent; DeRating Percentage For Orifice: 100 percent

Current Valve Information: Manufacturer: Camco; Type: R-20; Specification: Normal

Port Size	R. Value
8	0.017
12	0.038
16	0.066
20	0.103
24	0.147
28	0.2
32	0.26

Figure 5.9: Gas lift design input: Main screen (Case 1 revised)

After the introduction of the basic data input, the design process takes place. The optimum injection rate calculated by PROSPER can be seen at the top of Figure 5.10. The gas lift performance curve is plotted in Figure 5.11. The optimum gas injection rate according to the calculations is 8 MMscf/day, the maximum gas injection rate available.

Calculated Rate							
GLR Injected	Liquid Rate	Oil Rate	VLP Pressure	IPR Pressure	Standard Deviation	Design Rate	Oil Production
scf/STB	STB/day	STB/day	psig	psig		MMscf/day	STB/day
1826.8	9337.0	4668.5	3359.2	2417.8	71.5992	8.000	3300.9

Get Rate Plot

Objective Gradient				
Measured Depth	True Vertical Depth	Pressure	Temperature	Gas Injection Pressure
feet	feet	psig	deg F	psig
12000.0	9065.8	1638.6	242.9	2104.8

The OIL RATE is being checked for conformance with the IPR.  
 The GAS INJECTION RATE may be changed to ensure consistency.  
 This option is slower so please be patient...  
 Valve Number 1 @ 4398.52 (md) 3690.61 (tvd) (feet)  
 Valve Number 2 @ 8225.73 (md) 6396.76 (tvd) (feet)  
 Valve Number 3 @ 10801.3 (md) 8218.05 (tvd) (feet)  
 Operating Valve Number 4 @ 12000 (md) 9065.75 (tvd) (feet)

Design Plot Results Main Done Help

Results			
Liquid Rate	Oil Rate	Injected Gas Rate	Injection Pressure
STB/day	STB/day	MMscf/day	psig
6601.73	3300.87	7.62765	1650

Valve Details			
Valve Type	Manufacturer	Type	Specification
Casing Sensitive	Camco	R-20	Normal

Figure 5.10: Gas lift design: Calculation screen (Case 1 revised)

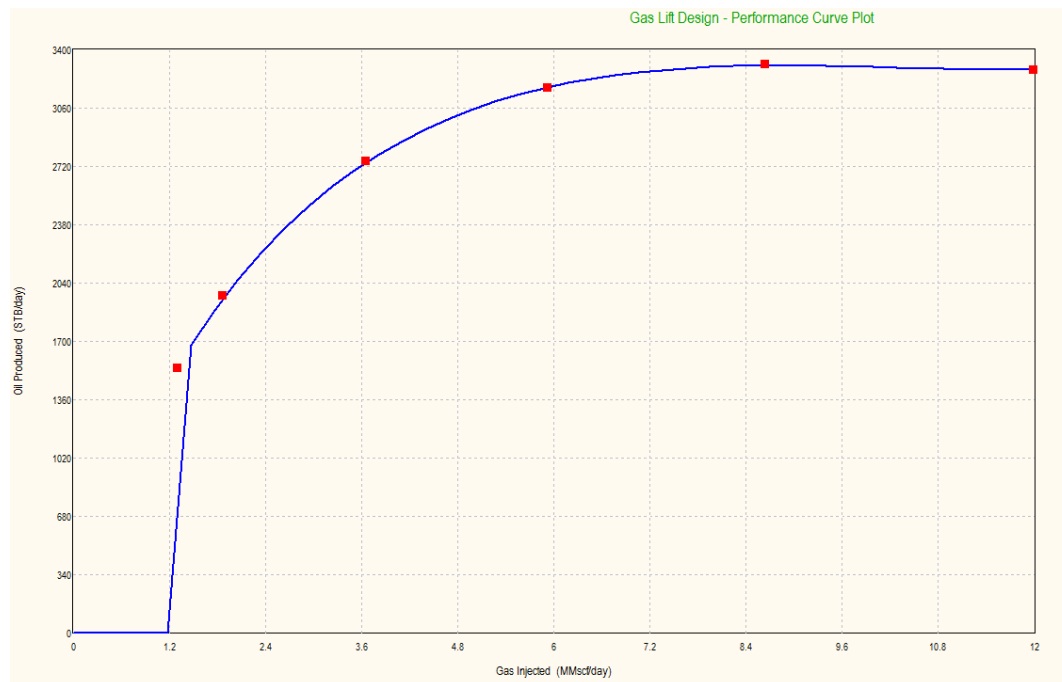


Figure 5.11: Gas lift performance curve (Case 1 revised)

If Figure 5.10 is recurred, at the bottom of the design screen and after the valve spacing process, the final operating conditions are visible. A constant gas injection rate of 7.63 MMscf/day with an injection pressure of 1,650 psi, can deliver 3,301 bbl/day of oil.

**Table 5.2** presents the basic information of the valves spacing. More information on calculated results can be found on **APPENDIX A-3**. The maximum depth of injection of 12,000' MD has been reached by the PROSPER design. The port size of the orifice is 31 64<sup>th</sup> inch.

**Table 5.2:** Valve spacing results (Case 1)

Valve	Valve type	MD (ft)	TVD (ft)	Tubing pressure (psig)	Casing pressure (psig)	Opening CHP (psig)	Gas lift gas rate (MMscf/day)	Port size (64 <sup>th</sup> inch)
1	Valve	4398.5	3690,6	776	1974.8	1800	0,76	12
2	Valve	8225.7	6396.8	1196.1	2043,8	1750	0,76	12
3	Valve	10801.3	8218.1	1492.1	2065.6	1700	0,76	12
4	Orifice	12000	9065.8	1638.6	2104.8	1650	7.63	31

The Pressure vs Depth plot is given in the following **Figure 5.12**. Positioning of the valves, valves opening and closing pressures and the flowing pressure gradient in the tubing are visible. An important observation is that in this revised scenario of **Case 1**, 3 unloading valves before the orifice are required, unlike the scenario of gas injection at 14,000' seen previously, where 4 unloading valves and 1 orifice were required. The main reason is that the injection point is shallower and less valves are necessary. Gas injection pressure is now sufficient to displace all annular fluids down to 12,000'. Optimum gas injection rate is 7.63 MMscf/day, slightly less than the optimum initially calculated. 7.63 MMscf/day of gas is the optimum gas injection rate for the specific valve configuration.

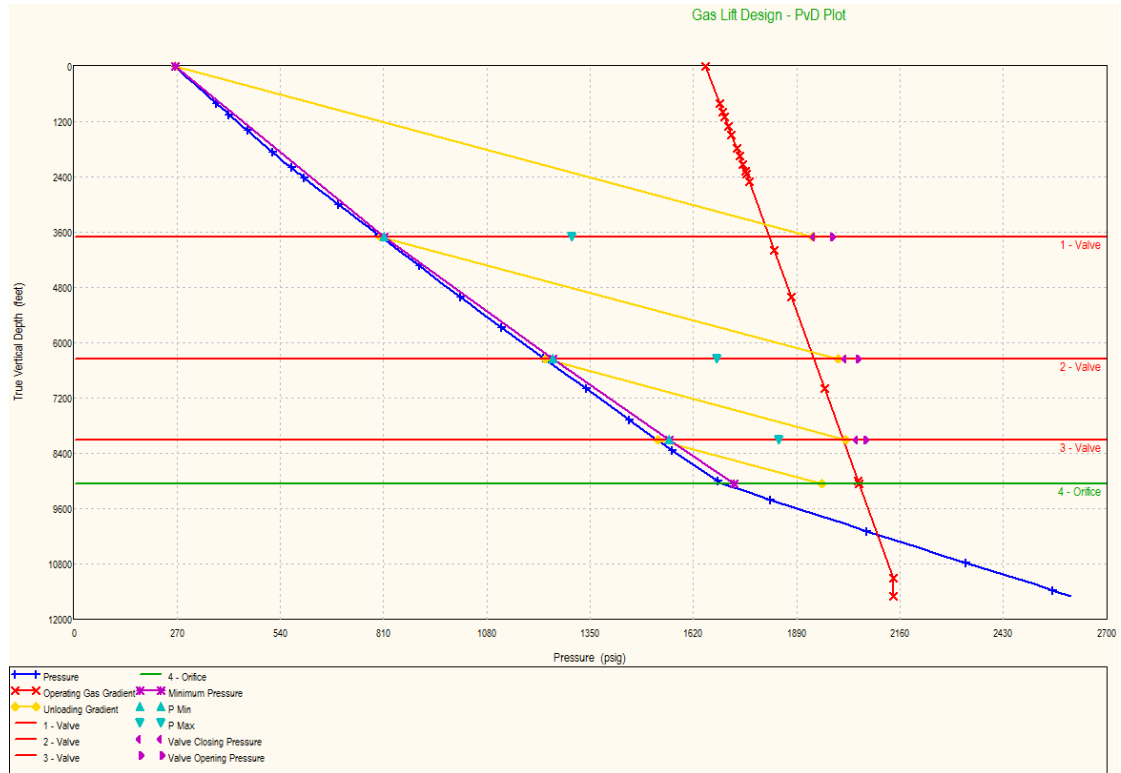


Figure 5.12: Gas lift design: PvD plot (Case 1 revised)

Finally, the gas lift stability criteria are checked. In this case, **Criteria F1 and F2 are equal to 2.03 and -1.83 respectively (Fig. 5.13), indicating a stable gas lift system.** More information on gas lift stability criteria are given in **Section 5.5.**

Since a stable scenario is found, it will be used as groundwork for the following operating conditions as discussed at **Chapter 5.2.**

Done      Main      Export      Help		
<b>Inflow Response Criterion</b>		
Lift Gas Density @ Standard Conditions	0.053662	lb/ft3
FVF of Gas @ Injection Point	0.0084053	ft3/scf
Lift Gas Flow Rate @ Standard Conditions	7.62765	MMscf/day
Liquid Flow Rate @ Standard Conditions	6601.73	STB/day
Productivity Index Of Well	23.6553	STB/day/psi
Orifice Efficiency Factor	0.9	fraction
Injection Port Size	0.18427	in2
<b>F1</b>	<b>2.03268</b>	
<b>Pressure-Depletion Response Criterion</b>		
Tubing Volume Downstream Of Injection Point	1325.36	scf
Gas Conduit Volume	978.475	scf
Acceleration Due To Gravity	32.174	ft/sec/sec
Vertical Depth To Injection Point	9065.75	feet
Tubing Pressure @ Injection Point	1638.58	psig
Reservoir Fluid Density @ Injection Point	53.1849	lb/ft3
Lift Gas Density @ Injection Point	6.36279	lb/ft3
Liquid Flow Rate @ Injection Point	7543.69	STB/day
Lift Gas Flow Rate @ Injection Point	0.064113	MMscf/day
<b>F2</b>	<b>-1.82727</b>	
F1 or F2 should be greater than 1 for Stable Flow.		
Ref. "Criteria for Gas-Lift Stability" - Harald Asheim - JPT November 1988		

**Figure 5.13:** Stability criteria (Case 1 revised)

An overview of the pressures and liquid hold up in the tubing along depth is given in **Figure 5.14**. Recall that liquid hold up is expressed as the fraction of an element of pipe which is occupied by liquid. When oil enters the wellbore, pressure has already dropped below  $P_b$  and a small amount of gas is produced with the oil. As the oil travels upwards, more gas is coming out of the solution. At 12,000', gas injection occurs and gas is the dominant phase in the tubing above this point. **Figure 5.14** shows that at the injection point, hold up is instantly decreased from 0.81 to 0.21. As a result, pressure gradient above that point is decreased as the mild slope of the pressure line indicates. More gas in the tubing leads to a less dense column, hence the mild slope observed.

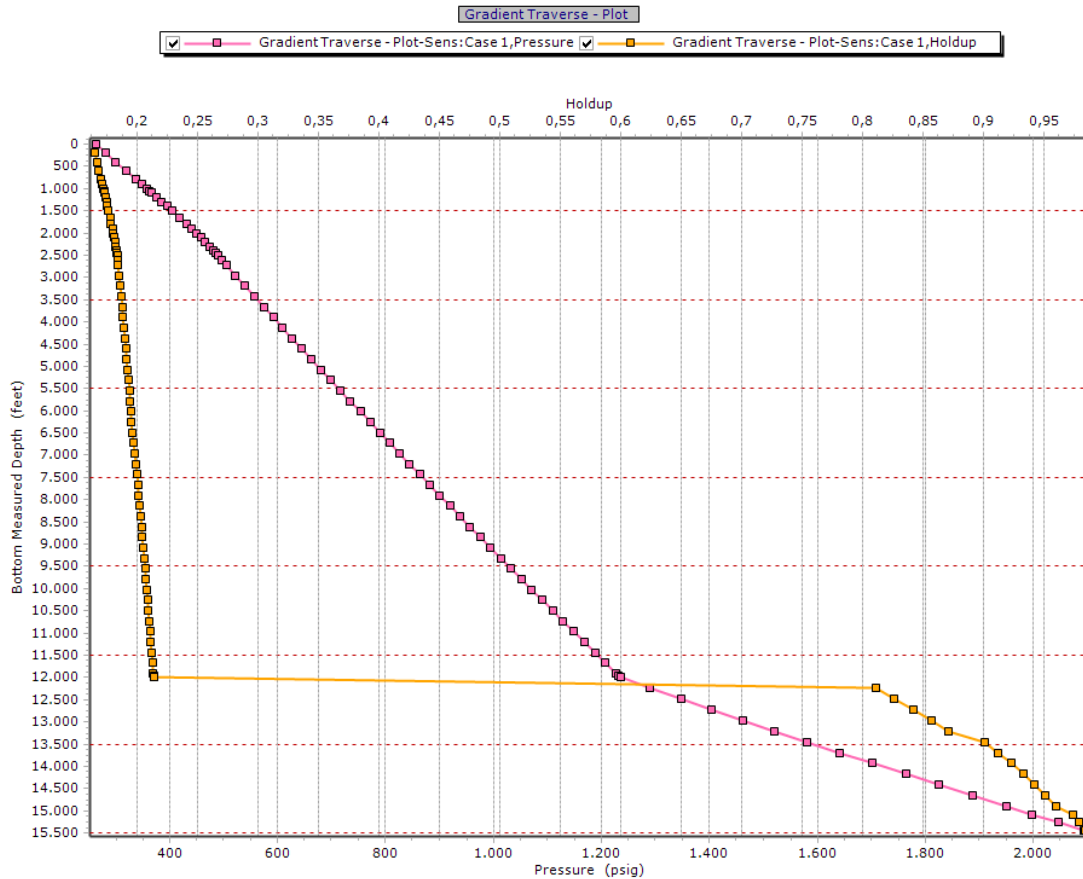


Figure 5.14: Pressure and liquid hold versus depth (Case 1 revised)

### 5.6 Gas lift design process for $\bar{P}_r = 3,100$ psi and water cut 40% (Case 2)

The second case examines the operating conditions at which the reservoir pressure will be 3,100 psi and the water cut 40%. In **Section 5.2**, it is explained that after the design of the gas lift system is carried out for the worst case scenario, the positions of the side pocket mandrels (SPM) will be considered as fixed for all remaining cases. Placing of the valves or the orifice is thus restricted to the existing positions of the SPM.

Once more, the IPR is updated with the new data corresponding the reservoir pressure and water cut level and the design process is initiated.

The option selected this time is not a “New well” but an “Existing mandrels” one. In the main screen, all input data remain the same as previously.

The optimum gas injection rate reported is again 8 MMscf/day, the maximum available (**Fig. 5.15**).

Calculated Rate							
GLR Injected	Liquid Rate	Oil Rate	VLP Pressure	IPR Pressure	Standard Deviation	Design Rate	Oil Production
scf/STB	STB/day	STB/day	psig	psig		MMscf/day	STB/day
1554.0	9337.0	5602.2	3297.4	2657.3	142.533	8.000	4744.8
Get Rate		Plot					

Objective Gradient				
Measured Depth	True Vertical Depth	Pressure	Temperature	Gas Injection Pressure
feet	feet	psig	deg F	psig
11999.9	9065.8	1837.8	243.3	2050.9

The program will look for the completion liquid level in the wellbore and will dummy the valves above.  
 The OIL RATE is being checked for conformance with the IPR.  
 The gas injection may be changed to ensure consistency.  
 This option is slower so please be patient...

Design Plot Results Main Done Help

Results			
Liquid Rate	Oil Rate	Injected Gas Rate	Injection Pressure
STB/day	STB/day	MMscf/day	psig
7907.97	4744.78	5.79704	1700

Valve Details			
Valve Type	Manufacturer	Type	Specification
Casing Sensitive	Camco	R-20	Normal

Figure 5.15: Gas lift design: Calculation screen (Case 2)

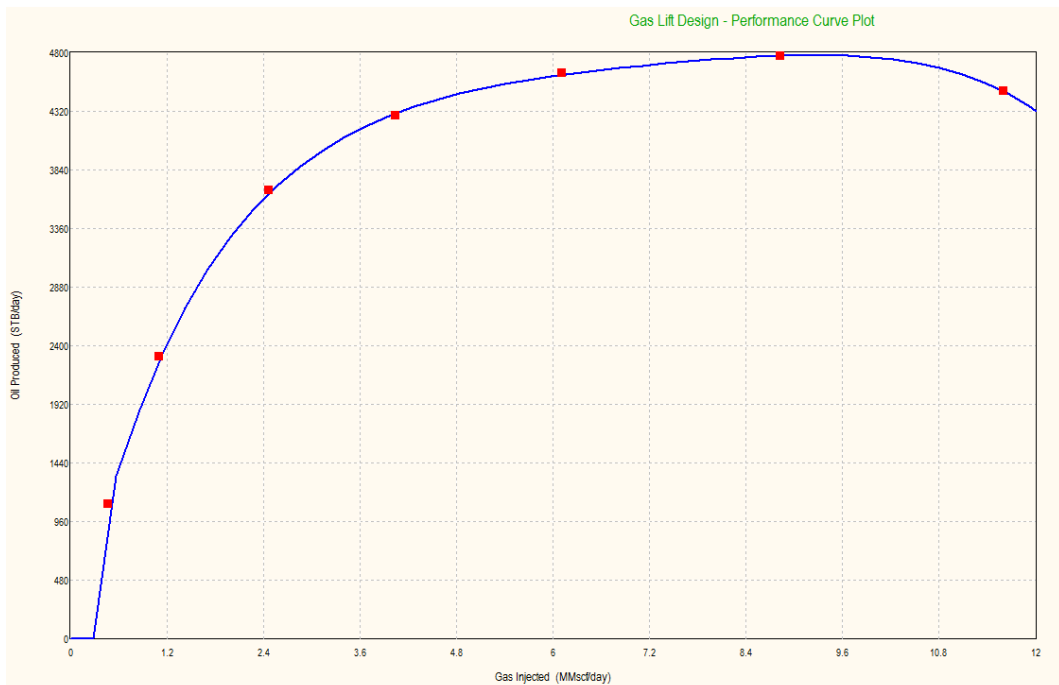


Figure 5.16: Gas lift performance curve (Case 2)

**The valve spacing calculations indicate an operating gas injection rate equal to 5.8 MMscf/day injected at 1,750 psi. This amount of gas yields an oil rate of 4,745 stb/day.**

The difference between the present case and the initial one is that now, not all mandrels contain unloading valves. The first side pocket mandrel contains a dummy valve (**Table 5.3**), (**Fig. 5.17**). A dummy valve is an isolation tool that prevents liquids to flow from the annulus to the tubing and vice versa. This point remains inactive and as a result, the unloading process can be achieved by using valves at higher depths as gas injected in the annulus is capable of displacing annular fluids up to about 8,200' (position of the 2<sup>nd</sup> SPM). **Figure 5.17** indicates that since the well, in these operating conditions (without gas lift), is not flowing (dead well), the surface of the fluids in the annulus is considerably below the casing head. This is proven by the pressure gradient of the casing fluid. Static pressure of annular fluid begins to increase below 2,000'. No need to unload the well at shallow depths, hence a dummy valve is set in the first mandrel, as already mentioned.

The injection depth remains at 12,000' MD, the maximum depth allowed. The injection rate is similar to the first case and equal to 5.8 MMscf/day once again lower than the optimum gas injection rate initially calculated.

**Table 5.3:** Valve spacing results (Case 2)

Valve	Valve type	MD (ft)	TVD (ft)	Tubing pressure (psig)	Casing pressure (psig)	Opening CHP (psig)	Gas lift gas rate (MMscf/day)	Port size (64 <sup>ths</sup> inch)
1	Dummy	4398.5	3690.6	0	0	1800	0	0
2	Valve	8225.7	6396.8	1290.4	2050.8	1800	0.58	8
3	Valve	10801.3	8218.1	1653.6	2069	1750	0.58	12
4	Orifice	12000	9065.8	1837.8	2050.9	1700	5.8	32

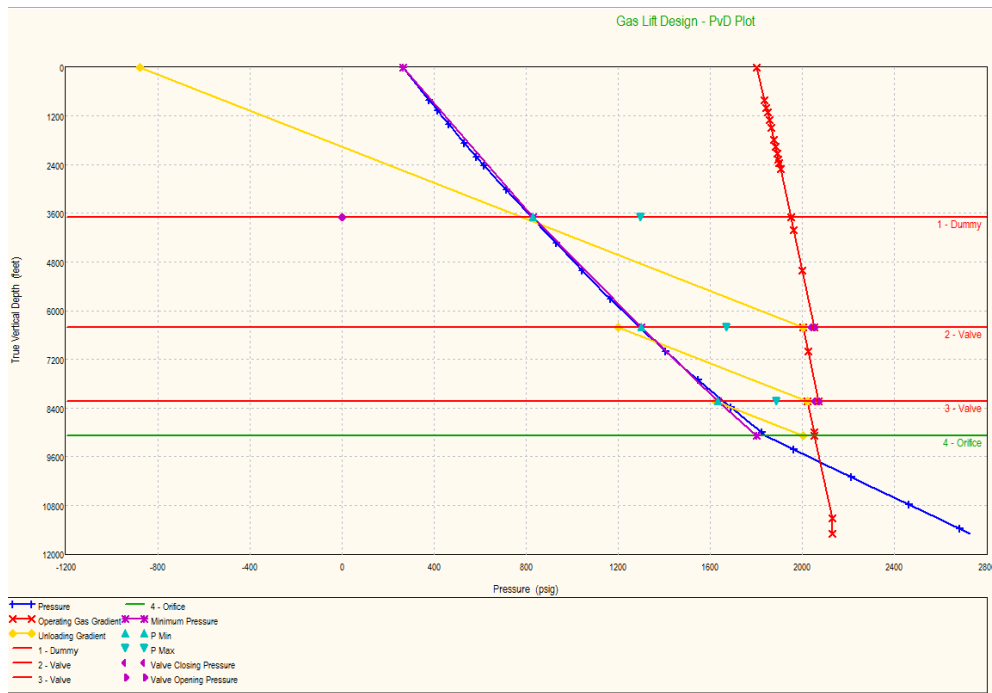


Figure 5.17: Gas lift design: PvD plot (Case 2)

The stability analysis of the second case yields stability criteria  $F1=0.94$  and  $F2=18.7$ , indicating a stable gas lift system (Fig. 5.18).

Done    Main    Export    Help		
<b>Inflow Response Criterion</b>		
Lift Gas Density @ Standard Conditions	0.053662	lb/ft3
FVF of Gas @ Injection Point	0.0086365	ft3/scf
Lift Gas Flow Rate @ Standard Conditions	5.79704	MMscf/day
Liquid Flow Rate @ Standard Conditions	7907.97	STB/day
Productivity Index Of Well	23.0923	STB/day/psi
Orifice Efficiency Factor	0.9	fraction
Injection Port Size	0.19635	in2
<b>F1</b>	<b>0.86589</b>	
<b>Pressure-Depletion Response Criterion</b>		
Tubing Volume Downstream Of Injection Point	1325.36	scf
Gas Conduit Volume	978.475	scf
Acceleration Due To Gravity	32.174	ft/sec/sec
Vertical Depth To Injection Point	9065.75	feet
Tubing Pressure @ Injection Point	1837.83	psig
Reservoir Fluid Density @ Injection Point	51.0409	lb/ft3
Lift Gas Density @ Injection Point	6.19246	lb/ft3
Liquid Flow Rate @ Injection Point	9305.67	STB/day
Lift Gas Flow Rate @ Injection Point	0.050066	MMscf/day
<b>F2</b>	<b>12.8429</b>	
F1 or F2 should be greater than 1 for Stable Flow.		
Ref. "Criteria for Gas-Lift Stability" - Harald Asheim - JPT November 1988		

Figure 5.18: Stability criteria (Case 2)

An overview of the pressures and liquid hold up in the tubing along depth is given in **Figure 5.19**. Note that the fluid entering the wellbore is undersaturated because a value of hold up equal to 1 indicates the absence of free gas. As soon as the fluid travels just a few feet upwards, pressure decreases below  $P_b$  and gas evolves from the oil. Liquid hold up in the injection point decreases from 0.84 to 0.27, slightly higher than the previous case. That difference between the present case and the previous one lies on the fact in the first case, pressure around the wellbore has already dropped below  $P_b$  so gas and oil and water are entering the tubing. However, in the second case, the fluid entering the wellbore is undersaturated. This means that less quantities of gas will evolve for the same distance travelled by the fluid. Once more, the effect of the lighter fluid column above the injection point is visible as a change in slope of pressure lines.

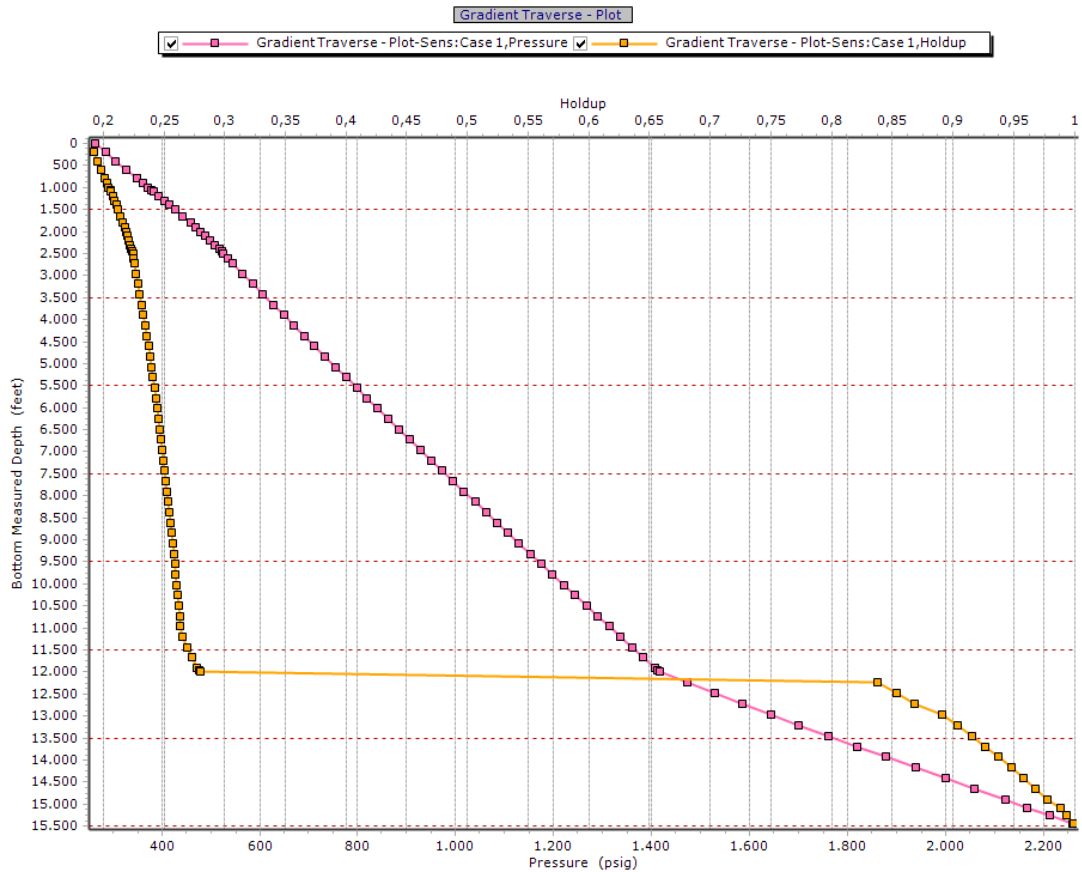


Figure 5.19: Pressure and liquid hold versus depth (Case 2)

### 5.7 Gas lift design process for $\bar{P}_r = 3,400$ psi and water cut 30% (Case 3)

The third case examines more favorable operating conditions, where the reservoir pressure will be 3,400 psi and the water cut 30%. As seen in case 2 in the previous section, the positions of the side pocket mandrels are again fixed i.e. the positions initially calculated (see **Section 5.5**). The procedure followed is the same as case 2.

The optimum gas injection rate is found to be equal to 7.87 MMscf/day, slightly less than previously (**Fig. 5.20**).

Calculated Rate							
GLR Injected	Liquid Rate	Oil Rate	VLP Pressure	IPR Pressure	Standard Deviation	Design Rate	Oil Production
scf/STB	STB/day	STB/day	psig	psig		MMscf/day	STB/day
1398.9	9337.0	6535.9	3195.8	2943.3	505.729	7.873	6709.4

Get Rate Plot

Objective Gradient				
Measured Depth	True Vertical Depth	Pressure	Temperature	Gas Injection Pressure
feet	feet	psig	deg F	psig
10801.3	8218.1	1800.0	239.2	2066.4

The program will look for the completion liquid level in the wellbore and will dummy the valves above.  
 The OIL RATE is being checked for conformance with the IPR.  
 The gas injection may be changed to ensure consistency.  
 This option is slower so please be patient...  
 The gas required to achieve this rate is higher than the gas available. Target Oil Production will be reduced.  
 A new rate is proposed -->> 6575.22 (STB/day)

Design Plot Results Main Done Help

Results			
Liquid Rate	Oil Rate	Injected Gas Rate	Injection Pressure
STB/day	STB/day	MMscf/day	psig
9393.17	6575.22	5.752	1750

Valve Details			
Valve Type	Manufacturer	Type	Specification
Casing Sensitive	Camco	R-20	Normal

Figure 5.20: Gas lift design: Calculation screen (Case 3)

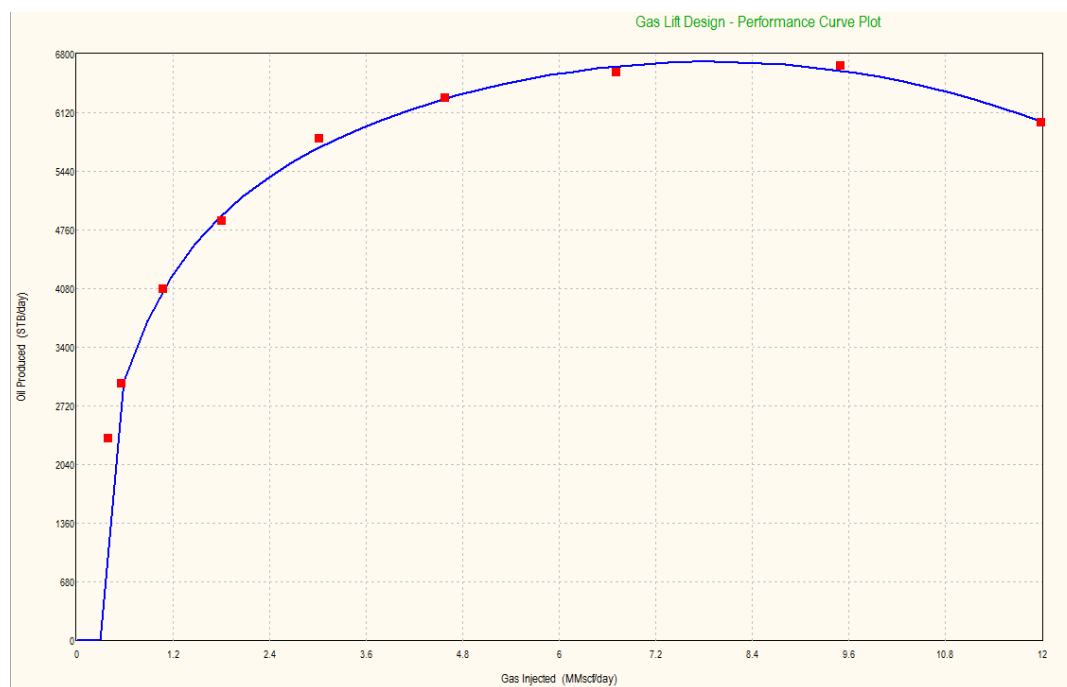


Figure 5.21: Gas lift performance curve (Case 3)

The valve spacing calculations indicate an operating gas injection rate equal to 5.75 MMscf/day injected at 1,750 psi. This amount of gas yields an oil rate of 6,575.22 stb/day.

In this particular case, except for the dummy valve seen on Case 2, which was placed in the first mandrel, there is also a dummy valve at the point where the orifice was previously placed (12,000' MD) in the two previous cases. This means that the injection point is now at 10,643' MD at the third SPM. Analytical results of the calculations are given in **Table 5.4**.

**Table 5.4:** Valve spacing results (Case 3)

Valve	Valve type	MD (ft)	TVD (ft)	Tubing pressure (psig)	Casing pressure (psig)	Opening CHP (psig)	Gas lift gas rate (MMscf/day)	Port size (64 <sup>th</sup> inch)
1	Dummy	4398.5	3690.6	0	0	0	0	0
2	Valve	8225.7	6396.8	1391.3	2048.4	1800	0.58	12
3	Orifice	10801.3	8218.1	1800	2066.5	1750	0.58	30
4	Dummy	12000	9065.8	0	0	0	5.75	0

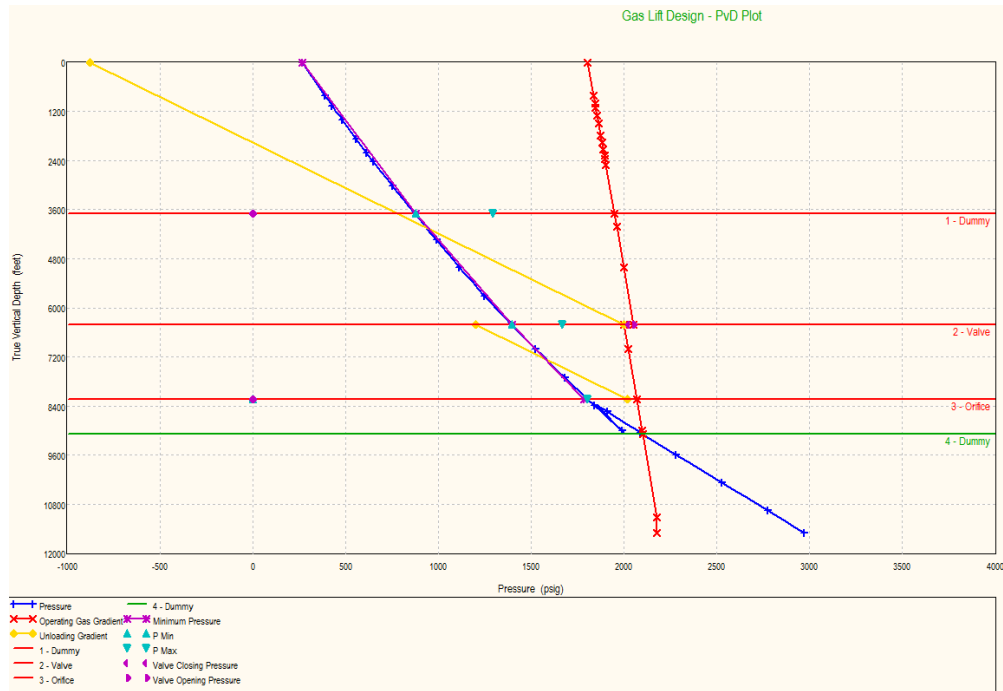


**Figure 5.22:** Gas lift design: PvD plot (Case 3)

It should be noted that, even though more favorable conditions are examined in this section, the injection point is set at a shallower depth than previously. To interpret this effect, consider that a greater injection depth means that the lift gas will be injected at a point where little or no amounts of liberated gas (if pressure at this depth is above  $P_b$ ) will be present in the tubing. Thus, the gas lift system will reduce the density of a heavy fluid column. The opposite occurs at shallower depths where significant amounts of gas previously dissolved in oil will be already in the tubing and the efficiency of the gas lift will be seriously affected.

The objective of gas lift is to reduce the density of heaviest fluid column possible. The present valve spacing and injection depth do not serve this cause.

An important observation from **Figure 5.22** is that gas pressure cannot overcome the static pressure of the annular fluid. The KO injection pressure in all cases is decided to be set at 1,800 psi. It is already mentioned that, pressure restriction of the casing is 2,000 psi. In the next section, the revised scenario of this section will examine the increase in KO injection pressure at 1,900 psi, very close to the restriction, and its effect on the valve positioning.

### 5.7.1 Revision of Case 3

The KO pressure is now at 1,900 psi always below casing restriction. **Figure 5.23** shows that, indeed, the injection point is now transferred to the last mandrel and the initial assumption made in **Section 5.7** have been verified to be correct. Optimum gas rate is 5.21 MMscf/day which is capable of delivering 6,714 stb/day.

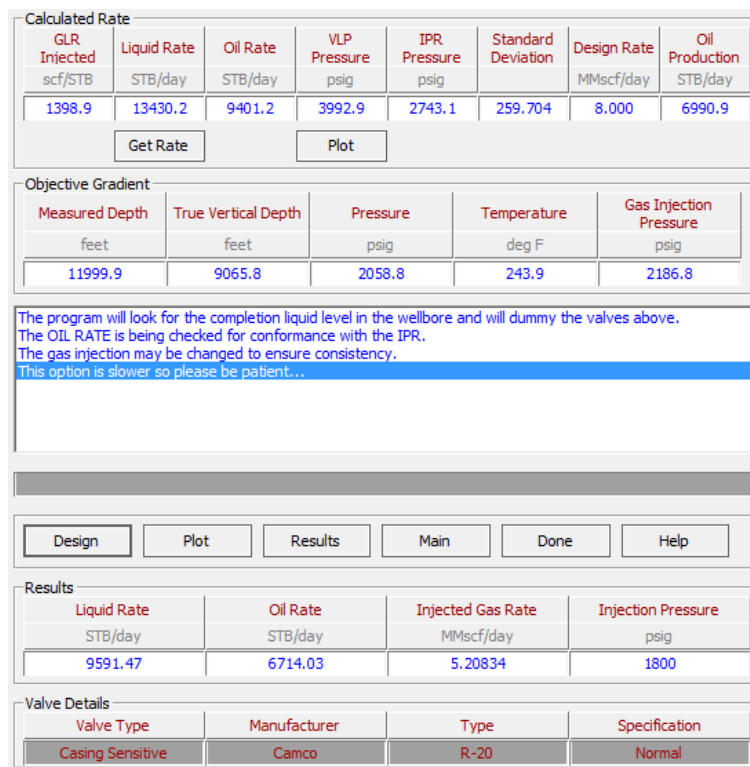


**Figure 5.23:** Gas lift design (Case 3 revised)

The new gas lift design plot can be seen in the following figure (**Fig. 5.24**). Dummy valve newly place at the first mandrel and the orifice lies at the deepest point possible (12,000’).

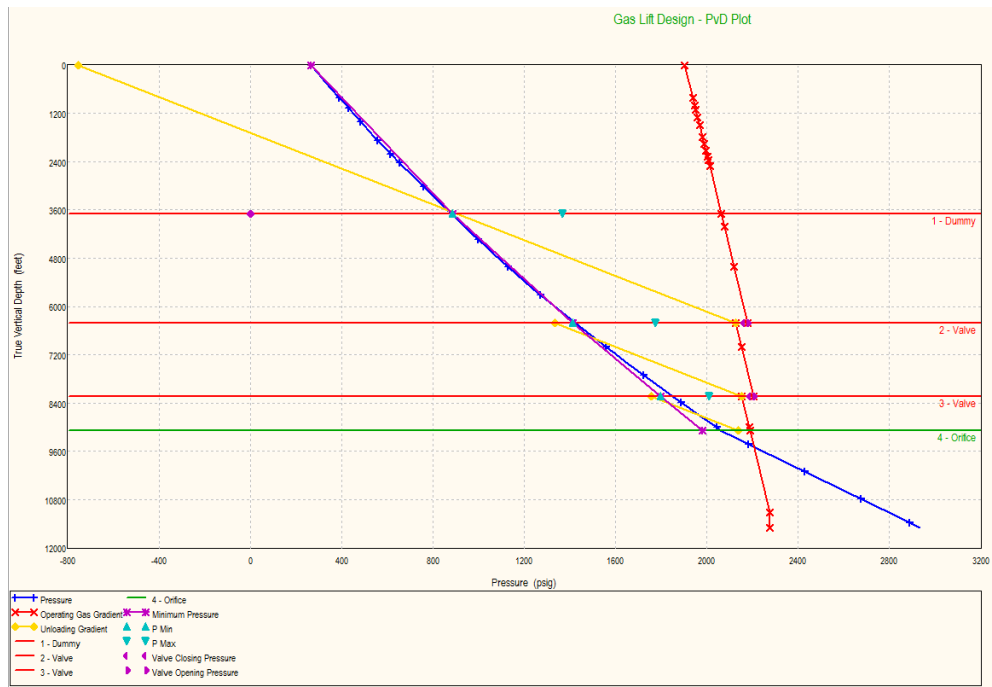


Figure 5.24: Gas lift design: PvD plot (Case 3 revised)

Table 5.5: Valve spacing results (Case 3 revised)

Valve	Valve type	MD (ft)	TVD (ft)	Tubing pressure (psig)	Casing pressure (psig)	Opening CHP (psig)	Gas lift gas rate (MMscf/day)	Port size (64ths inch)
1	Dummy	4398.5	3690,6	0	0	1900	0	0
2	Valve	8225.7	6396.8	1420.5	2175	1900	0.52	12
3	Valve	10801.3	8218.1	1846.23	2201.1	1850	0.85	34
4	Orifice	12000	9065.8	2058.8	2186.8	1800	5.21	0

Stability of the revised system is ensured by the Pressure-Depletion Response Criterion  $F2 = 2.92$  (Fig. 5.25).

Done      Main      Export      Help		
<b>Inflow Response Criterion</b>		
Lift Gas Density @ Standard Conditions	0.053662	lb/ft3
FVF of Gas @ Injection Point	0.0081059	ft3/scf
Lift Gas Flow Rate @ Standard Conditions	5.20834	MMscf/day
Liquid Flow Rate @ Standard Conditions	9591.47	STB/day
Productivity Index Of Well	22.3852	STB/day/psi
Orifice Efficiency Factor	0.9	fraction
Injection Port Size	0.22166	in2
<b>F1</b>	<b>0.41141</b>	
<b>Pressure-Depletion Response Criterion</b>		
Tubing Volume Downstream Of Injection Point	1325.36	scf
Gas Conduit Volume	978.475	scf
Acceleration Due To Gravity	32.174	ft/sec/sec
Vertical Depth To Injection Point	9065.75	feet
Tubing Pressure @ Injection Point	2058.8	psig
Reservoir Fluid Density @ Injection Point	48.8001	lb/ft3
Lift Gas Density @ Injection Point	6.5978	lb/ft3
Liquid Flow Rate @ Injection Point	11695.9	STB/day
Lift Gas Flow Rate @ Injection Point	0.042218	MMscf/day
<b>F2</b>	<b>2.92398</b>	
F1 or F2 should be greater than 1 for Stable Flow.		
Ref. "Criteria for Gas-Lift Stability" - Harald Asheim - JPT November 1988		

**Figure 5.25:** Stability criteria (Case 3 revised)

An overview of the pressures and liquid hold up in the tubing along depth is given in **Figure 5.26**. Similarly to case 2, the fluid enters the wellbore undersaturated and liberated gas is evolving at 14,000' when  $P_b$  is reached. The liquid hold up is even larger when the fluid reaches the injection point, in comparison to the previous cases and it is equal to 0.9. The injected gas reduced the liquid hold up to 0.41. The effect of the injected gas to the pressure gradient of the fluid is again visible above and below the injection point. As operating conditions get more favorable, the combination of lower optimum gas rates and less gas evolving from oil result to a quite satisfying value of liquid hold up just below the wellhead equal to 0.25.

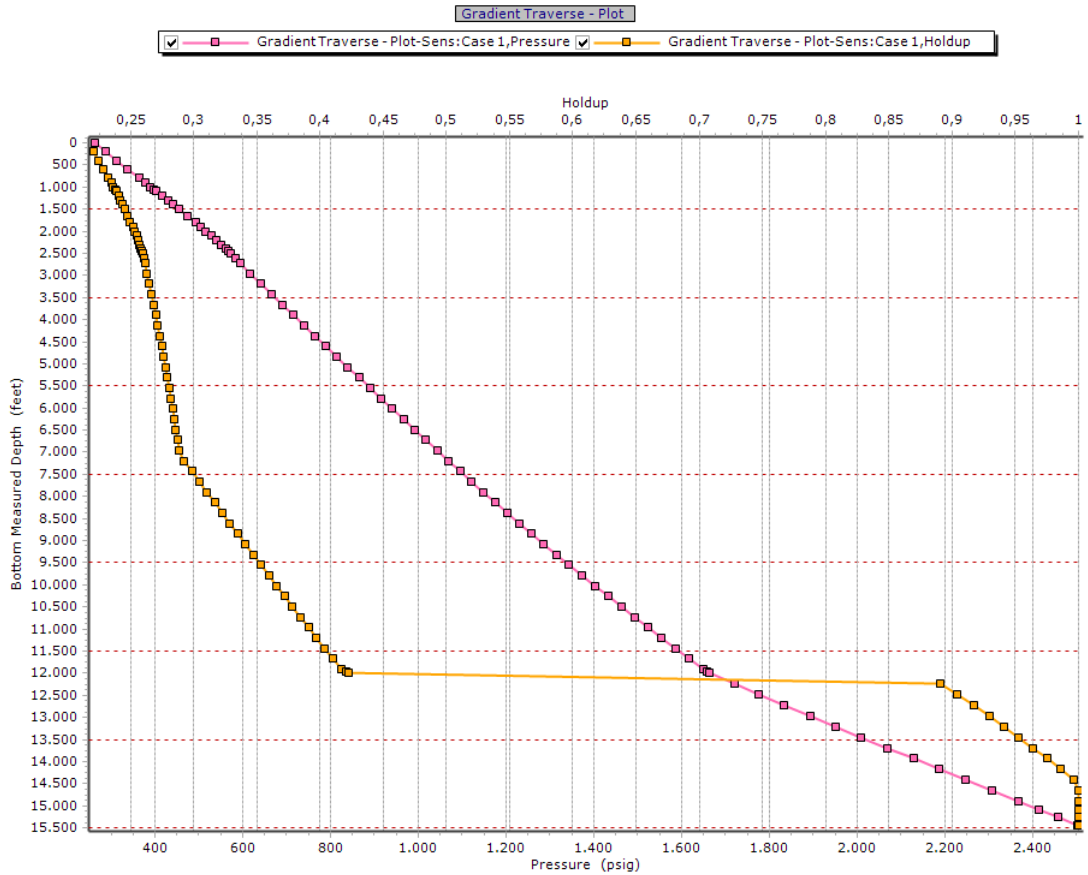


Figure 5.26: Pressure and liquid hold versus depth (Case 3 revised)

### 5.8 Gas lift design process for $\bar{P}_r = 3,795.2$ psi and water cut 20.3% (Case 4)

The fourth and last case examines the current operating conditions. The IPR is newly updated. The optimum gas injection rate is found to be equal to 8 MMscf/day (Fig. 5.27).

Calculated Rate							
GLR Injected	Liquid Rate	Oil Rate	VLP Pressure	IPR Pressure	Standard Deviation	Design Rate	Oil Production
scf/STB	STB/day	STB/day	psig	psig		MMscf/day	STB/day
1054.1	13430.2	10703.9	3830.5	3108.9	487.523	8.000	9323.5

Get Rate Plot

Objective Gradient				
Measured Depth	True Vertical Depth	Pressure	Temperature	Gas Injection Pressure
feet	feet	psig	deg F	psig
10801.3	8218.1	1998.8	239.4	2094.4

The program will look for the completion liquid level in the wellbore and will dummy the valves above.  
 The OIL RATE is being checked for conformance with the IPR.  
 The gas injection may be changed to ensure consistency.  
 This option is slower so please be patient...

Design Plot Results Main Done Help

Results			
Liquid Rate	Oil Rate	Injected Gas Rate	Injection Pressure
STB/day	STB/day	MMscf/day	psig
10782.1	8593.36	4.12486	1700

Valve Details			
Valve Type	Manufacturer	Type	Specification
Casing Sensitive	Camco	R-20	Normal

Figure 5.27: Gas lift design: Calculation screen (Case 4)

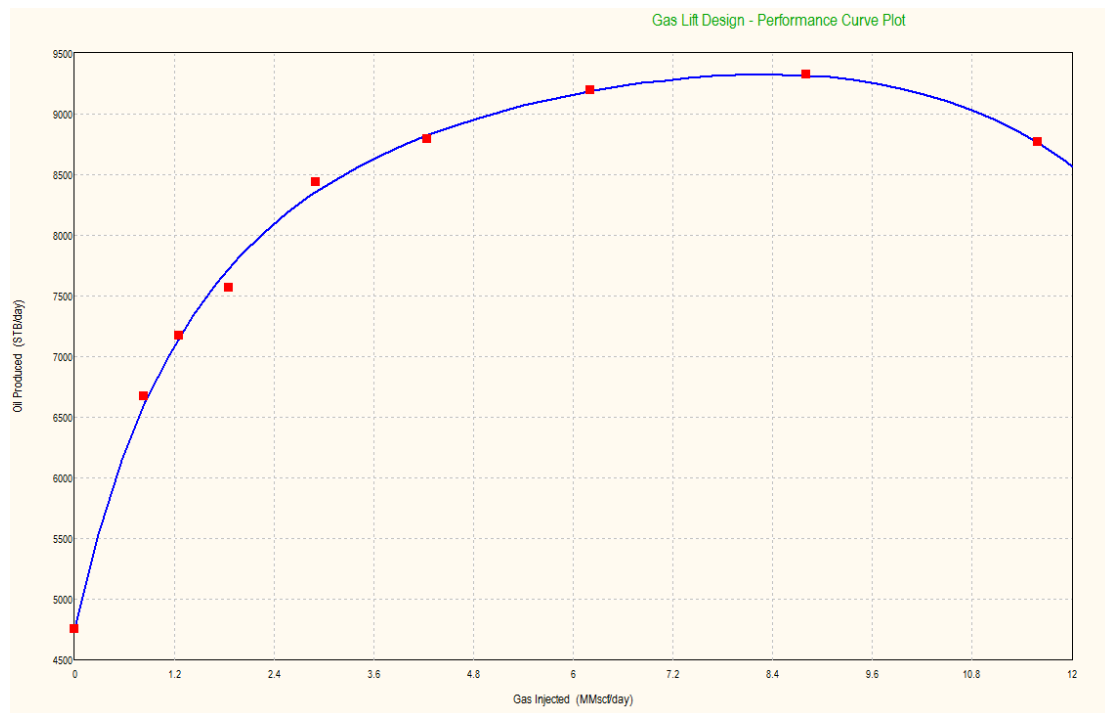


Figure 5.28: Gas lift performance curve (Case 4)

The valve spacing calculations indicate an operating gas injection rate equal to 4.12 MMscf/day injected at 1,700 psi. This amount of gas yields an oil rate of 8,593 stb/day.

This case exhibits the same valve spacing configuration as Case 3 in **Section 5.7 (Table 5.6), (Fig. 5.29)**. The dummy valve at the first SPM is now replaced by an unloading valve. In **paragraph 3.4.4.1**, it is already discussed that before the unloading process, all valves are open, and the tubing and annulus are connected. Pressure equilibrium occurs, and due to the fact that the well is now flowing, the pressure at the casing head will now be 264 psi equal to the wellhead pressure. Gas lift will now have to beat the annular fluid pressure gradient that starts from the surface at 264 psi. This is the reason why a valve is newly placed at the first mandrel in order to achieve the unloading process. The injection point is not at 12,000' and questions are again raised on whether the system is designed optimally or not. An attempt to increase the injection depth by increasing the injection pressure at the casing head, as tested in **Section 5.7**, is again tested in the next paragraph.

**Table 5.6:** Valve spacing results (Case 4)

Valve	Valve type	MD (ft)	TVD (ft)	Tubing pressure (psig)	Casing pressure (psig)	Opening CHP (psig)	Gas lift gas rate (MMscf/day)	Port size (64ths inch)
1	Valve	4398.5	3690.6	916.7	1957.2	1800	0	0
2	Valve	8225.7	6396.8	1525.1	2019.1	1750	0.631	12
3	Orifice	10801.3	8218.1	1998	2094.5	1700	0.631	12
4	Dummy	12000	9065.8	0	0	0	0	0

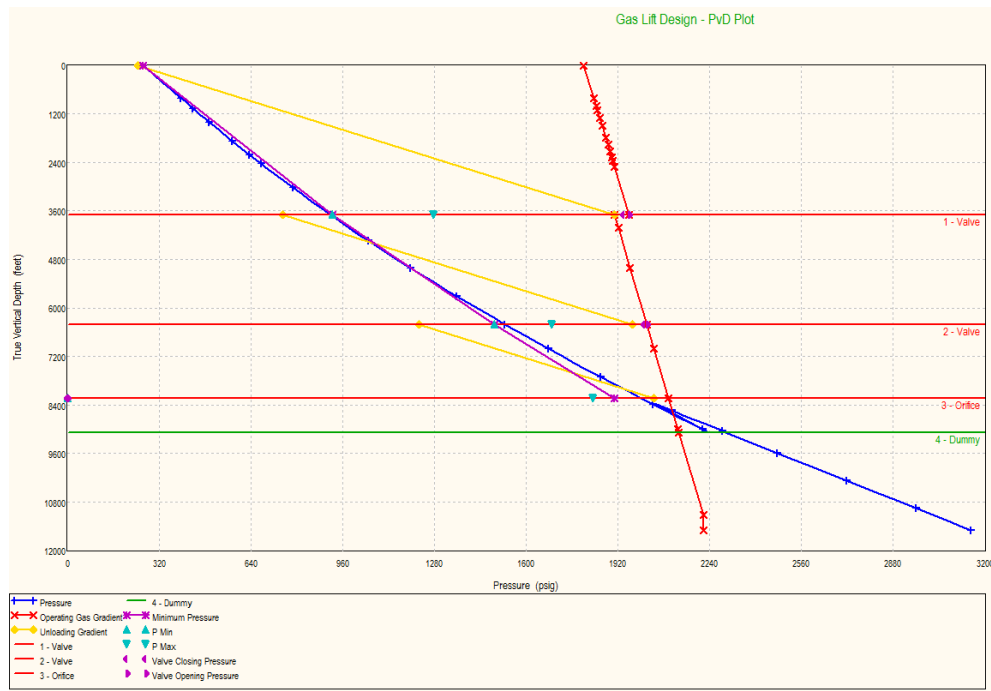


Figure 5.29: Gas lift design: PvD plot (Case 4)

### 5.8.1 Revision of Case 4

The same strategy as the revised case 3 is applied in this paragraph. The KO injection pressure is again raised at 1,900 psi to investigate whether the deepest point of injection can be reached at the unloading process.

Figure 5.30 illustrates that the application of this excess pressure is not capable of transferring the injection depth to the last SPM at 12,000', so the initial design occurs, as the conservative approach of 1,800 psi injected is judged to be more appropriate even though the oil rate is greater in the second case (9,299 stb/day).

Calculated Rate							
GLR Injected	Liquid Rate	Oil Rate	VLP Pressure	IPR Pressure	Standard Deviation	Design Rate	Oil Production
scf/STB	STB/day	STB/day	psig	psig		MMscf/day	STB/day
1054.1	13430.2	10703.9	3562.4	3108.9	378.428	8.000	9299.1
Get Rate			Plot				

Objective Gradient				
Measured Depth	True Vertical Depth	Pressure	Temperature	Gas Injection Pressure
feet		psig	deg F	psig
10801.3	8218.1	2038.4	240.2	2141.4

The program will look for the completion liquid level in the wellbore and will dummy the valves above.  
 The OIL RATE is being checked for conformance with the IPR.  
 The gas injection may be changed to ensure consistency.  
 This option is slower so please be patient...

Design	Plot	Results	Main	Done	Help
--------	------	---------	------	------	------

Results			
Liquid Rate	Oil Rate	Injected Gas Rate	Injection Pressure
STB/day	STB/day	MMscf/day	psig
11667.7	9299.15	5.50319	1800

Valve Details			
Valve Type	Manufacturer	Type	Specification
Casing Sensitive	Camco	R-20	Normal

Figure 5.30: Gas lift design: Calculation screen (Case 4 revised)

The stability analysis of the fourth case yields stability criteria  $F1=0.29$  and  $F2=2.37$ , indicating a stable gas lift system (Fig 5.31).

Done			Main			Export			Help		
Inflow Response Criterion											
Lift Gas Density @ Standard Conditions	0.053662	lb/ft3									
FVF of Gas @ Injection Point	0.0083824	ft3/scf									
Lift Gas Flow Rate @ Standard Conditions	4.1178	MMscf/day									
Liquid Flow Rate @ Standard Conditions	10772.5	STB/day									
Productivity Index Of Well	21.4271	STB/day/psi									
Orifice Efficiency Factor	0.9	fraction									
Injection Port Size	0.19635	in2									
F1	0.28884										
Pressure-Depletion Response Criterion											
Tubing Volume Downstream Of Injection Point	1192.97	scf									
Gas Conduit Volume	880.735	scf									
Acceleration Due To Gravity	32.174	ft/sec/sec									
Vertical Depth To Injection Point	8218.05	feet									
Tubing Pressure @ Injection Point	1998.15	psig									
Reservoir Fluid Density @ Injection Point	47.4166	lb/ft3									
Lift Gas Density @ Injection Point	6.38017	lb/ft3									
Liquid Flow Rate @ Injection Point	13292.6	STB/day									
Lift Gas Flow Rate @ Injection Point	0.034517	MMscf/day									
F2	2.37292										
F1 or F2 should be greater than 1 for Stable Flow.											
Ref. "Criteria for Gas-Lift Stability" - Harald Asheim - JPT November 1988											

**Figure 5.31:** Stability criteria (Case 4)

An overview of the pressures and liquid hold up in the tubing along depth is given in **Figure 5.32**. This case represents the most favorable operating conditions seen so far. Liquid hold up equal to 0.55 after the injection point is by far the largest value observed compared to all previous examined cases. The fluid is entering the wellbore with a larger pressure and in combination with the fact that the bubble point is reached well above bottomhole, more gas remains dissolved in the oil until the fluid reaches the surface. The pressure gradient has not significant differences before and after injection of gas because the amount of evolved gas is much less in this case and the fluid column is heavier in respect to all the previous cases. Changes in the shape of the hold up line at lower depths corresponds to the change from bubble to slug flow.

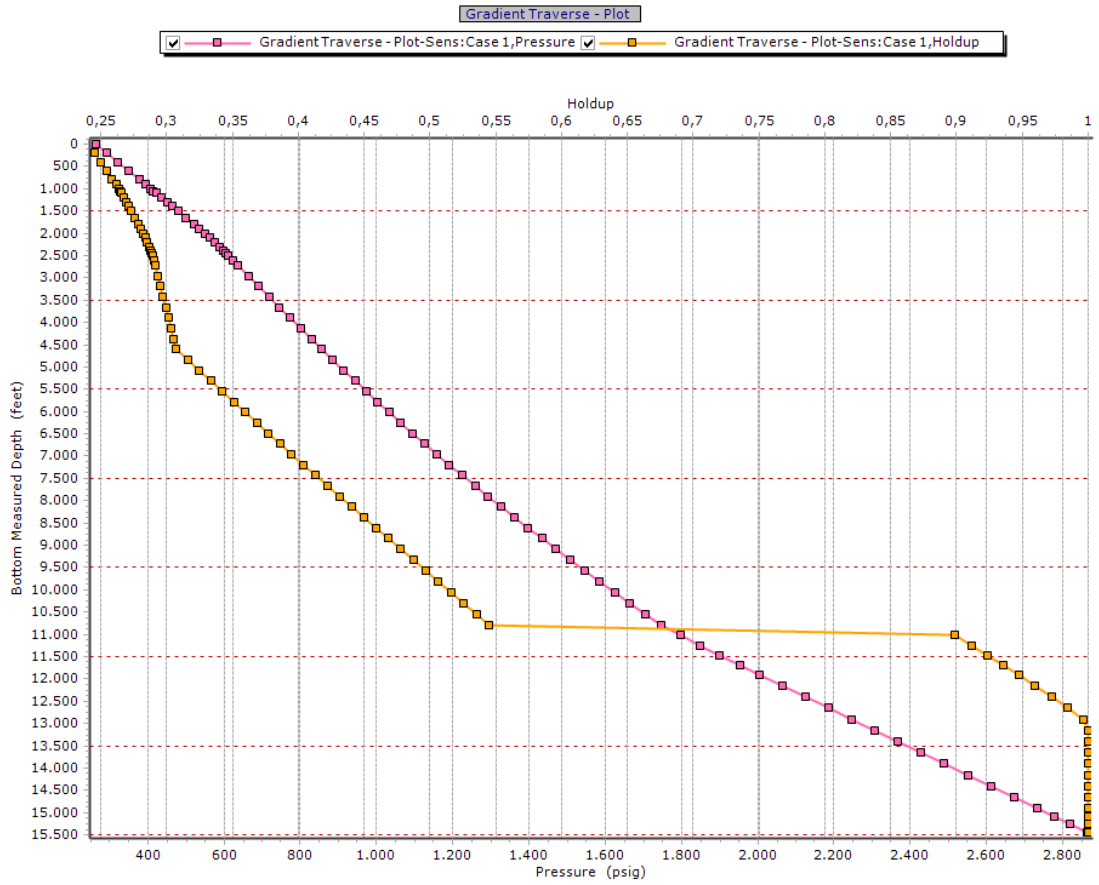


Figure 5.32: Pressure and liquid hold versus depth (Case 4 revised)



## 6. Conclusions

The purpose of the present MSc thesis was to design a continuous gas lift system for a well whose current design and operating conditions are severely affecting its productivity and it is about to cease flowing in the upcoming months.

A mathematical model, consisting of many submodels, was created in PROSPER to predict achievable fluid production rates in various operating conditions. The modelling of all parameters such as the IPR curve, the PVT data, downhole equipment and the temperature profile along the well was carried out without any issue. Although, during the VLP/IPR matching process, deviations between modeled and measured data for the well tests provided, were observed. Since the VLP curve was already matched, the IPR curve had to be revised. PROSPER gives the opportunity to adjust the average reservoir pressure and the skin factor. The investigation of the effect of these two variables, the ones with the highest amount of uncertainty, showed that both parameters can be adjusted individually without any significant effect on the validity of the model. The investigation includes adjustment of the IPR in terms of either  $P_r$  or  $S$  and at the same time a set of sensitivity analyses on various (a) water cut levels, (b) with and without the implementation of an ESP and (c) various top node pressures. Results showed no significant deviations in the liquid rates whatsoever. This means that both parameters, for this system, almost equally affect the inflow performance of the well and it is the engineer's choice, which parameter is more suitable to be altered. Finally, the reservoir pressure is adjusted and calculations continued with the revised value of pressure.

As far as the gas lift design process is concerned, sensitivity analysis on tubing diameters up to 4.5" indicated that the gas slip effect on the well deliverability, which could lead to significant productivity reduction for enhanced tubing diameters, is minimal. Therefore, the new production tubing, upon which the gas lift design took place, is chosen to be the maximum possible, i.e. 4.5" ID due to casing ID restriction (6.4" ID) so as to maximize production. However, for future recompletions, the tubing size must be reconsidered when larger quantities of gas (gas lift gas and gas coming out of solution) are anticipated.

The design of the gas lift system was run so that the production was optimized for all examined cases. Under these optimal design, the obtained oil rates exceed by far the economic limit which was set at 2,000 stb/day. The achieved oil rates vary from 3,300 to 8,593 stb/day depending on the operating conditions. Those production rates, in combination with a single recompletion workover for a wide range of reservoir pressure and water cut levels, provide an economically efficient design which can deliver large quantities of liquid with the same well configuration for several months after the examined period.

The valve spacing based on the worst case scenario ( $P_r=2,850$  psi, water cut 50%) fits adequately to the rest of the scenarios. Maximum injection depth was set at 12,000' because pre-calculations showed that the stability of the gas lift

system is at stake if injection of gas is about to take place at a very deep point (14,000') even though the increased injection depth yields greater oil rates. In Case 3, in **Section 5.7**, the injection pressure at the casing head was not sufficient to unload casing fluids and reach the last valve. The system was pushed to its limits, in terms of casing strength and the pressure it can withstand. A slight increase of 100 psi in the injection pressure, indeed, fits the purpose and production was optimized. Likewise, at current conditions where the highest  $P_r$  and lowest water cut are exhibited, the deepest valve at the last SPM could not again be reached. The same technique of increasing injection pressure was applied with no results. Nevertheless, despite the shallower point of gas injection, the production levels were satisfactory thus avoiding the need to run future multiple recompletion projects.

It should be noted that, even though the work done in this thesis led to successful results, in reality, production optimization problems are far too complex and every well cannot be optimized individually. When more wells are present an optimization software like GAP from PETEX is necessary to achieve full field optimization and maximize revenue.

.

---

## References

---

- [1] Beggs H. (2008), *Production Optimization Using Nodal Analysis*, Oil & Gas Consultants, 2nd edition.
- [2] Ahmed, T. (2010). *Reservoir Engineering Handbook*. Reservoir Engineering Handbook. Elsevier. doi:10.1016/B978-1-85617-803-7.50001-8
- [3] Evinger, H.H. and Muskat, M. (1942). *Calculation of Theoretical Productivity Factor*, Trans., AIME 146, 126.
- [4] Vogel, J.V. (1968). *Inflow Performance Relationships for Solution-Gas Drive Wells*. J. Pet. Technol. 20 (1): 83–92. SPE 1476-PA
- [5] Production Technology (2011), Heriot Watt University, Institute of Petroleum Engineering 2011
- [6] PetroWiki, (2015). *Wellbore flow performance* [http://petrowiki.org/Wellbore\\_flow\\_performance](http://petrowiki.org/Wellbore_flow_performance), (accessed 04 September, 2015).
- [7] Golan, M., & Whitson, C. H. (1991). *Well performance*. Englewood Cliffs, N.J: Prentice Hall.
- [8] Boyun, G., (2007). *Petroleum Production Engineering, A Computer-Assisted Approach*, 1st Edition | ISBN 9780750682701
- [9] Norwegian Society for Oil and Gas Measurement (NFOGM), (2005). *Handbook of Multiphase Flow Metering*
- [10] Gaurav, N. (2008). *Flow regime transitions during condensation in microchannels*, MSc thesis. Georgia Institute of Technology
- [11] Ali F., (2009). *Two phase flow in large diameter vertical riser*, Phd Thesis. Cranfield University, School of Engineering
- [12] Guo B.; Lyon W.,Ghalambor, (2007). *Petroleum Production Engineering: A Computer Assisted Approach*. Gulf Professional Publishing, ISBN: 9780750682701
- [13] PetroWiki, (2015). *Artificial Lift*. [http://petrowiki.org/Artificial\\_lift](http://petrowiki.org/Artificial_lift) (accessed 10 August, 2015)
- [14] Clegg, J. D., (2007). *Petroleum-Engineering-Handbook-Volume-IV-Production-Operations-Engineering*. Dallas, Texas: Society of Petroleum Engineers. ISBN 978-1-55563-118-5.

- [15] American Petroleum Institute, (1961). *History of Petroleum Engineering*. New York: American Petroleum Institute.
- [16] PetroWiki, (2013). *Sucker Rod Lift*. [http://petrowiki.org/Sucker-rod\\_lift](http://petrowiki.org/Sucker-rod_lift), (accessed 10 August, 2015)
- [17] Takacs, G., (2003). *Sucker-Rod Pumping Manual*. PennWell Books: Tulsa, OK, USA
- [18] Economides, J. M., Hill A. D., Ehlig-Economides C. (1994), *Petroleum Production Systems*. Prentice Hall.
- [19] Gamboa, J., Olivet, A., González, P. and Iglesias, J., (2002). *Understanding the Performance of a Progressive Cavity Pump with a Metallic Stator*, Proceedings of the 20th International Pump Users Symposium
- [20] PetroWiki, (2015). *Progressive cavity pump (PCP) systems* [http://petrowiki.org/Progressing\\_cavity\\_pump\\_\(PCP\)\\_systems](http://petrowiki.org/Progressing_cavity_pump_(PCP)_systems), (accessed 12 August, 2015)
- [21] Karassik, I. J., (2001). *Pump Handbook*, 3rd Edition. McGraw-Hill, New York
- [22] PetroWiki, 2015. *Phase characterization of in-situ fluids* [http://petrowiki.org/Phase\\_characterization\\_of\\_in-situ\\_fluids](http://petrowiki.org/Phase_characterization_of_in-situ_fluids) (accessed 12 August, 2015).
- [23] Kirkpatrick, C. V., (1959). *Advances in gas lift technology*.
- [24] Schlumberger. *Gas Lift Design and Technology*. Well Completions and Productivity. Chevron Main Pass 313 Optimization Project 09/12/00
- [25] American Petroleum Institute, (1994). *API gas lift manual*, Book 6 of the Vocational Training series, Exploration and Production Department, Washington DC 2005-4070, USA, third edition
- [26] Avery, D. J., Evans R.D. (1988). *Design Optimization of Plunger Lift Systems*. Society of Petroleum Engineers (SPE)
- [27] McCain, W. D. (1990), *The Properties of Petroleum Fluids*. 2<sup>nd</sup> ed. Tulsa, OK: Pennwell
- [28] Petroleum Experts, *Prosper User Manual*, Single Well Systems Analysis, Version 13.0, June 2014.
- [29] Duns, H., Jr. and Ross, N. C. J. (1963). *Vertical Flow of Gas and Liquid Mixtures in Wells*.

- [30] Ruiz, R., Marquez, J., Brito, A., (2014). *Evaluation of Multiphase Flow Models to Predict Pressure Gradient in Vertical Pipes With Highly Viscous Liquids*. Society of Petroleum Engineers (SPE). SPE-169328-MS

Asheim, H., (1988). *Criteria for Gas-lift Stability*. Journal of Petroleum Technology, Vol. 40, p. 1452-1456



## Nomenclature

$\gamma_{\text{gas}}$ : gas specific gravity

$\mu$ : viscosity, cp

$\Delta P_f$ : Pressure loss due to friction, psi

$\Delta P_g$ : Pressure loss potential energy change, psi

$\Delta P_k$ : Pressure loss due kinetic energy change, psi

$\Delta P_{\text{pump}}$ :  $\Delta P$  created by the pump, psi

$\rho_{\text{fluid}}$ : Density of the fluid, lbm/ft<sup>3</sup>

$A_{\text{gas}}$ : Pipe area occupied by gas, ft<sup>2</sup> or in<sup>2</sup>

$A_{\text{liquid}}$ : Pipe area occupied by liquid, ft<sup>2</sup> or in<sup>2</sup>

$A_{\text{pipe}}$ : Cross section area of the pipe, ft<sup>2</sup> or in<sup>2</sup>

$B_o$ : Formation volume factor, bbl/stb

$\bar{C}_p$ =Weighted average specific heat capacity for all the phases, BTU/lb/°F

$C_{p,\text{gas}}$ : average heat capacity of gas, BTU/lb/°F

$C_{p,\text{oil}}$ : average heat capacity of oil, BTU/lb/°F

$C_{p,\text{water}}$ : average heat capacity of water, BTU/lb/°F

$D$ : Pipe diameter, inches

$f$ : Moody friction factor

$g$ : Acceleration due to gravity, ft/s<sup>2</sup>

$G_2$ : Geothermal gradient, °F/ft

GOR: Produced gas to oil ratio, scf/stb

$G_s$ : Static fluid pressure gradient, psi/foot

$h$ : Reservoir thickness, ft

$J$ : Productivity index, stb/day/psi

$k$ : permeability, md

$L$ : Length of the pipe, ft

$N_{re}$ : Reynolds number

$P_b$ : Bubble point, psi

$\bar{P}_r$ : Average reservoir pressure, psi

$P_{wf}$ : Downhole flowing pressure, psi

$q$ : flow rate, ft<sup>3</sup>/day

$q_{\max}$ : AOF, ft<sup>3</sup>/day

$r_e$ : External drainage radius, ft

$R_s$ : Gas solubility, scf/stb

$r_w$ : wellbore radius, ft

$S$ : Skin factor

$T(x)$ : ambient temperature at a segment depth  $x$ , °F

$T_{a1}$ : ambient temperature at  $L_1$ , °F

$T_{\text{fluid, ave}}$ : The average temperature of the fluid in a segment depth  $x$ , °F

$T_{\text{in}}$ : Temperature of the fluid before entering segment  $x$ , °F

$T_{\text{out}}$ : Temperature of the fluid after exiting segment  $x$ , °F

$T_{\text{res}}$ : Reservoir temperature, °F

$u$ : Velocity, ft/s

$U$ : overall heat transfer coefficient, BTU/hr/ft<sup>2</sup>/F

$V_s$ : Slip velocity, ft/s

$V_{s, \text{gas}}$ : Gas superficial velocity, ft/s

$V_{s, \text{liquid}}$ : Liquid superficial velocity, ft/s



After 1,000', the inclination angle is being built with a constant angle rate of 3°/100 ft. The measured depth when the objective angle  $\theta$  (45°) is built, is:

$$MD = \frac{45^\circ}{\frac{3^\circ}{100 \text{ ft}}} + 1,000 \text{ ft} = 2,500 \text{ ft} \quad \text{Eq. A-2}$$

The TVD at 2,500 ft MD needs to be calculated. First of all, the arc length BD in **Figure A-1** is known and equal to the MD calculated in **Eq. A-2**. The radius is derived by the following expression:

$$r = \frac{180^\circ \cdot BD}{45^\circ \cdot \pi} = 1,909 \text{ ft} \quad \text{Eq. A-3}$$

The radius is now constant for all angles. The chord length BD is then calculated:

$$BD = 2 \cdot r \cdot \sin\left(\frac{45^\circ}{2}\right) = 1,461.08 \text{ ft} \quad \text{Eq. A-4}$$

BOD is an isosceles triangle as it has two sides equal to the radius r. The inclination angle  $\theta = 45^\circ$ , so the angle y or else  $\widehat{D\hat{B}O}$  is:

$$y = \frac{180^\circ - \theta}{2} = 67.5^\circ \quad \text{Eq. A-4}$$

In the right triangle BKD, the length of the side KD plus 1,000', corresponds to the true vertical depth at 2,500 MD, hence the true vertical depth can be computed as follows:

$$\begin{aligned} \sin y &= \frac{KD}{BD} \Leftrightarrow KD = BD \cdot \sin y = 1461.08 \cdot 0.92 = 1,349.87 \text{ ft} \Rightarrow \\ 1,349.87 \text{ ft} + 1,000 \text{ ft} &= 2,349.87 \text{ ft (TVD)} \quad \text{Eq. A-5} \end{aligned}$$

The same procedure is followed for all pairs of TVD and MD at the section where the inclination angle is equal to objective one.

Below 2500' MD or 2349,87 TVD, the two different types of depths represent the two sides of a right isosceles triangle. The measured depth can be calculated by the following expression:

$$MD = 2,500 \text{ ft} + \frac{TVD - 2,349.87 \text{ ft}}{\frac{\sqrt{2}}{2}} \quad \text{Eq. A-6}$$

APPENDIX A-2

Calculate	Design	Done	Cancel	Report	Export	Help
<b>Input Data</b>						
Pump depth (Measured)	10000	feet				
Operating Frequency	70	Hertz				
Maximum OD	6	inches				
Length Of Cable	10000	feet				
Gas Separator Efficiency	0	percent				
Design Rate	10000	STB/day				
Water Cut	20.3	percent				
Total GOR	493	scf/STB				
Top Node Pressure	264	psig				
Motor Power Safety Margin	0	percent				
Pump Wear Factor	0	fraction				
Pipe Correlation	Beggs and Brill					
Tubing Correlation	Petroleum Experts 2 1.03 1.00					
Gas DeRating Model	<none>					

Figure A-2.1: ESP input data screen: Pump depth is set at 10000', designed liquid rate is 10000 stb/day

Done	Calculate	Main	Export	Sensitivity	Help
Well Head Pressure	264	(psig)			
Flowing Bottomhole Pressure	3224.98	(psig)			
Water Cut	20.3	(percent)			
Pump Frequency	70	(Hertz)			
Pump Intake Pressure	1966.02	(psig)			
Pump Intake Temperature	229.31	(deg F)			
Pump Intake Rate	12988	(RB/day)			
Free GOR Entering Pump	61.4741	(scf/STB)			
Pump Discharge Pressure	2436.16	(psig)			
Pump Discharge Rate	12511.3	(RB/day)			
Total GOR Above Pump	493	(scf/STB)			
Mass Flow Rate	3311843	(lbm/day)			
Total Fluid Gravity	0.7466				
Average Downhole Rate	12654.3	(RB/day)			
Head Required	1453.99	(feet)			
Actual Head Required	1453.99	(feet)			
Fluid Power Required	101.006	(hp)			
GLR @ Pump Intake (V/V)	0.059109	(fraction)			
Gas Fraction @ Pump Intake	0.05581	(fraction)			
Bo @ Pump Intake	1.27263	(RB/STB)			
Bg @ Pump Intake	0.0083225	(ft3/scf)			
Average Cable Temperature	194.165	(deg F)			

Figure A-2.2: ESP design calculations

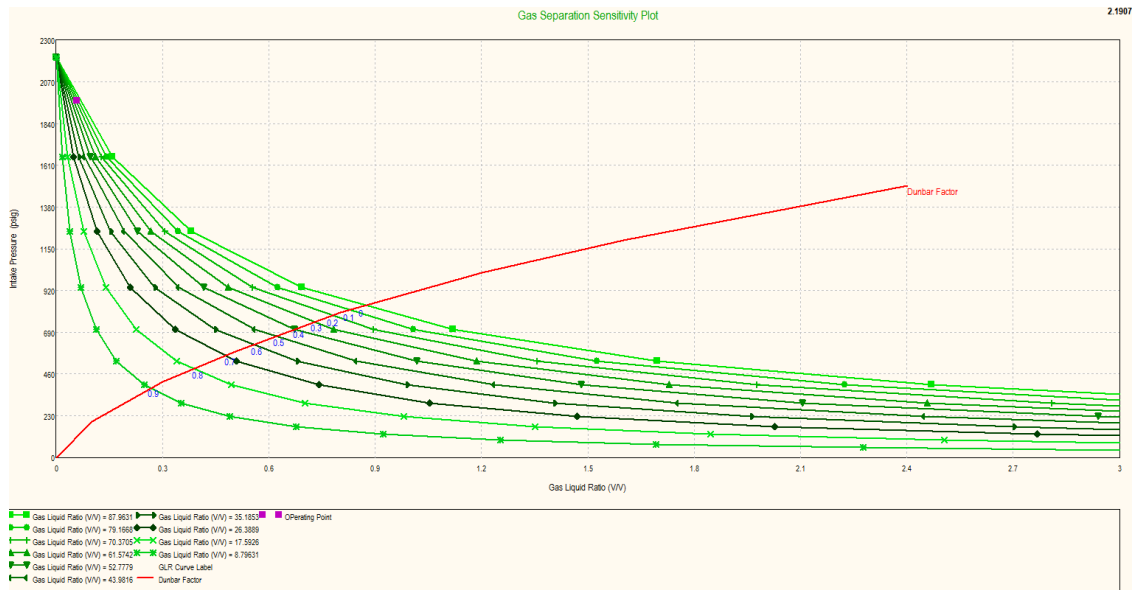


Figure A-2.3: Gas separation sensitivity plot (Red lines corresponds to the Dunbar factor)

Done	Cancel	Main	Help	Plot
------	--------	------	------	------

**Input Data**

Head Required	1292.37	feet	Pump Intake Pressure	2017.07	psig
Average Downhole Rate	12617.7	RB/day	Pump Intake Rate	12879.3	RB/day
Total Fluid Gravity	0.74876	sp. gravity	Pump Discharge Pressure	2436.16	psig
Free GOR Below Pump	48.6193	scf/STB	Pump Discharge Rate	12511.1	RB/day
Total GOR Above Pump	493	scf/STB	Pump Mass Flow Rate	3311843	lbm/day
Pump Inlet Temperature	229.31	deg F	Average Cable Temperature	194.165	deg F

Select Pump	ESP TE11000XHT_COMP 5.38 inches (8000-14000 RB/day)
Select Motor	ODI 70KM300-E 126HP 1545.83V 56A
Select Cable	#1 Aluminium 0.33 (Volts/1000ft) 95 (amps) max

**Results**

Number Of Stages	25		Motor Efficiency	90.2706	percent
Power Required	127.885	hp	Power Generated	127.885	hp
Pump Efficiency	72.0278	percent	Motor Speed	4104.01	rpm
Pump Outlet Temperature	230.67	deg F	Voltage Drop Along Cable	205.019	Volts
Current Used	50.1442	amps	Voltage Required At Surface	1750.85	Volts
Surface KVA	152.066		Torque On Shaft	163.66	lb. ft

Figure A-2.4: Pump selection screen

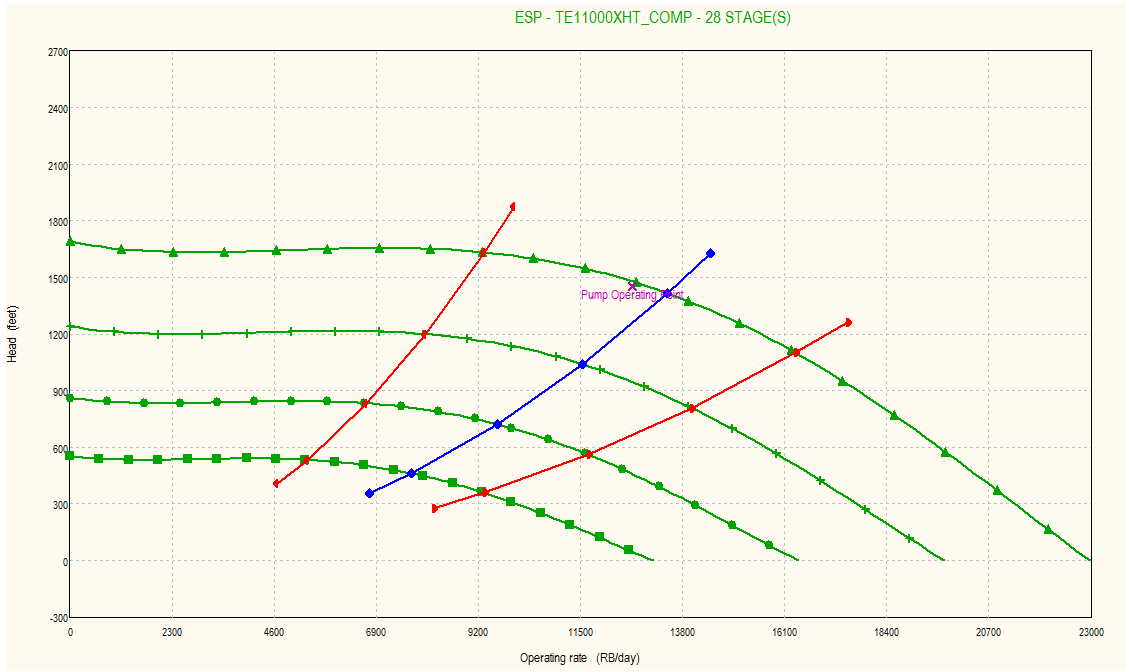


Figure A-2.5: Pump efficiency plot

### APPENDIX A-3

Valve Data																	
Valve	Number Of Valves	Valve Type	Measured Depth	True Vertical Depth	Tubing Pressure	Casing Pressure	Transfer Pressure	Temperature @ Valve	Gaslift Gas Rate	Port Size	R Value	Valve Opening Pressure	Valve Closing Pressure	Dome Pressure	TestRack Opening Pressure	Opening CHP	Closing CHI
			(feet)	(feet)	(psig)	(psig)	(psig)	(deg F)	(MMscf/day)	(64ths inch)		(psig)	(psig)	(psig)	(psig)	(psig)	(psig)
1	1	Valve	4394.78	3687.96	789.921	1973.58	1085.84	195.106	0.71194	12	0.038	1973.58	1928.6	1458.84	1516.47	1800	1755.02
2	1	Valve	8166.65	6354.99	1215.26	2040.09	1421.47	223.179	0.71194	12	0.038	2040.09	2008.74	1446.89	1504.05	1750	1718.66
3	1	Valve	10661.2	8118.96	1515.98	2059.05	1651.75	237.382	0.71194	12	0.038	2059.05	2038.41	1434.08	1490.73	1700	1679.36
4	1	Valve	12159.6	9178.61	1711.11	2042.82	1794.04	243.702	2.0926	20	0.103	2042.82	2008.66	1400.29	1561.09	1650	1615.83
5	1	Orifice	12562.1	9463.2	1764.97	1864.97	1764.97	244.925	7.1194	43							

Figure A-3.1: Gas lift Case 1 results

Valve Data																	
Valve	Number Of Valves	Valve Type	Measured Depth	True Vertical Depth	Tubing Pressure	Casing Pressure	Transfer Pressure	Temperature @ Valve	Gaslift Gas Rate	Port Size	R Value	Valve Opening Pressure	Valve Closing Pressure	Dome Pressure	TestRack Opening Pressure	Opening CHP	Closing CHI
			(feet)	(feet)	(psig)	(psig)	(psig)	(deg F)	(MMscf/day)	(64ths inch)		(psig)	(psig)	(psig)	(psig)	(psig)	(psig)
1	1	Valve	4398.52	3690.61	776.002	1974.77	1075.69	193.793	0.76276	12	0.038	1974.77	1929.22			1800	1754.45
2	1	Valve	8225.73	6396.76	1196.05	2043.77	1407.98	222.812	0.76276	12	0.038	2043.77	2011.56			1750	1717.79
3	1	Valve	10801.3	8218.05	1492.13	2065.63	1635.5	237.678	0.76276	12	0.038	2065.63	2043.83			1700	1678.21
4	1	Orifice	12000	9065.75	1638.58	2104.78	1638.58	242.899	7.62765	31							

Figure A-3.2: Gas lift Case 1 revised results

APPENDIX

Valve Data																	
Valve	Number Of Valves	Valve Type	Measured Depth	True Vertical Depth	Tubing Pressure	Casing Pressure	Transfer Pressure	Temperature @ Valve	Gaslift Gas Rate	Port Size	R Value	Valve Opening Pressure	Valve Closing Pressure	Dome Pressure	TestRack Opening Pressure	Opening CHP	Closing CHP
			(feet)	(feet)	(psig)	(psig)	(psig)	(deg F)	(MMscf/day)	(64ths inch)		(psig)	(psig)	(psig)	(psig)	(psig)	(psig)
1	1	Dummy	4398.52	3690.61	0	0	0	0	0	0						1800	1800
2	1	Valve	8225.73	6396.77	1290.51	2050.26	1290.51	224.257	0.58288	8	0.017	2050.26	2037.34	1463.88	1489.19	1800	1787.08
3	1	Valve	10801.3	8218.05	1653.43	2068.28	1653.43	238.399	0.58288	12	0.038	2068.28	2052.52	1441.16	1498.09	1750	1734.24
4	1	Orifice	12000	9065.75	1837.48	2050.08	1837.48	243.329	5.82878	32						1700	

Figure A-3.3: Gas lift Case 2 results

Valve Data																	
Valve	Number Of Valves	Valve Type	Measured Depth	True Vertical Depth	Tubing Pressure	Casing Pressure	Transfer Pressure	Temperature @ Valve	Gaslift Gas Rate	Port Size	R Value	Valve Opening Pressure	Valve Closing Pressure	Dome Pressure	TestRack Opening Pressure	Opening CHP	Closing CHP
			(feet)	(feet)	(psig)	(psig)	(psig)	(deg F)	(MMscf/day)	(64ths inch)		(psig)	(psig)	(psig)	(psig)	(psig)	(psig)
1	1	Dummy	4398.52	3690.61	0	0	0	0	0	0						1800	1800
2	1	Valve	8225.73	6396.77	1391.27	2048.41	1391.27	225.821	0.5752	12	0.038	2048.41	2023.44	1450.7	1508.01	1800	1775.03
3	1	Orifice	10801.3	8218.05	1800.01	2066.45	1800.01	239.166	5.752	30						1750	
4	1	Dummy	12000	9065.75	0	0	0	0	0	0							

Figure A-3.4: Gas lift Case 3 results

Valve Data																	
Valve	Number Of Valves	Valve Type	Measured Depth	True Vertical Depth	Tubing Pressure	Casing Pressure	Transfer Pressure	Temperature @ Valve	Gaslift Gas Rate	Port Size	R Value	Valve Opening Pressure	Valve Closing Pressure	Dome Pressure	TestRack Opening Pressure	Opening CHP	Closing CHI
			(feet)	(feet)	(psig)	(psig)	(psig)	(deg F)	(MMscf/day)	(64ths inch)		(psig)	(psig)	(psig)	(psig)	(psig)	(psig)
1	1	Dummy	4398.52	3690.61	0	0	0	0	0	0						1900	1900
2	1	Valve	8225.73	6396.77	1420.48	2174.99	1420.48	226.071	0.52083	8	0.017	2174.99	2162.16	1544.28	1570.99	1900	1887.17
3	1	Valve	10801.3	8218.05	1846.23	2201.11	1846.23	239.287	0.85364	12	0.038	2201.11	2187.63	1528.62	1589	1850	1836.51
4	1	Orifice	12000	9065.75	2058.8	2186.78	2058.8	243.86	5.20834	34						1800	

Figure A-3.5: Gas lift Case 3 revised results

Valve Data																	
Valve	Number Of Valves	Valve Type	Measured Depth	True Vertical Depth	Tubing Pressure	Casing Pressure	Transfer Pressure	Temperature @ Valve	Gaslift Gas Rate	Port Size	R Value	Valve Opening Pressure	Valve Closing Pressure	Dome Pressure	TestRack Opening Pressure	Opening CHP	Closing CHI
			(feet)	(feet)	(psig)	(psig)	(psig)	(deg F)	(MMscf/day)	(64ths inch)		(psig)	(psig)	(psig)	(psig)	(psig)	(psig)
1	1	Valve	4398.52	3690.61	916.725	1957.24	916.725	200.214	0.41178	8	0.017	1957.24	1939.55	1453.96	1479.11	1800	1782.31
2	1	Valve	8225.73	6396.77	1525.07	2019.12	1525.07	226.329	0.41178	8	0.017	2019.12	2010.72	1440.86	1465.78	1750	1741.6
3	1	Orifice	10801.3	8218.05	1998.15	2094.5	1998.15	239.413	4.1178	32						1700	
4	1	Dummy	12000	9065.75	0	0	0	0	0	0							

Figure A-3.6: Gas lift Case 4 results

Valve Data																	
Valve	Number Of Valves	Valve Type	Measured Depth	True Vertical Depth	Tubing Pressure	Casing Pressure	Transfer Pressure	Temperature @ Valve	Gaslift Gas Rate	Port Size	R Value	Valve Opening Pressure	Valve Closing Pressure	Dome Pressure	TestRack Opening Pressure	Opening CHP	Closing CHP
			(feet)	(feet)	(psig)	(psig)	(psig)	(deg F)	(MMscf/day)	(64ths inch)		(psig)	(psig)	(psig)	(psig)	(psig)	(psig)
1	1	Valve	4398.52	3690.61	952.489	2056.84	952.489	203.336	0.55032	8	0.017	2056.84	2038.06	1516.27	1542.49	1900	1881.23
2	1	Valve	8225.73	6396.77	1567.48	2117.11	1567.48	227.989	0.55032	8	0.017	2117.11	2107.77	1502.72	1528.7	1850	1840.66
3	1	Orifice	10801.3	8218.05	2038.38	2141.36	2038.38	240.213	5.50319	36						1800	
4	1	Dummy	12000	9065.75	0	0	0	0	0	0							

Figure A-3.7: Gas lift Case 4 revised results